Analysis of the role of the *Arabidopsis thaliana* ABC transporter AtMRP3 in heavy metal and herbicide detoxification

Dissertation

zur

Erlangung der naturwissenschaftlichen Doktorwürde
(Dr. sc. nat.)

vorgelegt der

Mathematisch-naturwissenschaftlichen Fakultät

der

Universität Zürich

von

Louis AZEVEDO

aus

Portugal

Promotionskomitee:

Dr. Markus Klein, Universität Zürich

Prof. Dr. Enrico Martinoia, Universität Zürich (Vorsitz)

Prof. Dr. Beat Keller, Universität Zürich

Dr. Ute Krämer, Max-Planck-Institut für Molekulare Pflanzenphysiologie, Postdam-Golm, Deutschland

Zürich, 2006

Table of contents

Results

I. Introduction

Among the various stresses to which living organisms are exposed, toxic compounds constitute one important factor. All living organisms have evolved specific detoxification mechanisms to cope with toxic substances. Plants as sessile organisms can not simply avoid the toxic compounds present in their close environment and so have developed structural (e.g. morphological), physiological and biochemical adaptations to avoid toxic stress.

The xenobiotics to which plants are exposed can be mainly divided into two major categories: metals/metalloids and organic xenobiotics. Among metals and metalloids, heavy metals are the most harmful.

I.1.1. Heavy metals

Heavy metals are defined as metals (and metalloids) whose density exceeds 5000 Kg m^{-3}. 53 metals correspond to this definition, but mainly eleven of them are problematic for plants. The 11 dangerous heavy metals are arsenic (As), cadmium (Cd), chromium (Cr), cobalt (Co), copper (Cu), lead (Pb), mercury (Hg), nickel (Ni), tin (Sn), vanadium (V) and zinc (Zn). Copper, zinc and nickel are essential for plant life while cobalt is essential for legumes ; vanadium is not essential for plant growth, but is essential for animals. Small amounts in the plants help therefore the herbivores consuming these plants to survive. Arsenic, cadmium, chromium, lead, mercury and tin are up to now considered to have only deleterious effects on living organisms. Other heavy metals either are not soluble enough or have a too high toxicity threshold to be harmful under physiological conditions. For example, iron (Fe) only reaches toxic concentrations in the vicinity of some industrial installations and mines or when bacteria reduce large amounts of Fe^{3+} ions to Fe^{2+} in flooded environments (He et al. 2005).

Concentrations of heavy metals in soils vary greatly. On the one hand, the amounts of metals in soils depend on the parental materials that contribute to soil formation : some rocks, such as malachite ($Cu_2(OH)_2CO_3$), smithsonite ($ZnCO_3$) or awaruite (Ni_3Fe), for example, are composed of large amounts of heavy metals and thus give birth to soils naturally rich in the corresponding metals. On the other hand anthropogenic inputs, such as industrial pollution, fertilizers, manures, chemical treatments, air pollution, are a major cause of heavy metal contamination in soils. Of course, inputs, extraction and consumption of these metals by living organisms, water flow, erosion and other factors, also contribute to overall heavy metal concentrations (He et al., 2005).

Element	Contents reported in the literature (mg kg^{-1})	1990 US Survey median (mg kg^{-1})
Zn	101-49000	725
Cd	<1-3410	7
Cu	84-17000	463
Ni	2-8330	29
Pb	13-26000	106
Hg	0.6-110	2
Cr	10-99000	40

Table I.1. : Observed concentrations of some heavy metals in soils.
(taken from He et al., 2005)

I.1.2. Mechanisms of metal transport and homeostasis in plants

In order to understand the mechanisms by which plants deal with heavy metals, it is important to analyse the pathways plants have evolved to absorb and distribute nutrient metallic ions between different organs and cell types and the mechanisms that maintain homeostasis of these ions. Indeed, toxic ions enter plants and are transported through the entire organism using similar ways as nutrient ions. Many mechanisms established to maintain optimal levels of nutrient ions in various organs are at the same time involved in the allocation, redistribution and detoxification of heavy metals. In fact, some nutrient ions, such as copper, iron or zinc, are toxic to the plant if their concentrations inside the organism bypasses a certain threshold. Membrane transporters play a central role in all these processes and some of them having already been described. Known transporters belong to various protein families : (i) The P-type ATPases protein family, which includes the *Arabidopsis* heavy-metal-transporting P-type ATPases (AtHMA) subfamily. AtHMA members are known to transport Zn^{2+},Cd^{2+},Pb^{2+},Co^{2+},Cu^{1+} and Ag^{1+} ions (Cobbett et al., 2003 ; Williams and Mills, 2005). (ii) The cation diffusion facilitator (CDF) family are metal/proton antiporters, one of them, AtMTP1, is suggested to mediate vacuolar sequestration of Zn^{2+} (van der Zaal et al., 1999 ; Mäser et al., 2001 ; Bloss et al., 2002 ; Kobae et al., 2004 ; Desbrosses-Fonrouge et al., 2005). (iii) The Yellow stripe-like (YSL) family is potentially involved in import of metallic ions complexed to phytosiderophores or to nicotianamine (Curie et al., 2001). (iv) Members of the natural resistance-associated macrophage proteins (NRAMP) family are divalent cation transporters (Colangelo and Guerinot, 2006). (v) The membrane proteins of the zinc-regulated

transporter ZRT-iron regulated transporter IRT-like protein (ZIP) family generally act as cation importers to the cytoplasm (Colangelo and Guerinot, 2006). (vi) The Ctr family of copper transporters (COPT) is not well studied, but AtCOPT1 as been demonstrated to play a role in Cu^{2+} uptake in roots (Sancenon et al., 2004).

Metallic ions enter the plant at the root level where they cross the plasma membrane through transport proteins and enter into the cytoplasm of the epidermal root cells, either as free metal ions or complexed with root exudates. For example, in *Arabidopsis* the ZIP transporter IRT1 is known to play a central role in the absorption of Fe^{2+} ions at this level. However IRT1 also facilitates transport of the heavy metals cadmium, manganese, cobalt and zinc. Thus IRT1 represents an entry point for toxic metal ions (Vert et al., 2002).

Once inside the root, the metals must be translocated to parenchyma cells, to be loaded in the xylem sap and translocated to the aerial parts of the plant. Again this step is facilitated by plasma membrane transporters which translocate the metallic ions from the cytoplasm of the endodermis and pericycle cells to the xylem parenchyma cells and from the xylem parenchyma cells into the vessels. In A*rabidposis*, the P-type ATPases AtHMA2 and AtHMA4 are thought to load zinc to the xylem (Eren and Arguello, 2004 ; Verret et al., 2005 ; Mills et al., 2005), and the YSL protein AtYSL2 is suspected to play a similar role for iron, copper or zinc (DiDonato et al., 2004 ; Schaaf et al., 2005) . Interestingly, both AtHMA2 and AtHMA4 have been demonstrated to transport heavy metals - cadmium in the case of AtHMA2, cadmium, zinc and lead in the case of AtHMA4 - indicating that they could play a role in the root to shoot transport of toxic heavy metals. At the level of the shoot and leaves, the ions leave the xylem. It is hypothesized that on this level the ion flux is divided into two streams here : some ions simply follow the transpiration stream of water in the apoplast, while another part is loaded into the symplast in cells of the bundle sheet. Again cell uptake requires the action of plasma membrane transporters (Karley et al., November 2000). The association of AtHMA2 and AtHMA4 with the vascular system at the leaf level could mean that these transporters also play a role during xylem unloading (Colangelo and Guerinot, 2006). Metallic ions are then differentially distributed between the various cell types of leaves, and it is suggested that differential import catalysed by various transporters facilitates cell-type specific uptake into the cytoplasm (Karley et al., March 2000, November 2000).

Once inside the cytoplasm of any cell type, the metallic ions will be translocated to the different organelles, either for immediate use in the organelle or for storage. Especially for toxic ions, subcellular sequestration for protection of cytosolic proteins is important. For short and long-term storage, ions mainly enter the central vacuole (Vögeli-Lange and Wagner,

1990 ; Brune et al., 1994 ; Krämer et al., 2000) (vacuolar sequestration of metallic ions will be further discussed in chapter I.1.3.). Some transporters distributing metals in other organelles have been described : in *Arabidopsis*, the P-type ATPases AtHMA1 and AtHMA6 transport copper from the cytoplasm to chloroplasts (Shikanai et al., 2003 ; Abdel-Ghany et al., 2005 ; Seigneurin-Berny et al., 2006) while AtHMA7 loads copper from the cytoplasm into the Golgi apparatus (Hirayama et al., 1999 ; Woeste and Kieber, 2000). Nutrient ions or enzyme cofactors can be remobilized from storage compartments and diverse membrane transporters involved in ion remobilization have also been described : in *Arabidopsis*, for example, AtNRAMP3 and AtNRAMP4 transport iron from the vacuole to the cytoplasm (Thomine et al., 2003 ; Lanquar et al., 2005). All these transporters could also transport heavy metals. In the case of AtNRAMP3 evidence was presented that this is also a cadmium transporter (Thomine et al., 2000).

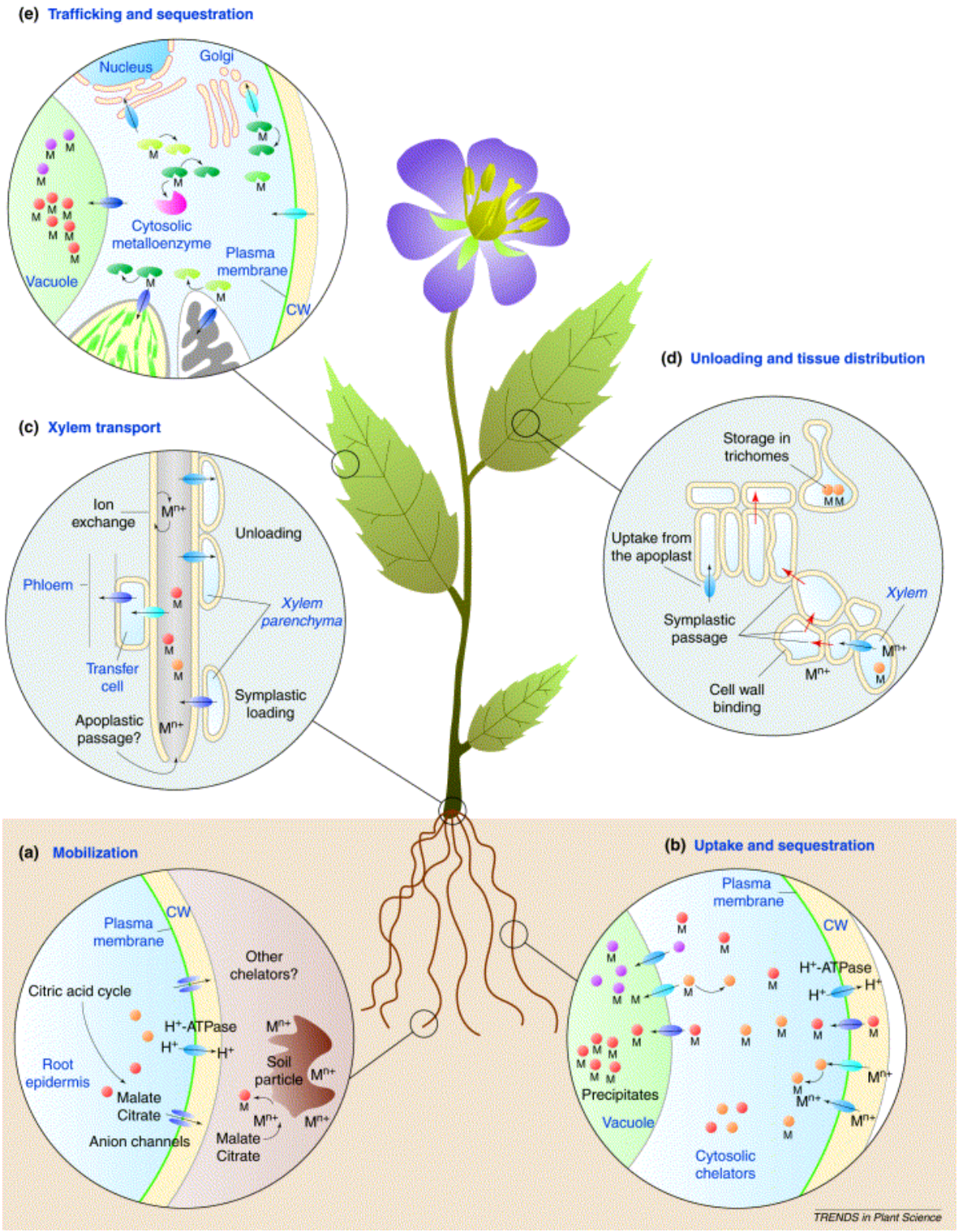

Figure I.1. : A general diagram of metal uptake, distribution and homeostasis in plants. Transporters act at all levels of metal homeostasis (a) at the roots, to excrete metal chelators to the soil (b) at the root, to import the metals (c) at the xylem, for loading and unloading the metallic ions (d) in the leaves, to distribute metals in all cell types (e) in the membranes of the cellular compartments, to distribute metallic ions among the various organelles or to remobilize stored metals (taken from Clemens et al., 2002).

I.1.3. Mechanisms of heavy metal detoxification in plants

Plants have developed various physiological and biochemical mechanisms to deal with heavy metals which can be generally classified into two categories : (i) *mechanisms of exclusion* aim at the limitation and prevention of a dangerous accumulation of heavy metals in the plant by avoiding their cellular entry (ii) *mechanisms of tolerance*. aim at the maintenance of the physiological functions of the organism despite the presence of high concentrations of heavy metals in the plant. As a consequence, the tolerant plant survives in a toxic environment. The efficiency of these mechanisms varies according to species or even ecotypes. Some plants, such as *Arabidopsis halleri*, *Thlaspi caerulescens*, or *Sebertia acuminata* are able to accumulate very high concentrations of heavy metals without suffering any adverse consequence (Lombi et al., 2000 ; Bert et al., 2003 ; Callahan et al., 2006). For example, the hyperaccumulator plant *Arabidopsis halleri* has been demonstrated to accumulate 3100 mg Zn^{2+}/kg dry weight when grown on a soil containing 100 ppm (100 mg/kg of soil) of Zn^{2+}, whereas the non-accumulator species *Arabidopsis thaliana* cultivated in the same conditions contained only 320 mg Zn^{2+}/kg dry weight (Plaza et al., 2005).

Mechanisms of exclusion mainly occur at the root level, through which heavy metals in soils enter the plant. A first strategy to avoid the entry of heavy metals is through complexation in a non-absorbable form in the soil. In this case, root exudates complex heavy metals before they enter the plant. Organic acids such as oxalate, citrate and malate or the amino acid histidine, which are actively secreted into the rhizosphere, have been demonstrated to play such a role (Ma et al., 1997, 2001 ; Salt et al., 2000 ; Yang YY et al., 2000 ; Hall, 2002). The excretion of these substances into the soil requires transporters.

The second mechanism of exclusion of heavy metals is through selective absorption of nutrient ions, via processes that selectively prevent import of toxic elements inside the plant together with the beneficial ions. In the case of mycorrhized roots, mycorrhizal fungi have been proposed to act as “filters” excluding the toxic ions (Jentschke and Godbold, 2000 ; Hall, 2002). Alternatively, metal-tolerant species may have evolved ion importers which exhibit a reduced affinity towards heavy metals (Meharg and Macnair 1990, 1992). Some authors have also proposed that binding of heavy metals to the root cell wall contributes to a “filtering process” (Bringezu et al., 1999). However, the specificity of such a mechanism with regard to heavy metals as opposed to nutrient ions is not well understood.

Another common exclusion mechanism in plants, is the excretion of heavy metals at the root level by secretion through specific transporters : heavy metals taken up are readily expelled from the cytosol to the soil (Hall, 2002). Finally, heavy metals can be accumulated in specific cell-types such as trichomes or are excreted through hydathodes at the leaf level, after their transfer from the root to the shoot (Choi et al., 2001 ; Larsen et al., 2005). Again, the concentration of heavy metals in these cells or organs needs the action of transport proteins.

Among the mechanisms conferring heavy metal tolerance, one strategy is the enhanced transfer of heavy metals from the root to the shoot. This strategy appears paradoxical at first sight since it results in increased concentrations of heavy metals in the aerial parts of the plant where photosynthesis occurs. However, it has been demonstrated repeatedly that hypertolerant plants have more efficient mechanisms of heavy metal translocation from root to shoot than related sensitive species. The data have been interpreted on the basis of a higher sensitivity of the root tissues towards heavy metal toxicity when compared to the shoot. Furthermore, a more widespread distribution of the heavy metals within the plant may result in reduced cell concentrations (Lassat et al., 1996, 2000 ; Bert et al., 2003). Increased translocation can be achieved through enhanced xylem loading at the root level or enhanced xylem unloading at the shoot level. Both processes rely on the activity of transport proteins (Clemens et al., 2002).

Probably the best described mechanism of heavy metal tolerance in plants is the *ligation mechanism*, by which heavy metals are complexed inside the cell. As a consequence, complexed heavy metals loose their deleterious capacity. The non-proteinogenic tripeptide glutathione as well as the glutathione polymers collectively referred to as *phytochelatins* ([γ-Glu-Cys]$_n$-Gly) act as efficient molecules enabling heavy metal complexation (Howden et al., 1995 ; Schmöger et al., 2000 ; Cobbett, 2000). Apart from glutathione and phytochelatins, other molecules are ligands including a class of polypeptides described as metallothionins, amino acids such as histidine and organic acids such as citrate and malate, nicotianamine and its derivatives, the phytosiderophores (Zhou and Goldsbrough, 1994 ; Krämer et al., 1996 ; Salt et al., 1999 ; Clemens, 2001 ; Callahan et al. 2006).

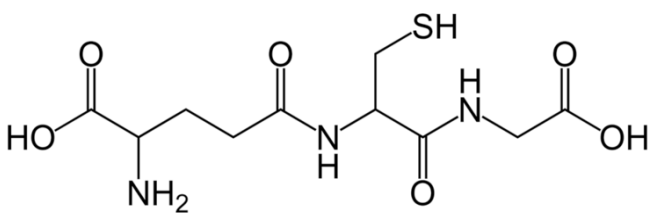

Figure I.2. : Chemical structure of the tripeptide glutathione.

With regard to glutathione, it is important to note that apart from chelating heavy metals it also acts as a powerful reducing agent and is involved in the detoxification of superoxid within the Halliwell cycle. Heavy metals such as Fe, Cu or Cd cause oxidative stress. Fe and Cu cause oxidative stress directly, by changing their oxidative state, while Cd causes oxidative stress indirectly, possibly by an interaction with thiols. Thus the antioxidative action of glutathione is an essential part of the resistance mechanisms against the effect of heavy metals (Marrs, 1996). In fact, all other molecules and enzymes involved in antioxidative processes play important roles in the resistance against these metals as well, including superoxide dismutase, catalase, acorbate peroxidase and ascorbate (Boominathan and Doran, 2003).

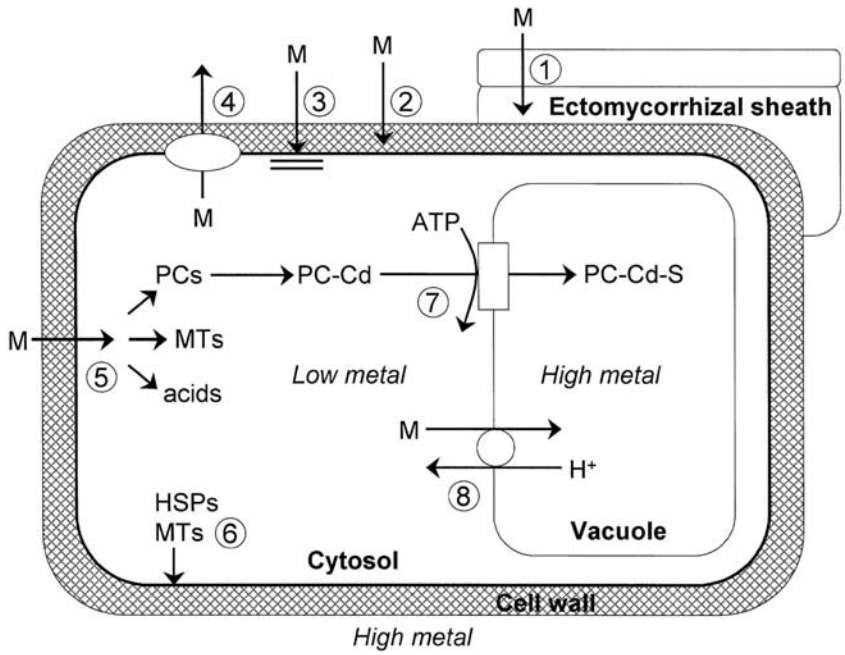

Figure I.3. : Summary of potential strategies available for metal detoxification and tolerance in plant cells. 1. Restriction of metal movement to roots by mycorrhizas. 2. Binding to cell wall and root exudates. 3. Reduced influx across the plasma membrane. 4. Active efflux into the apoplast. 5. Chelation in the cytosol by various ligands. 6. Repair and protection of the plasma membrane under stress conditions. 7. Transport of chelated metallic ions into the vacuole. 8. Transport and accumulation of free metal solutes into the vacuole. Abbreviations : HSPs, heat shock proteins ; M, metallic ion ; MTs, metallothioneins ; PC, phytochelatin. (taken from Hall, 2002)

It has also been suggested that specific mechanisms protecting the plasma membrane exist. It has been speculated that heat shock proteins might play a role, but no direct evidence was presented for this hypothesis (Tseng et al., 1993 ; Wollgiehn and Neumann, 1999 ; Hall, 2002).

Finally, a tolerance mechanism of central interest to this thesis, is the sequestration of heavy metals into plant vacuoles. Various kinds of toxic molecules, including heavy metal ions, are known to be transported from the cytosol, where they can disturb many important biochemical processes, into the vacuolar space. This transport is again catalyzed by membrane transporters and the heavy metal ions are transported either alone or in a complex with one of the ligands previously mentioned . Some examples are documented. There are evidences that in pea Fe^{2+} ions are accumulated into the vacuole complexed with nicotianamine, although the transporter of this complex is still not known (Pich et al. 2006). In *Arabidopsis thaliana*, the metal/proton antiporter AtMTP1 (previously named ZAT1) of the CDF family is thought to mediate the vacuolar sequestration of Zn^{2+} (van der Zaal et al., 1999 ; Mäser et al., 2001 ; Bloss et al., 2002 ; Kobae et al., 2004). In *Avena sativa*, the existence of a Cd^{2+}/H^{+} antiporter – exporting H^{+} and importing Cd^{2+} – in the vacuolar membrane has been demonstrated (Salt and Wagner, 1993), as well as the import of Cd^{2+}-phytochelatin complexes (Salt and Rauser, 1995). In *Arabidopsis thaliana* there are indications that some of the Ca^{2+}/proton antiporters of the CAX family also transport Cd^{2+} into the vacuole (Hirschi et al., 2000 ; Shigaki et al., 2005 ; Koren'kov et al., 2006).

In conclusion to this chapter, we can say that membrane transport processes play a central role in the majority of the known mechanisms of heavy metal exclusion or tolerance.

I.1.4. Cadmium

Since cadmium is the central heavy metal of this study, the specific characteristics and effects on plants are shortly outlined in this section.

Presence of cadmium in soils is mainly due to human activities although naturally occurring sites of high cadmium soil concentration are known. Industrial pollution, human waste (cadmium is used, for example, to produce batteries, pigments or coatings) and mineral fertilizers made from rocks containing a high percentage of cadmium are the main sources of anthropogenic pollution.

Cd^{2+} ions are known to enter the plants through Ca^{2+} channels (Perfus-Barbeoch et al., 2002) and Fe^{2+} transporters such as the IRT1 ZIP-type protein (Vert et al., 2002). Many membrane proteins transporting essential metallic ions also exhibit an affinity towards cadmium. As a consequence, the heavy metal is distributed throughout the plant by the action of unspecific transport processes. Apart from the proteins already introduced in paragraph I.1.2., the ZIP1, ZIP2 and ZIP3 transporters of *Arabidopsis thaliana* have to be particularly mentioned because they play a role in zinc homeostasis but also have an affinity for cadmium (Grotz et al., 1998). Inside the plant, Cd^{2+} causes oxidative stress, leads to proteins denaturation by binding to sulfhydryl residues, displaces cofactors of various proteins and perturbs the water status (Clemens et al., 1998 ; Thomine et al., 2000 ; Perfus-Barbeoch et al., 2002).
Sequestration of Cd^{2+} ions into the vacuole is regarded as the central mechanism of cadmium detoxification at the cellular level in plants. As discussed in paragraph I.1.3., the transporters responsible for this sequestration are partially known. Interestingly, it has been demonstrated that *Thlaspi caerulescens*, a Cd^{2+} hyperaccumulator and close relative of *Arabidopsis thaliana*, has a high-affinity Cd^{2+} transport activity in the roots in addition to extraordinarily high catalase activity in *Thlaspi* roots when compared to *Nicotiana tabacum*. Furthermore, Cd^{2+} mainly accumulates in *Thlaspi* vacuoles (Lassat et al., 1996, 2000 ; Lombi et al., 2001 ; Boominathan and Doran, 2003 ; Ma et al., 2005).

I.2.1. Organic xenobiotics

In contrast to heavy metals, toxic organic compounds with which plants were confronted during evolution were primarily of biological origin. Biotoxic compounds are mainly synthesized by microbial pathogens. Plants synthesize allelochemicals in order to control growth of other plant species or to defend themselves against attacks of herbivores. However, the quantity and variety of organic xenobiotics plants have to handle have dramatically increased during the last decades due to massive use of synthetic organic compounds produced by humans. Some of these novel toxic compounds are pollutants, byproducts of industrial activity, others are directly applied to plants such as agrochemicals (herbicides and pesticides). By today, more than 3000 different commercial agrochemical have been licensed for use in the field in Europe (Coleman et al., 1997).
In contrast to heavy metals, which enter the plant mainly through roots, organic xenobiotics enter the plant either through the roots or through leaves in the case of organic volatiles or of sprayed herbicides. Due to their lipophilic nature, organic xenobiotics penetrate the plant

easily, diffusing through the cellular membranes. Penetration through roots is quick because root cells are devoid of cuticular wax or suberin layers superimposed to the cell wall protecting aerial plant parts. In general, after being absorbed and partially detoxified by the roots, organic xenobiotics are systemically distributed in the plant via the vascular system, some of them already modified by the detoxification processes occurring in the root cells and some of them without changes in their molecular structure. Although entry through leaves is limited by the cuticle covering the epidermis constituting a barrier. Nonetheless lipophilic compounds are able to diffuse through the cuticular layer into the epidermal cells with time, and xenobiotics can also enter the leaves through the stomata. (Coleman et al., 1997 ; Korte et al., 2000).

Herbicides are one of the major categories of organic xenobiotics toxic to plants. Different families of organic compounds with herbicidal activity have been developed. According to their molecular structure and principle of action they can be roughly categorized as herbicides inhibiting photosynthesis (triazines, uracils, phenylcarbamates, pyridazinones, benzothiadiazoles, etc), herbicides inhibiting synthesis of phospholipids (aryloxyphenoxyproprionates, cyclohexanediones), herbicides inhibiting amino acid biosynthesis (chloracetamides, sulfonylureas, imidazolinones, sulfonanilides), herbicides disturbing auxin regulation (auxin analogs), herbicides inhibiting carotenoid synthesis (triazoles, isoxazolidinones), herbicides inhibiting chlorophyll synthesis, herbicides inhibiting cellulose synthesis or herbicides disturbing the cell membranes (Kreuz et al., 1996).

I.2.2. Detoxification of organic xenobiotics in plants

The prevailing physiological protective mechanism plants have evolved to survive treatment with a toxic xenobiotic substance is an increase in the detoxification capacity. In contrast, only few examples are known where a given herbicide is unable to bind to its target protein due to structural modifications of the enzyme which results in the inactivity of the herbicide in the tolerant species (Kreuz et al., 1996).

In rare cases, organic xenobiotics absorbed by plants can be excreted by roots or leaves. Tolerance towards a xenobiotic compound is mainly established by a biochemical detoxification pathway which generally involves three phases. In phase I, xenobiotics which enter the cytosol mostly by passive diffusion undergo a chemical activation In the following phase II, activated phase I products are conjugated. Finally, in phase III, the conjugated xenobiotic is transported into the vacuole or out of the cell. Once inside the vacuole, the

organic molecules undergo final processing including further oxidation, by which they are ultimately degraded (Coleman et al., 1997 ; Korte et al., 2000).

The phase I activation reactions occur in the cytosol and involve hydrolytic or oxidation reactions. Hydrolysis is catalysed by esterases or amidases while oxidations involve diverse cytochrome P-450 oxidoreductases located at the endoplasmatic reticulum (Bolwell et al., 1994 ; Siminszky et al., 1999). The phase I reactions results in two major changes : by introduction of polar groups in the xenobiotic molecules, they make them slightly more hydrophilic, thus reducing their mobility through membranes; at the same time, reactive groups introduced allow the subsequent conjugation reactions occurring in phase II. Here the toxic compound is conjugated to a hydrophilic moiety which guarantees that it is no more freely diffusible. It should be noted that the activated molecules do not generally have a reduced toxic activity and, sometimes, they are even more toxic than the parent compound. This means, that phase I reactions are not sufficient for detoxification (Kreuz et al., 1996).

One of the possible molecules attached to phase I products is glutathione : it conjugates itself, either spontaneously or catalysed by glutathione-S-transferases, with a wide range of xenobiotic electrophiles. These electrophiles may have been activated by the phase I reactions before conjugation. However in most cases glutathione conjugates directly to the unmodified electrophilic xenobiotic, bypassing the phase I reactions. Homoglutathione, a close homolog of glutathione which appears in *Avena sativa* for example, can exert the same function. Molecules containing hydroxylic groups, amino groups or carboxyl groups often undergo glycosylation in plants with glucose, but also with other sugars (Kreuz et al., 1996 ; Korte et al., 2000). Finally, carboxyl groups can also be conjugated to amino acids such as glutamate or aspartate. Each of these conjugation reactions is catalysed by specific families of catalytic enzymes. For example, glucosylations are catalysed by O- and N-glucosyltransferases utilizing UDP-glucose as sugar donor (Kreuz et al., 1996).

In phase III, conjugated phase II products enter the vacuole with the help of vacuolar membrane transporters. In several cases it has been shown that this transport is strictly ATP-dependent and some of these transporters have been characterized (Martinoia et al., 1993; Li et al., 1995a, 1995b ; Gaillard et al., 1994 ; Klein et al., 1996).

The so-called phase IV of detoxification – the fate of the conjugated xenobiotics within the vacuole – is not well understood but may involve oxidation. Circumstantial evidence suggests that some xenobiotics are eventually converted into Krebs cycle acids or amino acids which re-enter the primary biochemical pathways of plant metabolism (Korte et al., 2000). For example, in the case of glutathione conjugates, a first step of degradation of the glutathione

part towards the γ-glutamylcysteinyl-S-conjugate of alachlor catalyzed by a vacuolar carboxypeptidase has been described (Wolf et al., 1996).

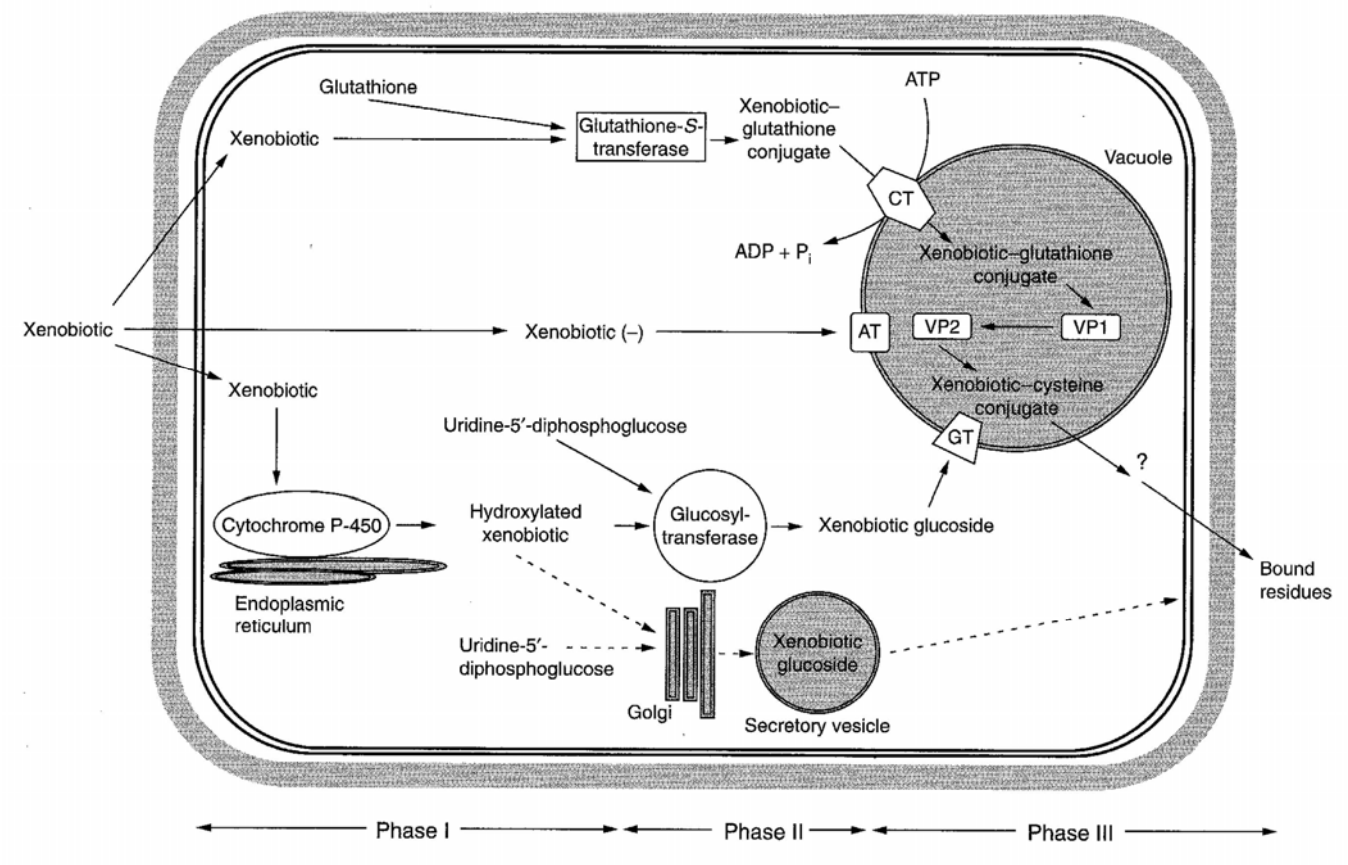

Figure I.4. : The three phases of xenobiotic detoxification are associated with several organelles. Different possible pathway of detoxification are represented and introduced in the text. Abbreviations : CT, glutathione conjugate transporter ; AT, ATP-dependant xenobiotic anion transporter ; GT, ATP-dependent glucoside-conjugate transporter ; VP, vacuolar peptidase. (Taken from Coleman et al., 1997)

I.2.3. Prosulfuron

Prosulfuron, a model herbicide used in this study, is an herbicide of the sulfonylurea group which inhibits acetolactate synthase. As a result, the plant is unable to produce acetolactate, an important intermediate of the synthesis of the branched amino acids valine, leucine and isoleucine (http://www.omafra.gov.on.ca/french/crops/facts/notes/prosuldic.htm).

Prosulfuron is detoxified by cytochrome P450-dependent hydroxylation in phase I (Moreland et al., 1996 ; Frear and Swanson, 1996) followed by glucosylation at the hydroxyl group during phase II. For hydroxyprimisulfuron-glucoside, a detoxification product of primisulfuron (an herbicide homologue to prosulfuron), an active, ATP-dependent transport into the vacuole has been demonstrated in barley (Klein et al.1996).

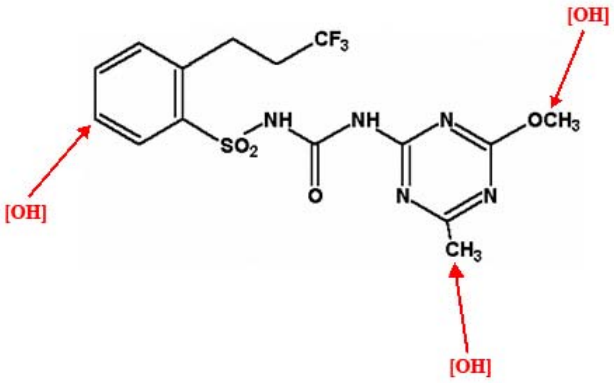

Figure I.5. : Prosulfuron and its possible sites of cytochrome P450 catalysed hydroxilations.

I.3.1. ABC transporters

The ATP-binding cassette transporters (ABC transporters) form a superfamily of membrane proteins which are present in all living organisms, from bacteria to humans. ABC transporters are found in all kinds of cellular membranes such as the plasma membrane, the vacuolar membrane, the endoplasmic reticulum membrane, the nuclear membrane or membranes of mitochondria (Jones and George, 2004).

ABC transporters are characterized by a typical and conserved structure. A functional ABC transporter consists of two hydrophobic transmembrane domains (TMD), usually composed of six membrane spanning α-helices, and two cytosolically oriented nucleotide binding domains (NBD), also known as the ABC domains (ABC for ATP-binding cassettes). The

ABC domains include the highly conserved Walker A and Walker B motifs and the so-called "ABC signature" motif LSGGQ. In eukaryotes, so called "full-size" ABC transporters are formed by a single protein which contains both TMDs as well as the two NBDs. Notable exceptions to these rules are known. In bacteria, all possible combinations exist to form a functional ABC transporter consisting of two TMDs and two NBDs : (i) each TMD and NBD can be encoded by separate open reading frames and the multimeric transporter consist of four subunits. (ii) One TMD and one NBD can be encoded by one open reading frame and associated either with another "half" consisting of a second TMD-NBD-halfmer or with separate TMD and NBD subunits. (iii) Either the two TMDs or the two NBDs can be encoded as a polypeptide that needs to associate itself either with a second polypeptide (comprising the two missing NBDs or TMDs respectively) or with two further subunits (two separate NBDs or TMDs respectively). (iv) The full-size ABC transporter can consist of the two TMDs and two NBDs encoded as a single protein (Linton and Higgins, 1998). In eukaryotes hemitransporters, also termed 'half-size' transporters, which include one TMD and one NBD, have been described. It is hypothesized that the half-size transporters in general have to dimerise to form a functional unit. "Soluble" ABC transporters, lacking contiguous TMDs exist in eukaryotes as well (Sánchez-Fernández et al., 2001).

ABC transporters usually mediate ATP-energized transport of a multitude of structurally diverse substrates. However, functions beyond simple transport catalysis have been defined for specialized ABC proteins which include ion channel or ion channel regulator functions, receptor, protease or protein sensor functions. As transporters, ABC transporters can be exporters as well as importers. It was thought a long time that only prokaryotic ABC transporters could function, not only as exporters of substrates from the cytoplasm, but also as importers, and that eukaryotic ABC transporters were limited to the role of exporters. But recently it was demonstrated that the *Coptis japonica* ABC transporter CjMDR1 was involved in alkaloid import to the cytoplasm (Shitan et al., 2003) and that the *Arabidopsis thaliana* ABC transporter AtPGP4 was involved in auxin import across the plasma membrane (Santelia et al., 2005). The variety of substrates translocated is impressive and includes ions, heavy metals, carbohydrates, drugs, amino acids, phospholipids, steroids, glucocorticoids, bile acids, proteic toxins, antigenic peptides, pigments, conjugated xenobiotics, vitamins (Bauer et al., 1999). The wide range of substrates of ABC transporters is reflected by large structural variations in the TMD domains, which allow interactions with very diverse molecular structures.

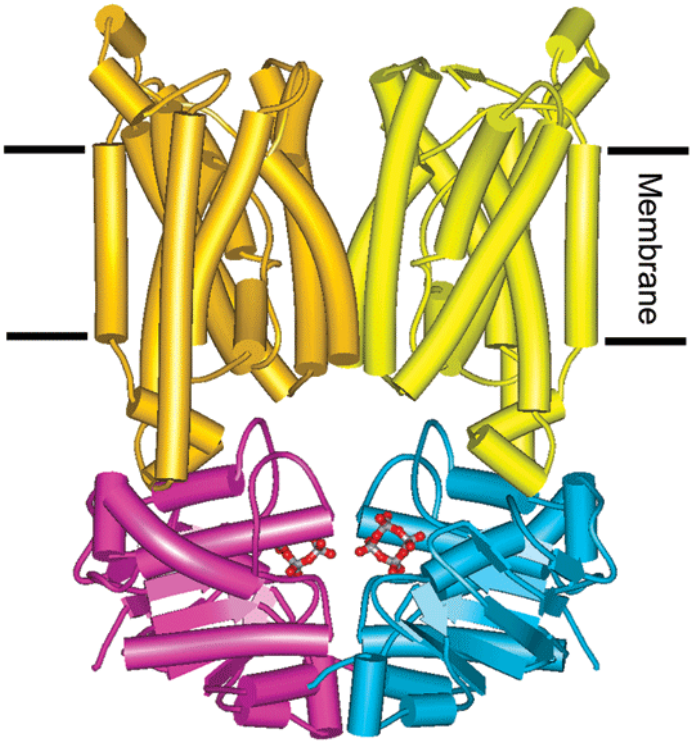

Figure I.6. : Three-dimensional structure of a typical ABC transporter. Vitamin B12 transporter BtuCD of *E. coli*. TMDs in gold and yellow, NBDs in magenta and blue. Two molecules of tetravanadate (shown in ball-and-stick) mimic nucleotides and are bound at the ATP-binding sites. (taken from Higgins and Linton, 2004)

Eukaryotic full-size ABC transporters are divided into several subfamilies based on their modular structure, in plant the three major classes are the pleiotropic drug resistance (PDR), the multidrug resistance (MDR) and the multidrug resistance-associated protein (MRP) subfamilies. Members of these subfamilies are classified according to phylogenetic and structural criteria (the order of the TMDs and NBDs) as well as differences in the substrate spectra accepted by members of the individual families.

PDRs, MDRs and MRPs have been established in many organisms as multidrug pumps which accept a large variety of endogenous and xenobiotic substrates, thereby preventing high concentrations of structurally diverse toxic compound. Consequently the action of ABC proteins has been linked to detoxification processes. In plants, apart from the examples discussed in I.3.2, different transporters of the ABC superfamily which comprises about 130 members in *Arabidopsis*, (Sanchez-Fernandez et al., 2001) several ABC transporters have been shown to protect the plant against toxic compounds. For example, the *Arabidopsis* ABC transporter AtPDR12 was demonstrated to play a major role in lead resistance (Lee et al., 2005) and the half-size *Arabidopsis* ABC transporter AtWBC19 was shown to confer resistance to the antibiotic kanamycin (Mentewab and Stewart, 2005).

I.3.2. MRPs and detoxification in plants

The first discovered multidrug resistance-associated protein (MRP) was found in a human lung cancer cell line, where it mediated resistance to chemotherapeutic drugs by exporting them (Cole et al., 1992). Generally, MRPs possess two characteristic features that distinguish them from other ABC transporters : they have a deletion of 13 amino acids between the Walker A and the Walker B domains of the NBD when compared to the classical multidrug resistance (MDR) proteins and they are often larger than other full length ABC transporters, because they contain an additional hydrophobic domain at the N terminus of the protein, the so-called TMD0. Thus, the domain structure of MRP proteins can be simplified as TMD0-TMD1-NBD1-TMD2-NBD2 (Hipfner et al., 1999 ; Jasinsky et al., 2003).

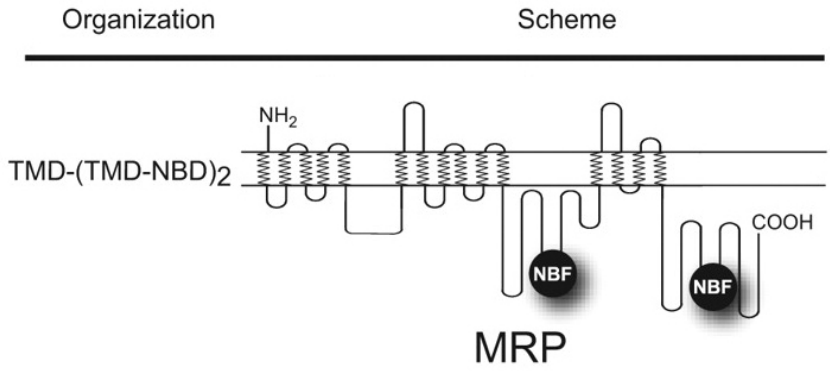

Figure I.7. : Organisation of a typical MRP-type ABC transporter with a first TMD and then alterned TMDs and NBDs (NBDs = NBFs : nucleotide binding folds). (taken from Jasinsky et al., 2003)

Animals have a very similar way to detoxify xenobiotics when compared to plants, including an activation phase, a conjugation phase and a transport phase, with the notable difference that the conjugated toxic compounds are secreted in animal cells, instead of being sequestrated into the vacuole. Studies in mammalian systems as well as with the Saccharomyces cerevisiae MRP-type pump YCF1 (yeast cadmium factor protein 1) demonstrated that the substrate spectrum of eukaryotic MRPs ranges from glutathionated, glucuronidated, sulphated compounds, which generally represent organic anions, to unchanged molecules which may be co-translocated together with reduced glutathione (König et al., 1999 ; Jungwirth and Kuchler, 2006 ; Cole and Deelay, 2006). Thus, by analogy, it as been hypothesized that plants transport glutathione conjugates inside the vacuole also through

MRPs. A first clue supporting this hypothesis was found in barley : barley vacuoles exhibited ATP-dependent transport of various glutathione conjugates (Martinoia et al., 1993). The hypothesis was further supported when the first three *Arabidopsis thaliana* MRP-type ABC transporters cloned and expressed in yeast, named AtMRP1, AtMRP2 and AtMRP3, exhibited ATP-dependent transport of glutathione conjugates (Lu et al., 1997, 1998 ; Tommasini et al., 1998). Furthermore, the expression of one of these three *Arabidopsis thaliana* MRPs, *AtMRP3*, was increased by xenobiotic treatment (Tommasini et al., 1997). Thus, AtMRP3, in contrast to AtMRP1 and 2, exhibited both increase of expression under xenobiotic stress and transport activity of conjugated xenobiotics.

I.3.3. *Arabidopsis thaliana* MRPs

Based on homology and expression data, 15 genes coding for MRPs have been identified in the *Arabidopsis thaliana* genome and designated *AtMRP1* to *AtMRP15*. It is suspected that *AtMRP15* represents a pseudogene (Kolukisaoglu et al., 2002). *Arabidopsis* MRPs genes were first discovered by homology comparison to already known MRPs in man and yeast which resulted in cloning and initial transport characterisation of AtMRP1 to 5 (Lu et al. 1997, 1998 ; Tommasini et al., 1997, 1998 ; Sánchez-Fernández et al., 1998 ; Gaedeke et al. 2001). Expression analysis by RT-PCR revealed that the *Arabidopsis MRPs* 1 to 14 are expressed, at different levels, in all organs of the plant. Phylogenetic analysis demonstrates that *AtMRP* genes are generally divided in two clades, with the exception of *AtMRP13*, which is significantly different from all other *AtMRPs* (Kolukisaoglu et al., 2002).

For some *Arabidopsis* MRPs, transport activity with typical MRP-type substrates such as glutathione conjugates or estradiol-glucoronide has been demonstrated after heterologous expression in yeasts lacking the major yeast *MRP* genes and the localisation or function is known for some of them. Present evidence suggests that AtMRP1 and AtMRP2 are able to transport glutathione conjugates when expressed in yeast, while *AtMRP2* has also the ability to transport chlorophyll catabolites (Lu et al., 1997 ; Lu et al. 1998). In fact, AtMRP2 has finally been demonstrated to play a role in chlorophyll degradation *in vivo* (Frelet et al., submitted). AtMRP4 and AtMRP5 have functions in stomatal regulation : mutant plants lacking AtMRP4 are more susceptible to drought due to an increased stomatal opening, in contrast, mutants lacking AtMRP5 are more resistant to drought because of a smaller stomatal aperture in the light. The properties of AtMRP5, which localizes to the plasma membrane, have been linked to ion channel regulation in guard cells (Gaedeke et al., 2001 ; Klein et al.,

2003 ; Klein et al., 2004 ; Lee et al., 2004 ; Suh et al., 2006). In contrast to AtMRP1 and AtMRP2, AtMRP4 and AtMRP7 have been linked to cadmium detoxification. Both are localized in the plasma membrane of the cells (Klein et al., 2004 ; Plaza et al., 2005).

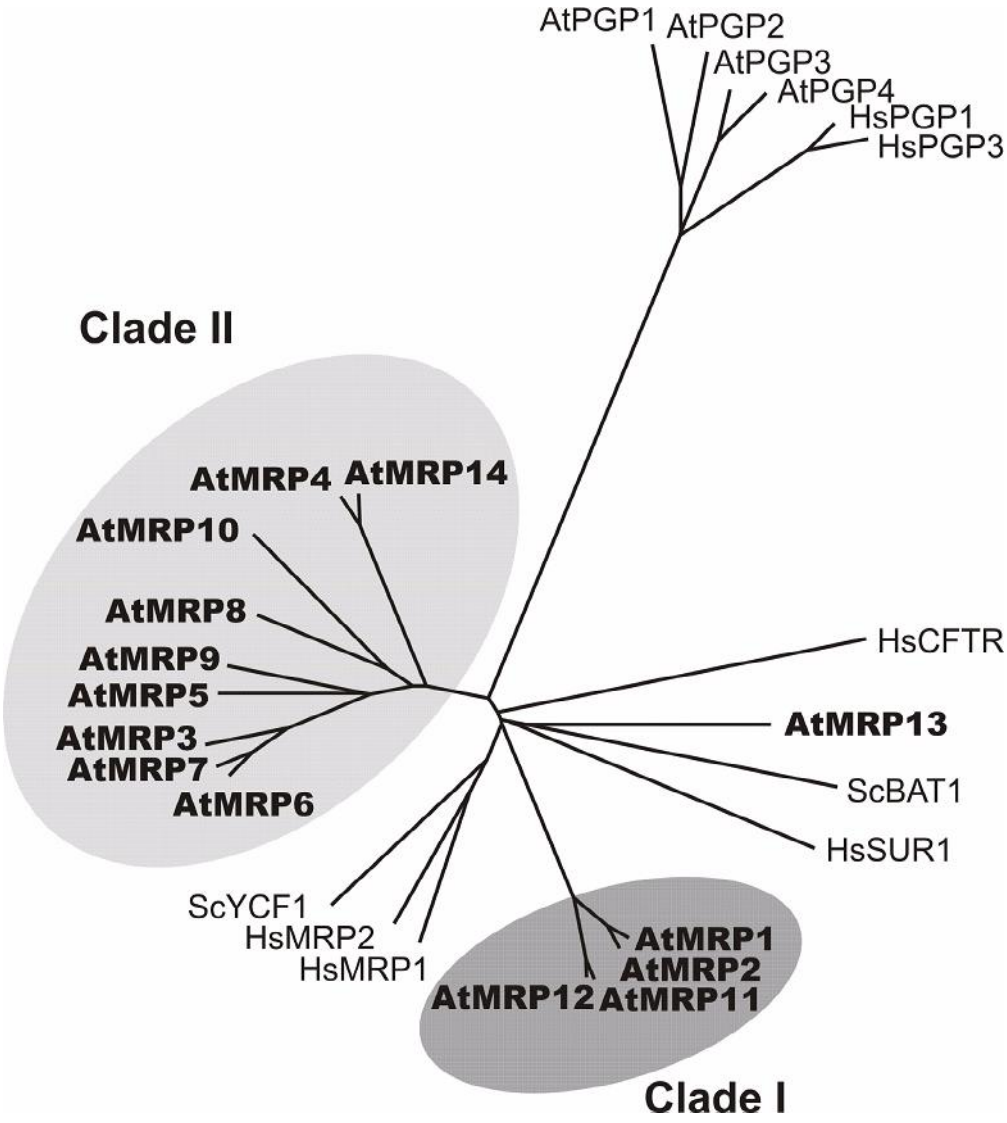

Figure I.8. : Phylogenetic tree of the *Arabidopsis* MRPs and of some other *Arabidopsis,* human and yeast ABC transporters. Abbreviations : At, *Arabidopsis thaliana* ; Hs, *Homo sapiens* ; Sc, *Saccharomyces cerevisiae* ; BAT, bile acid transporter ; CFTR, cystic fibrosis transmembrane conductance regulator ; MRP, multidrug resistance-associated protein ; PGP, P-glycoprotein ; SUR, sulphonylurea receptor ; YCF, yeast cadmium factor.

(taken from Kolukisaoglu et al., 2002)

I.3.4. AtMRP3

AtMRP3 and AtMRP1 were the first two Arabidopsis MRPs cloned and identified (Lu et al., 1997 ; Tommasini et al. 1998). Clues of the role of AtMRP3 in heavy metal and herbicide detoxification have been found since its discovery : a study on the differential expression under xenobiotic stress of four Arabidopsis expressed sequence tags exhibiting high homology to the yeast cadmium factor 1 (YCF1) transporter from *Saccharomyces cerevisiae* showed than one of them was indeed strongly induced upon primisulfuron (a herbicide structurally related to prosulfuron) and IRL 1803 (a herbicide inhibiting histidine synthesis) treatment of plants (Tommasini et al., 1997).

Later, the full-length cDNA of this gene was cloned and the gene was named *AtMRP3*. Expression of this protein in a mutant yeast strain lacking the YCF1 ABC transporter (Δycf1 strain) showed that it exhibited glutathion-S-conjugate transport activity, as well as chlorophyll catabolite transport activity. Perhaps the most interesting feature of this gene was that it partially restored cadmium resistance in the cadmium-sensitive Δycf1 yeast mutant (Tommasini et al., 1998). YCF1 is an ABC transporter present in *Saccharomyces cerevisiae*, one of the first studied ABC transporters in terms of transport. It was originally discovered by screening a yeast genomic library for the ability of DNA fragments to confer resistance to cadmium (Szczypka et al., 1994). YCF1 has been demonstrated to catalyse the transport of organic conjugates of glutathione and also the transport of cadmium-glutathione conjugates, in the form of bis(glutathionato)cadmium, into the vacuole of *S. cerevisiae* (Tommasini et al., 1996 ; Li et al., 1996 ; Li et al. 1997). In fact, the yeast strain Δycf1, which is deleted in the *YCF1* gene and is defective in GSH-dependent cadmium transport, is hypersensitive to cadmium. Complementation of the hypersensitivity phenotype of this mutant strain by expression of the gene of interest has been used in several studies as evidence for the ability of transporter coded by the gene to transport cadmium. These results were not only a strong indication of the role of AtMRP3 as a detoxifier of cadmium but also supported the hypothesis of AtMRP3 playing the same role in plants as YCF1 in yeast since AtMRP3 “replaced” a protein mediating vacuolar transport of cadmium-glutathione complexes. Thus AtMRP3 has been considered to act as a vacuolar importer of cadmium complexes.

More recent studies have demonstrated that *AtMRP3* expression is sharply inducible and regulated by cadmium (Bovet et al., 2003 ; Bovet et al., 2004) and under various herbicide treatments (prosulfuron, primisulfuron) (Glombitza et al., 2004). The presence of cadmium in

the culture medium enhanced expression of *AtMRP3* in the roots of adult plants and in the roots and leaves of seedlings. Enhanced expression of *AtMRP3* in the leaves of adult plants was also observed when, after removal of the roots, the leaves were directly fed with a medium containing cadmium. When green parts of adult plants were sprayed with a solution containing prosulfuron or primisulfuron, expression of *AtMRP3* in the leaves was enhanced as well.

I.4.1. Application aspects : phytoremediation, "safe food" and gene regulation strategies by manipulation of heavy metal transporters

As outlined above, AtMRP3 is a potential heavy metal transport protein. Consequently, it can be expected that manipulation of AtMRP3 activity changes the capacity to transport cadmium in the plant, depending on its expression and subcellular localization. In general, the understanding of plant mechanisms of heavy metal resistance in plants could lead to various applications. *Phytoremediation* is one of them. Soil pollution by heavy metals is an important concern and decontamination of the contaminated soils by phytoremediation as been explored as a cost effective solution for this problem (McGrath and Zhao, 2003). Decontamination of soils by phytoremediation makes use of plants to remove the toxic ions from the soil : the plants absorb the pollutant through their root, accumulate it in the aerial parts which can be harvested easily. Their content in heavy metals is thus removed from the ecosystem. Evidently, the effectiveness of this method depends on the quantity of heavy metals accumulated in the aerial parts, which has to be maximized. Two factors increase this quantity: high concentrations of heavy metals in the aerial parts and high biomass of the aerial parts. Hyperaccumulator plants could be interesting species to use in phytoremediation due their very high heavy metal content in aerial parts. However all known hyperaccumulator plants have a low biomass. To solve this problem, it has been proposed to engineer a plant producing high biomass with an enhanced capacity to accumulate heavy metals (Clemens et al., 2002). With a better understanding of the mechanisms underlying heavy metal translocation and accumulation, these properties could be transferred in the chosen high biomass plant to produce a transgenic high biomass hyperaccumulator. Modification of the heavy metal accumulation mechanisms could be altered at each level of ion transport in plants: (i) an increased heavy metal uptake from soil across the plasma membrane of the root epidermis should improve heavy metal xylem loading at the root level, (ii) maximizing heavy metal unloading from the xylem in the leaves and (iii) increasing heavy metal sequestration in

organelles (especially the vacuole) should lead to higher root-to-shoot translocation. Each of these transformations could lead to increased heavy metal accumulation in the transgenic plants. For example, overexpression of the vacuolar transporter YCF1 in *Arabidopsis* has already been demonstrated to produce plants exhibiting enhanced cadmium resistance and accumulation (Song et al., 2003). To increase heavy metal accumulation, the secretion of heavy metals into the rizosphere could be decreased. If AtMRP3 is indeed a heavy metal transporter *in planta*, one would hypothesize that its overexpression would lead to enhanced heavy metal accumulation, by increasing the transport at one of the steps of the heavy metals accumulation process. Or, if AtMRP3 functions in some kind of heavy metal exclusion mechanism (for example at the root epidermis level), knocking out the *AtMRP3* gene could lead to increased heavy metal accumulation.

Another potentially interesting application based on the knowledge of the mechanisms of heavy metal accumulation could be the engineering of crop plants with reduced contents of heavy metals ("safe food"). Heavy metals are deleterious to humans and one source of heavy metal penetration in the human body is through food, and thus through consumed crops, while another is through cigarette smoke, since heavy metals are accumulated in tobacco leaves. By reducing heavy metals accumulation in crops, we could theoretically produce healthier food and cigarettes. To reduce the accumulation of heavy metals in crops, the mechanisms of heavy metal accumulation could be modified at the same levels as for the engineering of hyperaccumulator plants, but the mechanisms could be manipulated into another direction when compared to hyperaccumulation : the transport steps should be decreased, including uptake from soil, loading into the xylem, unloading from the xylem or sequestration in the organelles. Alternatively, heavy metal exclusion mechanisms could be enhanced.

The understanding of the mechanisms leading to the enhanced transcription of some proteins, like AtMRP3, under xenobiotic stress could also have a practical interest. If DNA motives responsible for the specific activation of *AtMRP3* under a given stress (e.g. heavy metal contaminated soil) were unequivocally discovered, these motives could be used to construct transgenic reporter plants indicating the presence of the stress factor. In other words, heavy metal-stress-responsive DNA elements fused to a reporter gene could be used as indicators of heavy metal pollution in the soil after stable transformation into a suitable plant . A possible non-invasive reporter is the Arabidopsis *PAP1* gene encoding a R2R3-type Myb-type transcription factor which if overexpressed leads to massive anthocyanin accumulation and therefore red pigmented plants (Borevitz et al., 2000). One could think of more subtle applications also : in our previous examples of plants engineered for enhanced or reduced

heavy metal accumulation, one could imagine that the genes introduced to modify the accumulation of heavy metals would expressed under the control of these specific motives. Thus, expression of transgenes would appear only if the stress factor is present and the transgene would be expressed specifically in a stress-inducible manner. Similar applications can be discussed for plants engineered for herbicide resistance. If resistance genes are only activated when the plants are treated with herbicides, this activation of the introduced genes only on specific circumstances would probably lead to plants that do not need to permanently invest energy for the maintenance of the resistance mechanisms.

I.4.2. Aims of the present study

The present study aims at understanding the role of *AtMRP3 in planta*. Given the past observations of induction of *AtMRP3* under xenobiotic stress conditions and of its transport activities in yeast, the study will first try to prove or disprove the implication of AtMRP3 in resistance to xenobiotics *in planta*, focusing mainly on two toxic model compounds : cadmium and prosulfuron.

In the first place, knockout mutants in the *AtMRP3* gene are isolated and a genotype linked to xenobiotic stress is investigated

In order to make a sound hypothesis about the role of AtMRP3, the tissue-specific expression of *AtMRP3* and the subcellular localisation of the protein are analysed by molecular methods.

Using atmrp3 knockout mutants experiments are carried out to verify if the transport activities mediated by AtMRP3 as observed in yeast are also of significance *in planta*. To this end, the transport activities of protoplasts and vacuoles of wild type plants and knockout mutants will be compared.

Finally, the mechanism by which stress factors induce the transcription of *AtMRP3* is analysed using molecular methods. Since in preliminary studies using stable transformation into tobacco and *Arabidopsis* of a reporter gene construct under the control of the sole *AtMRP3* promoter resulted in only very low GUS activity induction by cadmium exposure (Klein and Martinoia, unpublished), it is investigated if the promoter region of the *AtMRP3* gene is sufficient to induce enhanced transcription under xenobiotic stress conditions or if the terminator region of the gene is also necessary.

II. Material and methods

II.1.1. Chemicals and material for molecular biology

Unless otherwise stated, all chemicals were from Sigma (Buchs, Switzerland). MS medium (Murashige and Skoog, 1962) was obtained from Duchefa (Harlem, The Netherlands ; M0233). Phytoagar was from Gibco (New York, USA). Pectolyase Y-23 and cellulase Y-C were from Kyowa Chemical Products (Japan). Radioactive cadmium – $^{109}Cd^{2+}$ – , tritiated water – $^{3}H_20$ – and radioactive glycerol – [U-^{14}C]glycerol – were from GE Healthcare (Otelfingen, Switzerland ; CUS1, CFB174, TRS3). Radiolabelled glutathione – [*glycine*-2-^{3}H]glutathione – was from ANAWA (Wangen, Switzerland ; ART-1180). The scintillation liquid used for the quantification of radioactivity with the scintillation counter was from Perkin Elmer (Schwerzenbach, Switzerland ; "Ultima Gold" 6013329). Prosulfuron was a kind gift of Dr. Klaus Kreuz, BASF AG, Ludwigshafen, Germany. Watery solutions and media containing prosulfuron were prepared by dilution of a 1 mM prosulfuron stock solution in methanol.

Enzymes and kits used for molecular biology were supplied by New England Biolabs (Allschwil, Switzerland) – restriction enzymes, ligases, NEBlot kit – ; Roche (Mannheim, Germany) – Expand polymerase – ; Promega (Wallisellen, Switzerland) – Pfu polymerase, pGEM-T easy, dNTPs, RQ1 DNAse, pSP-luc+ fusion Vector, MLV reverse transcriptase RNAse H minus point mutant – ; Invitrogen (Basel, Switzerland) – One-Step RT-PCR System with Platinum Taq DNA Polymerase – ; Qiagen (Hombrechtikon, Switzerland) – miniprep kits, DNA purification kits – ; AppliChem (Darmstadt, Germany) – spermidine – ; Serva (Wallisellen, Switzerland) – salmon sperm ; Merck (Dietikon, Switzerland) – lysozyme – ; Sigma (Buchs, Switzerland) – protease inhibitor cocktail. Unless otherwise stated, PCRs were carried out using a "home made" Taq polymerase.

II.1.2. Bacterial strains

The strains of *E. coli* used for cloning were XLI-blue, DH10b and DH5α from Stratagene (Amsterdam, The Netherlands) ; the strain of *Agrobacterium tumefasciens* used for plant transformation was GV3101/pMP90 (Koncz and Schell, 1986).

II.1.3. Growth of plants

Unless otherwise stated, plants were grown in pots in standard soil (ED 73+ Bims Einheitserde, Germany). For all experiments plants were grown in a 8/16-hour light/dark cycle, with a temperature of 22°C in the light period and of 21°C during the dark period, with a relative humidity of 70% and a light density of 200 µmol $m^{-2}s^{-1}$ PAR. For seed production and for some experiments indicated in Results, plants were grown in a 16/8-hour light/dark cycle, with a temperature of 22°C in the light period and of 21°C in the dark period, with a relative humidity of 70% and a light density of 200 µmol $m^{-2}s^{-1}$ PAR. Plants were watered twice a week.

Unless otherwise stated, sterile-grown seedlings were grown on plates in a 16/8-hour light/dark cycle at 24°C with a relative humidity of 70% and a light density of 200 µmol $m^{-2}s^{-1}$ PAR.. As indicated in the next paragraphs, sterile-grown seedlings were grown in a 8/16-hour light/dark cycle, with a temperature of 22°C in the light period and of 21°C in the dark period, with a relative humidity of 70% and a light density of 200 µmol $m^{-2}s^{-1}$ PAR in certain experiments. Unless otherwise stated, the medium used on plates was MS medium with 0.8% (w/v) phytoagar.

Seeds deposited on plates were surface sterilized using the following procedure : seeds were placed in a dessicator jar, in open plastic micro test tubes. In addition with a beaker containing 100 ml of 2% (w/v) NaClO was placed ; 3 ml of 37% (v/v) HCl was added to the hypochlorite solution which resulted in Cl_2 production and the jar was immediately sealed. The seeds were exposed to the Cl_2 vapor for 4 to 5 hours before being removed from the jar under a sterile bench. Sterile water was added to the seeds and the micro test tubes closed. In order to synchronize germination, seeds were then incubated at least for 18 hours at 4°C, in sterile water, before being deposited on plates.

II.2.1. Selection of *AtMRP3* knockout mutants generated by insertional mutagenesis

The *mrp3-1* mutant allele was obtained from the Syngenta SAIL collection. Syngenta SAIL collection was generated by large scale insertional mutagenesis and the position of the insertions was determined by sequencing of thermal asymetric interlaced PCR products obtained with a primer specific for the left border of the T-DNA (Sessions et al., 2002). In our case, the SAIL_351_B06 mutant was found by sequence comparison of the *AtMRP3* genomic

sequence with the SAIL database using the integrated BLAST tool.. Seeds of the T2 generation were germinated on ½ MS plates containing 1% (w/v) sucrose and the herbicide BASTA (glufosinate ammonium ; 25 mg/l). After two weeks, six resistant seedlings were transferred to soil pots and grown in 8 hours of light. Four additional weeks later, one leaf per plant was taken for DNA extraction and PCR analysis of the genotype. The *mrp3-2* mutant allele was obtained from the Cold Spring Harbour collection and was a gene trap transposon mutant (Martienssen, 1998). The mutant with the identifier GT10839 was found by searching the SIGnAL "T-DNA Express" Arabidopsis Gene Mapping Tool with the AGI Code At3g13080 (signal.salk.edu/cgi-bin/tdnaexpress). Seeds of the F3 generation were grown on ½ MS plates containing 1% (w/v) sucrose and kanamycin (50 mg/l), in 8 hours light conditions. All subsequent steps were performed as detailed above for the *mrp3-1* allele but twelve kanamycin-resitant seedlings transferred.

The *mrp3-3* mutant allele was obtained from the Arabidopsis Knockout Facility of the University of Wisconsin. Thus *Arabidopsis* mutant population was generated by large scale insertional mutagenesis (Krysan et al., 1996, 1999 ; Sussman et al., 2000). As for the *mrp3-2* allele, the mutant WiscDsLox481-484C11 was found by mining the SIGnAL "T-DNA Express" Arabidopsis Gene Mapping Tool. Seeds of the T2 generation were germinated on a ½ MS plate containing 1% (w/v) sucrose and BASTA (25 mg/l). Since only two seedlings were BASTA resistant, they were continued for seed production. T3 seeds of the two individual T2 lines were again selected on BASTA-containing MS plates. Twelve resistant seedlings were transferred into soil and leaf material was collected for DNA isolation and PCR genotyping.

II.2.2. DNA extraction, PCR and DNA gel blot analysis of *atmrp3* knockout mutants

Genomic DNA was extracted as described by Fulton et al. (1995). PCRs were performed on each leaf sample sample to ensure presence, orientation and position of the insertion in the *AtMRP3* gene in each mutant allele, and to analyse the genotype of each individual. Each mutant allele was analysed with the different primer combinations as listed below. The primers were either specific for the *AtMRP3* gene or for the T-DNA and transposon used for insertional mutagenesis (see Table II.1. for the sequences) :

- *mrp3-1* allele : LMRP3A_s/LMRP3A_as ; LMRP3A_s/LB2 ; LMRP3A_as/QRB3 ; LMRP3A_s/QRB3 ; LRMP3A_as/LB2 ; 3Cn-s/3Cn-as ; AtMRP3-s/AtMRP3-as.

- *mrp3-2* allele : 3-2ver-up/3-2ver-low ; 3-2ver-up/Ds5-4 ; 3-2ver-low/Ds3-4 ; 3-2ver-up/Ds3-4 ; 3-2ver-low/Ds5-4.
- *mrp3-3* allele : 3-2ver-up/3-2ver-low ; 3-2ver-up/p745 ; 3-2ver-low/p745.

The following PCR temperature cycling program was used : 10 min at 95°C ; 36 cycles of 1 min at 95°C / 1 min at 58°C / 2 min 30 sec at 72°C ; 5 min at 72°C. In case of the following primer combinations, the cycling programme was slightly modified: 3-2ver-up/3-2ver-low ; 3-2ver-up/p745 and 3-2ver-low/p745 : 10 min at 95°C ; 36 cycles of 1 min at 95°C, 1 min at 57°C and 2 min 30 sec at 72°C ; 5 min at 72°C .

Amplified PCR products allowing the determination of the position of the T-DNA or transposon were cloned into the pGEM-T easy vector following the manufacturers instructions. Plasmids containing the corresponding PCR products as verified by restriction and PCR analysis were subsequently sequenced with SP6 and T7 oligonucleotides (see Table II.1.)

The genomic DNA extracted from the *mrp3-1* leafs samples was analysed by DNA gel blotting. The DNA samples were digested with the PstI restriction enzyme, loaded on an agarose gel together with the controls (genomic DNA from Col-0 digested with PstI ; unlabelled samples of the hybridation probes, see further) and separated by gel electrophoresis. The resolved DNA was then transferred to a nylon membrane using the following procedure : first, the agarose gel was incubated 30 minutes in transfer solution (0.4 M NaOH, 0.6 NaCl). Then several layers of blotting paper soaked in transfer solution were stacked in a dish partially filled with this same solution and the agarose gel was deposited on top of these soaked papers and a nylon membrane and then a layer of blotting paper, both soaked in transfer solution, were deposited on top of the gel. Several layers of dry blotting paper were deposited over this setting, toghether with a weight on top of all. Finally, the setting was left overnight and the DNA blotted to the nylon membrane, driven by the transfer solution migrating by capillarity from the dish to the dry papers. The membrane was rinsed with solution A (0.3 M NaCl, 20 mM NaH_2PO_4, 2.5 mM EDTA/NaOH pH 7.4) and incubated 2 hours at 80°C to fix the DNA to it. The membrane was hybridized with two different radiollabeled DNA probes : a probe specific for the pCSA110 T-DNA – the GUS probe – and a probe specific for the *AtMRP3* gene – the 3C probe. The GUS probe was a fragment of the vector pCambia 1305.1 (http://www.cambia.org/daisy/cambia/585.html) obtained by digestion with the restriction enzymes SpeI and NheI. The 3C probe was synthetized by PCR using the *AtMRP3* cDNA present in the pNEV yeast vector (Tomassini et al., 1998) as template and the pair of primers 3C-s/3C-as (see Table II.1.). The following PCR temperature

cycling program was used : 2 min at 95°C ; 36 cycles of 1 min at 95°C / 1 min at 58°C / 2 min 30 sec at 72°C ; 5 min at 72°C. Each DNA probe was radiolabelled with ^{32}P-dCTP using the NEBlot kit following the manufacturers instructions and then purified with a DNA purification kit. Between each hybridization , the membrane was washed 1 hour at 95°C with a solution of 0.5% (v/v) SDS. Hybridizations were carried out using the following procedure : the nylon membrane was incubated for 2 hours at 65°C in hybridisation solution (1 g/l Ficoll, 1 g/l PVP K 30, 1 g/l BSA, 0.75 NaCl, 50 mM NaH_2PO_4, 6.25 mM EDTA/NaOH pH 7.4, 0.4% (v/v) SDS) containing 0.2 mg/ml of salmon sperm DNA (previously denatured by 5 minutes of incubation at 95°C). Then the membrane was gently shaken overnight at 65°C in hybridization solution containing 1.25 ng/ml of the purified probe and 0.3 mg/ml of salmon sperm DNA (both previously denatured by 5 minutes of incubation at 95 °C). Finally the membrane was washed twice for 5 minutes at 65°C in solution A containing 0.1% (v/v) SDS with gentle shaking. After each hybridization, the membrane was exposed to a Biomax MS Kodak film, for autoradiographic detection of the bands.

II.2.3. Segregation analysis of the *mrp3-1* and *mrp3-2* mutant alleles

T3 seeds of each single BASTA-resistant *mrp3-1* plant were individually harvested. Around 500 T3 seeds of each line were germinated on ½ MS / 1% (w/v) sucrose plates containing BASTA . After two weeks, sensitive and resistant seedlings were counted. A 3:1 ratio of resistant and sensitive seedlings was interpreted as a single insertion in the hemizygous state. Consequently, 100% resistant seedlings were scored as putative homozygous T3 lines. Results were compared with the PCR analysis of the genotype to verify cosegregation between resistance and insertional mutagen. For the *mrp3-2* allele, seeds were germinated on kanamycin-containing MS plates.

All following experiments using the insertional mutants were performed with homozygous lines based on genotype and resistance assays.

II.2.4. Analysis of *AtMRP3* transcription in the knockout mutant alleles by reverse transcription-PCR

RNA was extracted from rosette leaves of homozygous plants of the three different mutant alleles using the following procedure : first, leaves were ground in liquid nitrogen and 1 ml of solution A (aqueous solution containing 0.8 M guanidium thiocyanat, 0.4 M ammonium

thiocyanat, 0.1 M sodium acetat/acetic acid pH 5.0, 5% (v/v) glycerol, 38% (v/v) phenol) was added per 100 mg of plant tissue. This mix was homogenized during 1 minute by vortexing at room temperature and then incubated 5 additional minutes at room temperature. $CHCl_3$ was added to the samples, at a volume of 0.2 ml per ml of solution A used and then the samples were vigorously shaken for 15 seconds and incubated for 3 minutes at room temperature. The tubes containing the samples were centrifuged 15 minutes at 12000 g, at 4°C. The upper phases of the resulting separation, containing the RNAs, were transferred into new tubes. Isopropyl alcohol was added to each tube, at a volume of 0.5 ml per 1 ml of solution A used. The tubes were incubated 10 minutes at room temperature and then centrifuged 10 minutes at 12000 g, at 4 °C, to precipitate RNAs. The supernatants were removed from each tube and the pellets containing the RNAs were washed with 75% (v/v) ethanol. The tubes were centrifuged 5 minutes at 12000 g, at 4 °C, and the supernatants discarded. Finally the pellets were dried in a low vacuum system and dissolved in RNAse free water.

About 1 µg sample of extracted RNAs was treated with RQ1 DNAse for 25 minutes at 37 °C followed by addition of stop buffer (20 mM EGTA pH 8.0, supplied by the manufacturer) and incubation for 10 min at 65°C to inactivate the DNAse. Subsequently, first-strand cDNA synthesis was performed by addition of the M-MLV RNAse H minus, point mutant reverse transcriptase, following the protocol of the manufacturer in the presence of oligo-dT. Finally, gene-specific DNA fragments were obtained by PCR amplification using these first-strand cDNAs and two primer combinations (see Table II.1. for the sequences) : AtMRP3-s/AtMRP3-as (primers specific for the *AtMRP3* gene) and S16-s/S16-as (constitutive control: primers specific for the At5g18380 mRNA coding a 40S ribosomal protein). In pilot experiments it was found that good amplification results were observed if undiluted cDNAs were used for the amplification of a fragment of the *AtMRP3* cDNA while amplification of the constitutive control with the S16-s/S16-as primer pair were performed with cDNA templates that were diluted 1:10 with water. PCRs were performed using the Expand Polymerase and the following cycling program : 2 min at 94°C ; 10 cycles of 15 sec at 94°C / 30 sec at 57°C / 45 sec at 72°C ; 25 cycles of 15 sec at 94°C / 30 sec at 57°C / 45 sec + 5 sec per cycle at 72°C ; 7 min at 72 °C.

Furthermore, one-step reverse transcription-PCR was performed starting from total leaf RNA using the SuperScript One-Step RT-PCR System containing Platinum Taq DNA Polymerase, following the protocol of the manufacturer. Each reaction contained about 1 µg of total RNA. Primers used for amplification of the cDNA fragment of *AtMRP3* were 3-1ver-up/LMRP3A_as (see Table II.1 for the sequences, primers specific for the *AtMRP3* gene).

PCR cycling program : 30 min at 60°C ; 2 min at 94 °C; 40 cycles of 15 sec at 94°C / 30 sec at 60°C / 1 min at 68°C ; 5 min at 68°C.

II.3.1. Growth of plants under xenobiotic stress, preliminary experiments

In the case of direct exposure of seeds to the toxic compound, Columbia 0 (Col-0) and homozygous *mrp3-1* mutant seeds were grown with a photoperiod of 16 hours on sterile ½ MS plates under various stress conditions. Cd^{2+} was added as $CdCl_2$ prepared from a 5 mM stock solution in water. Prosulfuron was added from a 5 µM stock solution in water (watery stock solution was prepared from a 1 mM prosulfuron stock solution in methanol, resulting in a maximal methanol content of 0.001% (v/v) in the plates). Depending on the experimental setup, plates contained no, 0.5 or 1% (w/v) sucrose and 10 to 60 µM CdCl2 or 0.1 to 10 nM primisulfuron. Control plates contained ½ MS and the corresponding concentration of sucrose. In separate experiments, seedlings were transferred from control to stress exposure conditions after germination. In this case, seeds of stratified Col-0 and *mrp3-1* mutants were germinated on ½ MS medium with 1% (w/v) sucrose for three or four days as indicated in Results followed by transfer of visually identical seedlings to ½ MS / 1% (w/v) sucrose medium containing either no xenobiotic, up to 60 µM $CdCl_2$ or 8 nM prosulfuron, respectively. In separate experiments, the sucrose concentration was reduced to 0.5% (w/v).
In all cases, gowth of the seedlings was monitored for up to 17 days.

II.3.2. Xenobiotic stress exposure (main experiments) and chlorophyll determination

Col-0 , Landsberg erecta (Ler-0) plants and mrp3-1, mrp3-2, mrp3-3 homozygous mutants were grown on plates on ½ MS medium containing 0.5% (w/v) sucrose in the absence or presence of 45 µM $CdCl_2$ or 4 nM prosulfuron for 10 days. Subsequently, the aerial parts of individual seedlings were harvested and transferred into 80% aceton for chlorophyll determination (each seedling was incubated in 1 ml aceton). The chlorophyll content was spectrophotometrically measured in these extracts obtained after incubation at room temperature in the dark using the quantification formulas described by Lichtenthaler and Wellburn (1983) . Total chlorophyll represented the sum of the measured quantities of chlorphyll a and b.

Number of plants analysed : 99 Col-0 with no xenobiotic, 108 *mrp3*-1 with no xenobiotic, 101 *mrp3-3* with no xenobiotic, 102 Col-0 with 45 µM Cd^{2+}, 98 *mrp3-1* with 45 µM Cd^{2+}, 101 *mrp3-3* with 45 µM Cd^{2+}, 92 Col-0 with 4 nM prosulfuron, 90 *mrp3-1* with 4 nM prosulfuron, 91 *mrp3-3* with 4 nM prosulfuron, 35 Ler-0 with no xenobiotic, 44 *mrp3-2* with no xenobiotic, 41 *Lansberg erecta* with 45 µM Cd^{2+}, 43 *mrp3-2* with 45 µM Cd^{2+}, 39 *Lansberg erecta* with 4 nM prosulfuron, 42 *mrp3-2* with 4 nM prosulfuron.

II.4.1. Short term accumulation of cadmium in seedlings, phosphor-imaging and quantification by liquid scintillation counting

Col-0 and *mrp3-1* mutants were germinated on ½ MS / 1% (w/v) sucrose plates in the light (16h/d). After 6 days, seedlings were transferred on new ½ MS / 1% (w/v) sucrose plates. Care was taken to align all roots in a vertical direction. One day later, a ∅ 6 mm glassfiber disc (glass microfiber filters, Whatman, Bottmingen, Switzerland ; 1822 024) was deposited at the root tip of each seedling which was wetted before with 10 µl of an aqueous solution containing ⅛ MS, 1 mM $CaCl_2$, 10 µM $CdCl_2$ and radiolabelled with $^{109}CdCl_2$ ($3.7x10^7$ Bq/µmol). Two hours later, the discs were removed and the plates were positioned vertically After 2, 8 or 24h , seedlings were removed and carefully deposited between two layers of saran wrap paper. For the detection of the spatial distribution of the radioactive cadmium, wrapped seedlings were exposed overnight to storage phosphor screens followed by scanning of the screens with the "Cyclone Plus Storage Phosphor System" (Perkin Elmer, Schwerzenbach, Switzerland ; C431200) Subsequently, the saran wrap was removed and each seedlings was cut into aerial part (leaves and hypocotyls) and the root. The root was further separated into the upper root segment (1 cm from the root-shoot interphase) and the remaining root tip segment. The radioactivity of each segment was measured, after addition of 2 ml of the Ultima Gold scintillation liquid, by liquid scintillation counting. Counting was performed with a "Tri-Carb 2900TR Liquid Scintillation Analyzer" (Perkin Elmer, Schwerzenbach, Switzerland ; A290000). All values were corrected for quenching.

II.4.2. Long term accumulation of cadmium, preliminary experiment

Col-0 plants and *mrp3-1* mutants were first germinated on ½ MS / 1% (w/v) sucrose plates for 13 days with an 8 hours photoperiod. Then, they were cultured hydroponically in ½ MAMI

medium (½ MAMI medium : 0.73 mM KH_2PO_4, 0.38 mM $MgSO_4$, 168 µM $Ca(NO_3)_2$, 109 µM KNO_3, 8.75 mg/l Sequestren rapid (Syngenta Agro, Dielsdorf, Switzerland) 123 nM $MnCl_2$, 617 nM H_3BO_3, 21.3 nM $ZnSO_4$, 13.8 nM $CuSO_4$, 25.8 nM $NaMoO_4$, 6.4 nM $Ni(NO_3)_2$), (8 hours photoperiod). During the following eleven days of hydroponic culture, the plants were covered with a transparent plastic bag to avoid desiccation of the seedlings. Four days after transfer an aquarium pump was added to supply roots with oxygen. On day 19 of hydroponic culture, the medium was exchanged and either new ½ MAMI medium or ½ MAMI medium containing 1 µM $CdCl_2$ was added After one or two additional weeks of growth in the new medium, the aerial parts of the plants were harvested. 6 plants of each line which were cultivated in the same conditions were pooled together, in order to have enough material for the subsequent inductively coupled plasma-mass spectrometry (ICP-MS) analysis. Pooled plants were dried in an oven at 60°C and ground with mortar and pestle. All samples were digested and analysed by ICP-MS as described by Bovet et al. (2006).

II.4.3. Long term accumulation of cadmium, main experiments

Seedlings of Col-0, *mrp3-1* and *mrp3-3* mutants were first germinated on ½ MS / 1% (w/v) sucrose plates for one week, in a photoperiod of 8 hours. Then, they were cultured hydroponically in ⅓ MS medium, (8 hours of light). As in the preliminary experiment, during the following eleven days of hydroponic culture the plants were covered with a transparent plastic bag and four days after transfer an aquarium pump was added. On day 18 of hydroponic culture, the medium was exchanged for ½ MS medium, to provide more nutrients to the plants. Plants were grown 15 additional days and then, on day 33 of hydroponic culture, the medium was exchanged again : depending on the condition, either ½ MS, ½ MS containing 0.5 µM $CdCl_2$, ½ MS containing 1 µM $CdCl_2$ or ½ MS containing 2 µM $CdCl_2$ was added. After one additional week of growth in the new medium, the aerial parts of the plants were harvested. Groups of 4 or 8 plants of the same line which were cultivated under the same conditions were pooled together and analysed by ICP-MS. Pooled plants were dried and ground. Samples were calcinated by treatment at 550°C for 3 hours. Calcinated samples were dissolved with 1 ml 65% (v/v) HNO_3 and then diluted with H_20 to a total volume of 25 ml. The solution was filtered through a micropore filter (0.2 µM) and analysed with an `Agilent ICP-MS 7500c` (Agilent, Meyrin, Switzerland).

II.5.1. Cadmium transport in mutant and wild-type protoplasts

Col-0 plants and *mrp3-1* mutants were cultivated for 8 weeks on soil (8h light). Mesophyll protoplasts were prepared from each line according to the following protocol. The adaxial epidermial layer of leaves was abraded with emery paper (P 500, Carborundum Abrasives) and these leaves were then transferred to glass Petri dishes, adaxial side down, on medium A (500 mM sorbitol, 10 μM $CaCl_2$, 10 mM methyl ethane sulfonate/KOH pH 5.6) diluted in water (1:1 v/v water/ medium A, 1 mg/ml BSA). The digestion of the leaves was started by replacing the diluted medium with 10 ml of digestion buffer (medium A supplied with 0.03% (w/v) pectolyase Y-23 and 0.75% (w/v) cellulase Y-C). The leaves were incubated in this medium 90 min at 30°C. The digestion buffer was then carefully removed by aspiration and replaced by medium A and the protoplasts were released by gentle agitation. The solution containing the protoplasts suspension was transferred to 50 ml plastic test tubes ; 2 ml of Percoll pH 6 (500 mM sorbitol, 10 μM $CaCl_2$, 20 mM methyl ethane sulfonate pH 6 dissolved in Percoll) was added at the bottom of each plastic tube to form a cushion and the tubes were centrifuged at 200 g, 5 min, at room temperature to sediment mesophyll protoplasts onto the Percoll cushion. The supernatant was removed by aspiration while the protoplast suspension was mixed with the Percoll cusion. Additional Percoll pH 6 100 % was added to arrive at a suspension volume of 7.5 ml and on top of the protoplasts suspension, two layers were added to form a discontinuous gradient. The first (middle) phase of about 15 ml consisted of medium B (25 % (v/v) Percoll pH 6 prepared in medium A). On top, a layer of about 8 ml of medium C (7 % (v/v) Percoll pH 6 in medium A) was added. This gradient was centrifuged at 200 g, 10 min, at 4°C, and the protoplasts were then carefully recovered from the interphase between middle and uppermost phases using a micropipet with a cut plastic tip. The protoplasts were microscopically inspected for intactness.

The recovered protoplasts were subsequently diluted in medium D (500 mM glycine betain, 10 μM $CaCl_2$, 10 mM methyl ethane sulfonate/KOH pH 5.6, 1 mg/ml BSA) by addition of three volumes of medium D per volume of recovered protoplasts. Each isolation of protoplasts (isolation of Col-0 protoplasts and of *mrp3-1* protoplasts) was separated in two batches of equal volume and pipetted into plastic petridishes : one batch was used to measure $^{109}Cd^{2+}$ import while the protoplast volume was determined in the second batch by addition of $^{3}H_2O$. During all transport experiments, protoplast suspensions were exposed to the white light generated by three fluorescent tubes (Sylvania, Germany ; Sylvania standard

F36W/133), and the petridishes were cooled with a ventilator to avoid heating by the light bulbs. Furthermore, petridishes were regularly shaken. At time point 0, $^{109}CdCl_2$ (18.5 Bq per µl of protoplast suspension) and $^{3}H_2O$ (37 Bq per µl) were added to the appropriate batches. After incubation for the time intervals indicated in Results (chapter VI.), five 100 µl-aliquots of protoplast suspension were pipetted on top of a gradient prepared in 0.4 ml polyethylene tubes. The gradient consisted of 30 µl of 50% Percoll in water (bottom phase) and 200 µl of silicon oil (Polyphenyl-methylsiloxane AR200 ; Aldrich, Buchs, Switzerland) (middle phase). Incubation was terminated by centrifugation (15 seconds centrifugation at 10'000 g). During the centrifugation step, protoplasts were separated from their medium and sedimented through thesilicon oil into the bottom Percoll phase. Protoplast-associated radioactivity was determined by cutting off the bottom of each tube containing the protoplasts and transfer of the cut segment into 6 ml polyethylene vials. After addition of 3 ml of the Ultima Gold scintillation liquid, the protoplasts suspension was mixed with the scintillation liquid by vigorous shaking. The radioactivity in each sample was then quantified as described in paragraph II.4.1. In order to calculate the Cd^{2+} amount absorbed per protoplast volume, four samples of 10 µl each were removed from the protoplast suspension batches containing either $^{109}CdCl_2$ or $^{3}H_20$ prior to silicone oil centrifugation and the radioactivity was quantified correspondingly. The amount of Cd^{2+} absorbed per protoplast volume unit in a sample of protoplasts was calculated using the following formulas :

$$\mathbf{m_{Cd\ per\ V\ proto} = radio^{109}Cd\ /\ (specradio_{Cd})(V_{proto})}$$

$$\mathbf{V_{proto} = radio^{3}H_20\ /\ specradio_{3H20}}$$

$\mathbf{m_{Cd\ per\ V\ proto}}$ = pg of Cd^{2+} absorbed per µl of protoplasts
$\mathbf{radio^{109}Cd}$ = protoplast-associated ^{109}Cd radioactivity in a sample
$\mathbf{specradio_{Cd}}$ = specific radioactivity of Cd^{2+} per pg
$\mathbf{V_{proto}}$ = volume of protoplasts in a sample
$\mathbf{radio^{3}H_20}$ = protoplast-associated $^{3}H_20$ radioactivity in a sample
$\mathbf{specradio_{3H20}}$ = specific radioactivity of $^{3}H_20$ per µl of protoplast suspension

$\mathbf{radio^{109}Cd}$ was measured in each sample of protoplasts incubated with $^{109}CdCl_2$; $\mathbf{specradio_{Cd}}$ was determined in the samples of protoplast supsension taken from the batch containing $^{109}CdCl_2$; $\mathbf{radio^{3}H_20}$ was measured in each sample of protoplasts incubated with

$^3H_20$; **Specradio$_{3H20}$** was determined in the samples of protoplast supsension taken from the batch containing $^3H_20$.

The correction for unspecific binding of Cd^{2+} to the protoplasts was done by substracting from each result the amount of Cd^{2+} absorbed by the protoplasts at time point 0, amount calculated by a linear regretion over the early time point results.

II.6.1.Generation of a specific antibody against the *AtMRP3* protein

Raw serum containing the crude antibodies generated against a peptide corresponding to the amino acids 867 to 924 of AtMRP3 fused to a GST protein was supplied by Dr Markus Geisler and Thomas Eggman. They supplied also the plasmid coding for the fusion peptide.

II.6.2. Assay and purification of the *AtMRP3* specific antibody

Raw serum was assayed on diverse protein blots, charged with the AtMRP3-GST fusion protein, with the total extract of soluble proteins of *E. coli* expressing a GST, with the total protein extract of Col-0 leaves or with the two phases of a two phases partitionning of Col-0 leaves.

The AtMRP3-GST fusion protein was recovered as follows : *E. coli* transformed by electroporation with the *AtMRP3-GST* plasmid were grown overnight in 5 ml liquid LB medium containing the appropriate chemical selection, 100 mg/l ampicillin, at 37°C, with shaking. The 5 ml culture was poured in 200 ml of LB medium + ampicillin ; the now bigger culture left to grow 24 additional hours. 800 additional ml of LB medium + ampicillin were then added to the culture ; the subsequent growth was monitored by spectrophotometery. When OD_{600} of the culture attained a value between 0.5 and 1, 1 ml of 0.5 M IPTG was added to the culture, to induce synthesis of the fusion peptide by the transformed bacteria. The growth was then allowed to continue for four additional hours. The bacterial cells where then pelleted by centrifugation the culture at 2500 g for 30 min ; after removal of the supernatant, the pellet was resuspended in 50 ml of solution A (0.1 M NaCl, 0.1 M trishydroxymethylaminomethane/HCl ph 8.0, 50 mM EDTA, 2% (v/v) Triton X-100) and 36 µl of 0.1 M PMSF (in isopropanol) and 10 ml of 10 mg/ml lysozyme were added to the suspension. The suspension was mixed by inverting the tube containing it several times and then incubated 30 min on ice, to lyse the bacteria. The lysate was centrifugated at 12'000 g for 30 min and the supernatant was recovered. This supernatant was a total extract of the soluble

proteins of the bacteria. 2 ml of 50% (v/v) Glutathione Sepharose 4B (GE Healthcare), previously washed and equilibrated in medium A, was added to the soluble protein solution and this suspension was shaken 30 min at 4°C, to allow the *GST* of the fusion peptide to link itself to the glutathione bound to the matrix of the Glutathione Sepharose 4B. The beads of Glutathione Sepharose 4B were pelleted by centrifugation of the mix at 500 for 5 min ; the supernatant was discarded and the beads were washed three times with 20 ml of solution B (136 mM NaCl, 2.7 mM KCl, 10 mM Na_2HPO_4, 1.76 mM KH_2PO_4/KOH pH 7.4). The fusion peptide was eluted from the beads by incubation in 1 ml of solution C (10 mM glutathione, 50 mM trishydroxymethylaminomethane/HCl pH 8.0, 0.1 M NaCl) for 10 min, at room temperature, with shaking. The beads were pelleted by centrifugation and the supernatant, containing the fusion peptide, was recovered.

Total extract of soluble proteins of *E. coli* expressing a GST was obtained as described above, but using a culture of bacteria transformed with an empty pGEX vector (GE Healthcare, Otelfingen, Switzerland) instead of a culture *E. coli* transformed with the *AtMRP3-GST* plasmid.

Total protein extract of leaves was obtained as follows. Leaves of 8 weeks old plants (grown in 8 hours photoperiod) were grinded with small plastic mortars in micro test tubes. For 100 mg of tissue material, 300 µl of cold solution A (0.1 M NaCl, 50 mM trishydroxymethylaminomethane/HCl pH 7.5, 0.5% (v/v) Triton-X100, 10 mM β-mercaptoethanol, 1 mM PMSF) and 1.5 µl of protease inhibitor cocktail were added in the tubes. This mix was vortexed and then centrifugated at 20'000 g, 2 min, at 4°C. The supernatant was transferred into new tubes and for 200 µl of supernatant, 480 µl methanol and 160 µl $CHCl_3$ were added. The tubes were vortexed and centrifugated at 20'000 g, 1 min, at room temperature. The extracted proteins were at this step located at the interphase between the upper methanol-aqueous phase and the lower chlorophorm phase. The upper phase was carefully removed by aspiration and 480 µl of methanol were added. The tubes were vortexed and then centrifugated at 20'000 g, 5 min, at room temperature. All the liquid in the tube (methanol and chlorophorm) was removed and proteins were dryed in in a vacuum pump apparatus. The proteins were finally resuspended in solution B (12 mM trishydroxymethylaminomethane/HCl pH 6.8, 30 mg/ml SDS, 5% (v/v) glycerol, 0.2 mg/ml bromophenol blue, 0.18 M β-mercaptoethanol).

The two phase partionning is a method allowing the extraction of the membranes of plant cells and the separation of the plasma membranes from the other extracted membranes. These

membrane extract contain the correponding membrane proteins. The two phase partionning was carried out as follows (all steps carried out at 4°C) : 4.5 g of leaves of 8 weeks old plants (grown in 8 hours photoperiod) were homogenized in a blender with 30 ml of solution A (250 mM sorbitol, 50 mM trishydroxymethylaminomethane/HCl pH 8.0, 2mM EDTA, 0.6% (w/v) polyvinylpyrrolidone K 30 (Roth, Karlsruhe, Germany), 5 mM DTT, 0.2% (v/v) protease inhibitor cocktail (Sigma, Buchs, Switzerland ; P9599), 1 mM PMSF). This mix was filtered through 6 layers of cheese cloth and the obtained filtrate was then centrifuged at 6700 g for 10 min. The supernatant was recovered and centrifuged at 75'000 g for 45 min. The obtained pellet was recovered : it contained the crude membrane extract. 2 ml of crude membranes were homogeneized with a glass potter with 6 g of phase mixture (100 g of phase mixture were prepared by adding in the following order : 11.3 g of sucrose, 42.7 g of 20% (w/v) dextran 500, 21.3 g of 40% (v/v) PEG, 0.3 ml of 1M KCl, 2.5 ml of 0.2 M KH_2PO_4/KOH pH 7.8 and 370 µl of protease inhibitor cocktail ; H_2O was added to have a total of 100 g and the phase mixture was thoroughly mixed). The phases were recovered by centrifugation at 250 g for 15 min. The upper phase, which was enriched in plasma membranes, was recovered, diluted, in a ratio 1:3, in solution B (10 mM trishydroxymethylaminomethane/HCl pH 7.8, 330 mM sucrose) and centrifugated at >100'000 g for 45 min. The supernatant was discarded and the pellet, constituted of plasma membranes, was diluted in 100 µl of solution C (330 mM sucrose, 3 mM KCl, 5mM KH_2PO_4/KOH pH 7.8). The lower phase, which was enriched in the other cellular membranes, was treated as the upper, the final pellet being diluted in 200 µl of solution C.

The raw serum was purified by affinity chromatography through two different resins. To the first, designed to retain unspecific antibodies, were bound all soluble proteins of a bacterial culture expressing the pGEX empty vector. To the second designed to retain antibodies specific to th*e AtMRP3-GST* peptide, were bound AtMRP3-GST peptides. The two different preparations of proteins were extracted and purified as described above. The peptides were then linked to the matrix of the resine in the following manner : 1 g of CNBr-activated Sepharose 4B (GE Healthcare) was deposited on a filter paper (type coffee filter) in a vacuum pump and washed with 200 ml of 1 mM HCl, in 15 min. The resulting gel, constituted of humidified resin, was suspended in 5 ml of solution A (0.1 M $NaHCO_3$/HCl pH 8.3 , 0.5 M NaCl). An amount of protein preparation containing 10 mg of bacterial soluble proteins + GST (or 10 mg of the AtMRP3-GST fusion peptide) was added to the suspension. The suspension was incubated 2 hours at room temperature, to bind the proteins to the matrix. The

suspension was centrifugated at 500 g for 5 min, the resulting supernatant was discarded and 5 ml of a buffer of 0.1 M trishydroxymethylaminomethane/HCl pH 8.0 was added to the pelleted gel. This new suspension was incubated 2 hours at room temperature, with shaking. The gel was recovered by filtrating the suspension on a filter paper, using a vacuum pump and then washed successively with 5 ml of solution B (0.1 M sodium acetat/HCl pH 4.0, 0.5 M NaCl) and 5 ml of solution C (0.1 M trishydroxymethylaminomethane/HCl pH 8.0, 0.5 M NaCl). This washing step was repeated twice. The gel was finally suspended in solution D (136 mM NaCl, 2.7 mM KCl, 10 mM Na_2HPO_4, 1.76 mM KH_2PO_4/KOH pH 7.4, 0.01% (w/v) NaN_3). The volume of gel ready to use obtained with the starting 1 g of CNBr-activated Sepharose 4B was of 3.5 ml.

To purify the raw serum 8 ml of it were centrifugated at 20'000 g for 10 min. The obtained supernatant, containing the antibodies, was passed three times through a syringe containing 1 ml of the gel of resin bound to the soluble peptides of *E. coli* expressing GST. The antibodies having an affinity for the bacterial peptides or the *GST* were retained in this column. The resulting purified filtrate was the passed three times through 6 ml of the gel of resin with the AtMRP3-GST fusion peptide bound to its matrix. The antibodies having an affinity for the *AtMRP3-GST* fusion peptide were retained in the second column. The second column was washed with 10 ml of solution A (136 mM NaCl, 2.7 mM KCl, 10 mM Na_2HPO_4, 1.76 mM KH_2PO_4/KOH pH 7.4). The antibodies retained in it were eluted by passing through the resin 2 ml of solution B (50 mM glycine/HCl pH 2.3, 0.15 M NaCl). The eluate was buffered with 1 M trishydroxymethylaminomethane and stabilized with and NaN_3 (final concentration 0.01% (w/v)).

The purified antibodies were assayed on various protein blots, charged with the AtMRP3-GST fusion protein, with the total extract of soluble proteins of *E .coli* expressing GST, with the total protein extract of Col-0 or *mrp3-1* leaves (8 weeks old plants, 8 hours light conditions) or with the two phases of a two phases partitionning of Col-0 or *mrp3-1* leaves (8 weeks old plants, 8 hours light conditions ; plants in control condition or treated 24 hours before harvesting with a solution of 100 µM prosulfuron and 0.02% (v/v) Tween 20 (Bio-Rad, Reinach, Switzerland).

II.6.3. Cloning of a construct encoding an AtMRP3-GFP fusion

In order to obtain a fusion between AtMRP3 and the green fluorescent protein (GFP) positioned at the C-terminal end of AtMRP3, the *AtMRP3* cDNA was amplified by PCR

using the published pNEV-AtMRP3 construct as a template (Tomassini et al., 1998) and the primers atMRP3_NcoI_s/atMRP3_NcoI_as. The PCR was performed with Pfu polymerase and the reaction was prepared according to the protocol provided by the manufacturer. The temperature cycling program consisted of : 2 min at 95°C ; 20 cycles of 45 sec at 95°C / 1 min at 58°C / 9 min 30 sec at 72°C ; 5 min 30 sec at 72°C. As a result, a cDNA fragment lacking the stop codon of *AtMRP3* which was extended at the 5'- and 3'-ends with NcoI restriction sites was obtained. Care was taken to obtain the correct reading frame allowing the translational fusion with GFP via the 3' NcoI site in the final transient expression vector.

Since direct cloning of the NcoI-treated PCR product into the vector containing the GFP expression cassette appeared impossible, it was first subloned into pGEM T-easy. First, 3'-adenine overhangs were added by incubation of the PCR product for 30 min at 37°C with 2 U Taq and 1.25 mM dATP. The PCR product was purified by $CHCl_3$:isoamylalcohol 24:1 (v/v) extraction followed by precipitation in 70 % EtOH, 90 mM sodium acetate pH 5.2, (30 min centrifugation at 20'000 g and 4°C) and brief washing of the DNA pellet with 70% EtOH. After air drying of the DNA pellet, it was dissolved in 10 µl H_20 and ligated into the pGEM-T easy vector following the instructions of the manufacturer. After transformation into *E. coli* strain DH5α, positive clones containing *AtMRP3* were scored by NcoI-digestion of plasmid DNA. The resulting vector was termed *AtMRP3_NcoI_pGEM* and the absence of sequence errors was verified by sequencing of the *AtMRP3* insert.

In order to construct the $Pro_{CaMV\ 35S}$*::AtMRP3-GFP5::*Ter_{nos} cassette, the *AtMRP3* cDNA fragment released from *AtMRP3*_NcoI_pGEM (see above) by NcoI digestion and gel elution (Qiaex II kit from Qiagen) was cloned into NcoI-cut and dephosphorylated pCL60 ((Bauer et al., 2002). pCL60 is a pBluescript-based vector which contains a $Pro_{CaMV\ 35S}$*::(NcoI)-GFP5::*Ter_{nos} cassette allowing transient expression in plant cells. The resulting plasmid was termed *AtMRP3_pCL60*.

For all bacterial transformations, *E. coli* DH5α or XLI-Blue competent cells were transformed by electroporation (Gene Pulser, Bio-Rad, Reinach, Switzerland ; electroporation followed the instructions of the manufacturer ; settings : cuvette gap 0.2 cm ; voltage 2.5 kV ; field strength 12.5 kV/cm ; capacitor 25 µF ; resistor 200 Ω ; time constant 4.8 msec). In all cases, bacteria were grown at 28°C to maintain integrity of plasmids containing the *AtMRP3-GFP5* cassette. Correct orientation and absence of sequence errors was controlled by sequencing *AtMRP3_pCL60* with the following primers : pCL60_35S, 3Cn-s, 3Cn-as, MRP3_seq1, LMRP3A_s, 3An-s, MRP3_seq2, MRP3_seq3, MRP3_seq4, AtMRP3-s, GFP5'_200R.

II.6.4. Subcellular localisation of AtMRP3 by transient expression of *AtMRP3*-GFP.

To determine the subcellular localisation of the AtMRP3-GFP fusion protein, epidermial onion cells were transiently transformed by biolistic microprojectile delivery of plasmid *AtMRP3_pCL60*.

The plasmid *AtMRP3_pCL60* was delivered either with a vector carrying a gene coding for the p19 inhibitor of gene silencing (Voinnet et al., 2003), or with p19 and a vector containing a tonoplast marker : the *Pro$_{35S}$::DsRed2-TPK1* construct. *TPK1* has been repeatedly localized to the tonoplast (Czempinski et al., 2002). Cloning of the *Pro$_{35S}$::DsRed2-TPK1* construct which was kindly provided by Isabelle Debeaujon (INRA Versailles) is described in Marinova (2006).

DNA-coated microprojectiles were prepared in the following manner : either 7.5 µg DNA of *AtMRP3_pCL60* construct and 1 µg DNA of p19 or 7.5 µg DNA of *AtMRP3_pCL60* construct and 1 µg DNA of p19 and 0.75 µg DNA of *Pro$_{35S}$::DsRed2-TPK1* were added to1 mg of gold particles (size of the particles : ∅ 1.0 µm) resuspended in 1 ml of a 1:1 mixture of ethanol and glycerol. The suspension was carefully mixed with the DNAs. 20 µl of 0.1 M spermidine were added to 50 µl of 2 M $CaCl_2$ and this mixture was added to the gold particle suspension. The suspension was incubated 1 min on ice, then vortexed for 15 min and finally centrifuged for 15 sec at 3'700 g, to pellet the DNA-coated gold particles. The supernatant was discarded, and the gold particle pellet was washed twice with 200 and 100 µl 99.8% ethanol. Finally, the DNA-coated gold particles were thoroughly resuspended in 100 µl of ethanol and transferred to the rupture disks used in the particle inflow gun (10 µl of supension per rupture disk) and dried.

Onions (*Allium cepa*) bulbs were bought at the local food store and cut in order to have square bulb leaflet slices of around 4 cm X 4 cm. The DNA-coated microprojectiles were delivered to the adaxial epidermal layer by helium biolistic bombardment using a low pressure partical inflow gun, as described by Geisler et al. (2004). After transformation, the bulb slices were incubated in a petri dish supplied with a wet filter paper to avoid drying. After 24 hours, the transformed epidermial layer was carefully removed and insepcted by confocal laser scanning microscopy. Single optical sections were captured by confocal laser scanning microscopy (CLSM) using a TCS SP2-x1 full spectrum confocal microsope attached to a Leica DM IRE2 inverted fluorescence (Glattbrugg,

Switzerland). GFP and DsRed were simultaneously excited with a 488 nm Ar and a 543 HeNe laser and fluorescence emission images averaged over 8 frames were captured in independent channels (GFP: 500-520 nm, DsRed: 580-615 nm; DD488/543 beam splitter). Images were false-colored in green (GFP) or red (DsRed) using Adobe Photoshop 7.0 (Mountain View, CA).

II.7.1. Isolation of wild-type and mutant vacuoles

Col-0, , *mrp3-1* and *mrp3-3* plants were cultivated for 8 weeks on soil with a photoperiod of 8 hours. Vacuoles isolated from mesophyll protoplasts were prepared from Col-0 and *mrp3-1* plants in the first experiment, Col-0 and *mrp3-3* in the second experiment and Col-0, *mrp3-1*, *mrp3-3* in the third experiment) using the following protocol. As a first step, protoplasts were isolated from the leaves as described in paragraph II.5.1., but with the following modifications : medium A contained 500 mM sorbitol, 1 mM $CaCl_2$, 10 mM methyl ethane sulfonate/KOH pH 5.6 ; Percoll pH 6 contained 500 mM sorbitol, 1 mM $CaCl_2$, 20 mM methyl ethane sulfonate pH 6 dissolved in Percoll ; the uppermost phase of the discontinuous gradient consisted of a layer of about 8 ml of medium E (0.4 M sorbitol, 30 mM KCl, 20 mM hydroxyethyl piperazine ethane sulfonic acid/KOH pH 7.2, 1 mg/ml BSA).

The isolated protoplasts were lysed by addition of the same volume of medium F (0.2 M sorbitol, 10% (w/v) Ficoll, 20 mM EDTA, 10 mM hydroxyethyl piperazine ethane sulfonic acid/KOH pH 8, 0.16 mg/ml BSA) prewarmed to 42°C, followed by around 10 min of incubation at room temperature. The lysis was monitored by microscopy. When an optimum amount of intact vacuoles had been released by the protoplasts, the lysis was stopped by incubation of the tubes containing the suspension on ice. Then the lysate was transferred to 10 ml glass tubes and a discountinous gradient was prepared by addition of two layers on top of the suspension. The first (middle) phase of about 5 ml consisted of a 1:1 mixture of medium F and medium G (400 mM glycine betain, 30 mM KCl, 20 mM hydroxyethyl piperazine ethane sulfonic acid/KOH pH 7.2, 1 mg/ml BSA). On top a layer of about 2 ml of medium G was added. This gradient was centrifuged at 200 g, 5 min, at room temperature, and the vacuoles were then carefully recovered from the interphase between middle and uppermost phases using a micropipet with a cut plastic tip.

II.7.2. Uptake of glutathione into isolated wild-type and mutant mesophyll vacuoles

Transport experiments were performed immediately after vacuole isolation. Prior to the transport experiment, about 1/3 volume of Percoll pH 7.2 (Percoll with 500 mM sorbitol, 20 mM hydroxyethyl piperazine ethane sulfonic acid) was added per volume of vacuoles to the suspension.

Transport experiment started by adding 30 µl of vacuoles to 70 µl of transport medium already deposited at the bottom of 0.4 ml polyethylene tubes . The transport assay (based on 100 µl final volume) consisted of 31 % Percoll (pH 7.2), 0.4 M sorbitol, 30 mM KCl, 20 mM hydroxyethyl piperazine ethane sulfonic acid/KOH pH 7.2, 0.12% (w/v) BSA, 6 mM $MgCl_2$, 5 mM ATP, 200 µM GSH, 7400 Bq of [*glycine*-2-^{3}H]GSH and further compounds depending on the assay as indicated in chapter VII. The vacuolar volume was either measured using 3700 Bq of ^3H_2O in separate tubes or by double-labelling in the presence of 3700 Bq of [U-^{14}C]glycerol together with the [*glycine*-2-^{3}H]GSH. In the case of vanadate inhibition, 1 mM potassium *ortho*-vanadate was added.

The samples were rapidly overlayered with 200 µl of silicon oil (poly(dimethylsiloxane-co-methylphenylsiloxane) 550 ; Aldrich, Buchs, Switzerland) and 60 µl of water. The incubation was terminated after 18 min in the first experiment and after 20 min in the second and third experiment by flotation of the vacuoles through the silicon oil phase by centrifugation (10'000 g for 15 s). For each time-point, line and condition, five separate tubes were prepared. In each tube, vacuole-associated radioactivity was quantified by pipeting 50 µl of the upper aqueous phase, containing the vacuoles which floated through the silicone oil before they collapsed in the water phase, into 6 ml vials followed by liquid scintillation counting as indicated in paragraph II.5.1.. Furthermore, to calculate the uptake rates, the radioactivity in four 10 µl-aliquots of each specific transport medium (without the vacuoles) was determined. The amount of GSH absorbed per vacuole volume unit in a sample of vacuoles was calculated by dividing the radioactivity due to the ^{3}H isotope in the sample by the specific radioactivity of GSH per molar unit in the vacuole suspension and by the volume of vacuoles in the suspension. The specific radioactivity per molar unit of GSH in the suspension was deduced from the radioactivity of the ^{3}H isotope measured in the aliquots of the corresponding transport medium. In the first transport experiment, the volume of vacuoles in the suspension was calculated by dividing the vacuole-associated radioactivity incubated with $^3H_20$ by the $^3H_20$ radioactivity per unit of volume as determined in the transport mix. In the second and

third experiment, the volume of vacuoles in each sample was calculated by dividing the ^{14}C-glycerol radioactivity in the vacuolar sample by the ^{14}C-radioactivity per unit of volume as determined in the transport mix. This is summarized by the following formulas :

$$\mathbf{C_{GSH\ in\ vac} = radio^{3}H\text{-}GSH / (specradio_{GSH})(V_{vac})}$$

In the first experiment :

$$\mathbf{V_{vac} = radio^{3}H_20 / specradio_{3H20}}$$

In the second en third experiments :

$$\mathbf{V_{vac} = radio^{14}C\text{-}glycerol / specradio_{glycerol}}$$

$\mathbf{C_{GSH\ in\ vac}}$ = concentration of GSH inside vacuoles
radio^{3}H-GSH = vacuole-associated ^{3}H-GSH radioactivity in a sample
specradio$_{GSH}$ = specific radioactivity of GSH per µmol
$\mathbf{V_{vac}}$ = volume of vacuoles in a sample
radio^{3}H$_2$0 = vacuole-associated $^{3}H_20$ radioactivity in a sample
specradio$_{3H20}$ = specific radioactivity of $^{3}H_20$ per µl of transport mix
radio^{14}C-glycerol = vacuole-associated ^{14}C-glycerol radioactivity in a sample
specradio$_{glycerol}$ = specific radioactivity ^{14}C-glycerol of per µl of transport mix

II.8.1. Cloning of reporter gene cassettes including the *AtMRP3* promoter and different terminators

To allow the cloning of various constructs carrying cassettes with the *AtMRP3* promoter fused to different reporter genes and either the *CaMV 35S* or the *AtMRP3* terminator, a modular cloning strategy was developed. All construct were prepared in the pRTΩ vector (Überlacker and Werr, 1996) using the AscI restriction sites flanking the expression cassette in pRTΩ. As depicted in Figure II.1., a fragment of 2030 bp of the promoter and 5'UTR region of *AtMRP3* was amplified by PCR using the primers Pr3fwd-Asc, Pr3rev-AKN and the BAC clone MJG19 as template. The upper primer introduced an AscI restriction site at the 5'-end while the lower primer added 5'-NotI-KpnI-AscI-3' sites at the 3'-end of the promoter fragment.

The AscI-cut promoter fragment was ligated with AscI-cut pRTΩ vector, thereby replacing the CaMV 35S expression cassette. The resulting vector was termed *promM3*.

Next, a fragment of 918 bp of the 3'UTR and terminator region of *AtMRP3* (primers: Ter3fwd-NP/Ter3rev-Kpn; template BAC clone MJG19) and the *nos* terminator (primers: TerNosfwd-NP/TerNosrev-Kpn ; template: nos-GFP cassette of the pGREEN vector series ; Hellens, Edwards et al., 2000 ; Hellens, Mullineaux and Klee, 2000) were amplified by PCR. In both cases, the upper and lower primers introduced NotI and PacI restriction sites at the 5'-ends and a KpnI site at the 3'-ends of the terminator fragments. Subsequently, the terminator PCR products were ligated NotI-KpnI into *promM3* resulting in vectors *promM3-terM3* and *promM3-ternos*.

Finally, reporter genes were added. The *uidA* (*GUS*) gene and the *luc*+ reporter gene, an artificial gene derived from the native firefly luciferase gene, were amplified by PCR using pCambia 1305.1 (www.cambia.org) and pSP-luc+ fusion vector (Promega) as templates and NotGUSfwd/GUSPacRev and NotLUCfwd/LUCPacRev as primer combinations, respectively. These primers introduced 5'-NotI and 3'-PacI restriction sites which were used to introduce both reporter genes NotI-PacI into *promM3-terM3* and *promM3-ternos* resulting in plasmids *promM3-GUS-terM3* (reporter cassette Pro_{AtMRP3}*::GUS::*Ter_{nos}), *promM3-LUC-terM3* (Pro_{AtMRP3}*::LUC::*Ter_{nos}), *promM3-GUS-ternos* (Pro_{AtMRP3}*::GUS::*Ter_{AtMRP3}) and *promM3-LUC-ternos* (Pro_{AtMRP3}*::LUC::*Ter_{AtMRP3}).

Primers are listed in Table II.1. All PCRs were performed with Pfu polymerase, following the protocol given by the manufacturer. The following temperature profiles were used for PCR : (1) promoter : 2 min at 95°C ; 23 cycles of 45 sec at 95°C / 1 min at 56°C / 4 min 30 sec at 72°C ; 5 min 30 sec at 72°C. (2) terminator fragments : 2 min at 95°C ; 25 cycles of 45 sec at 95°C / 1 min at 64°C / 4 min at 72°C ; 5 min 30 sec at 72°C. (3) reporter genes: 2 min at 95°C ; 25 cycles of 45 sec at 95°C / 1 min at 56°C / 4 min 30 sec at 72°C ; 5 min 30 sec at 72°C. Restriction digestion, gel elution (QiaQuick kit, Qiagen), ligation and heat-shock transformation of *E. coli* XL1-blue followed standard procedures. All reporter cassettes were verified by sequencing.

In order to obtain binary vectors for Agrobacterium-mediated stable plant transformation, all four reporter cassettes were transferred *via* AscI into pGREENII 0179 vector (Hellens, Edwards et al., 2000) which was modified before to contain a unique AscI site within the multicloning site of the T-DNA region (Klein, unpublished). The resulting plasmids were termed *promM3-GUS-terM3_pG*, *promM3-LUC-terM3_pG*, *promM3-GUS-ternos_pG* and *promM3-LUC-ternos_pG*. Subsequently, the binary plasmids, each together with the pSoup

helper vector were transformed into *Agrobacterium tumefaciens* by electroporation. Transformants were selected on tetracycline + kanamycin. Six-week old, greenhouse-grown *Arabidopsis* of the Col-0 ecotype were used for stable transformation with *Agrobacteria* by floral dipping, as described by Clough and Bent (1998), with the following small modification : the inoculation medium contained 0.54 g/l MS salts, 50 g/l saccharose, 5 mM $MgCl_2$ and 0.05% (v/v) Silwet L-77 (Lehle Seeds, Round Rock, USA).

T1 seeds were selected for transgenic plants by hygromycine B (Duchefa, Haarlem, the Netherlands ; 29 mg/l) selection on ½ MS / 1% (w/v) sucrose plates. After two weeks, resistant seedlings were transferred into soil and T2 seeds of individual T1 transformants were collected.

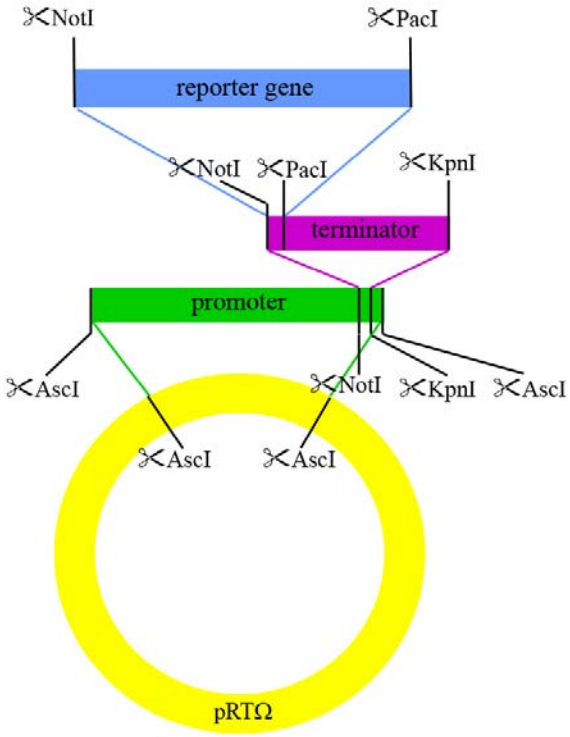

Figure II.1. : Modular cloning strategy to obtain *Pro$_{AtMRP3}$::Reporter::Ter* cassettes that allow the flexible introduction of either *uidA* or *luc+* as reporter genes and either *nos* or the *AtMRP3* 3'-UTR as terminator.

II.9.1. GUS staining of reporter plants and tissue fixation, embedding and sectioning

T2 seeds of independent lines of Columbia 0 transformed with Pro_{AtMRP3}*::uidA::*Ter_{AtMRP3} (in pBIN19) (Eggmann, Bovet and Klein, unpublished) were kindly provided by Dr Lucien Bovet, University of Fribourg. Homozygous transgenic plants were obtained by selection of T2 lines exhibiting a 3:1 $kan^{RESISTANT}$:$kan^{SENSITIVE}$ seedling ratio on kanamycin-containing growth media and 100% kan resistance of T3 seeds obtained from single T2 plants. Homozygous lines were labelled MTER B to MTER F. Two independent plants of Columbia 0 transformed with a Pro_{AtMRP3}*::GUS::*Ter_{nos} construct were obtained as described in paragraph II.8.1.

Seedlings of all the MTER lines were grown for 11 days in 16 hours of light on ½ MS / 1% (w/v) sucrose agar plates in the absence or presence of 10 µM $CdCl_2$. A third treatment consisted of growth on ½ MS / 1% (w/v) sucrose agar plates and spraying of seedlings with an aqueous solution of 500 nM prosulfuron six hours before GUS staining.

Seedlings where stained by immersion in GUS staining solution (1 mM X-Gluc (Bromo-4-Chloro-3-indolyl-β-D-glucuronicacid, from a 20 mM solution in dimethylformamide ; manufacturer : Biosynth AG, Staad, Switzerland), 50mM Na_2HPO_4/NaH_2PO_4 pH 7.0, 1mM NaEDTA, 0.3% (v/v) Triton X-100, 0.5 mM $K_4Fe(CN)_6$, 0.5 mM $K_3Fe(CN)_6$) followed by incubation for 6 hours at 37°C. Staining was stopped by removing the solution and clearing of the seedlings in 70% ethanol which was daily replaced for three days at 4°C.

For GUS analysis of rosette leaves and stem tissue, MTER and Pro_{AtMRP3}*::GUS::*Ter_{nos} lines were grown on soil for 4-8 weeks with a photoperiod of 8 hours. Leaves of individual plants were stained for GUS activity and cleared as described above. Microtome sections of leaves and stems of MTER plants were prepared in the following manner : small pieces of leaves (around 1 cm X 0.5 cm) and stems (around 1 cm of lenght) were cut and prefixed by 1 hour incubation on ice in solution A (4 mM sucrose, 0.5% (w/v) paraformaldehyde, 0.1% (v/v) Triton X-100, 10 mM β-mercaptoethanol, 0.1 M Na_2HPO_4/NaH_2PO_4 pH 7.2) ; the pieces were subsequently stained for GUS activity for 18 hours at 37°C in GUS staining solution . These tissue fragments were then fixed by incubation on ice in solution B (1% (w/v) paraformaldehyde, 0.1 M Na_2HPO_4/NaH_2PO_4 pH 7.2) for 3 hours. Clearing and dehydration was performed by successive incubation in an ethanol series at 4°C (1 hour 30% ethanol, 1 hour 50% ethanol, 1 hour 70% ethanol, 1 hour 100% ethanol, 18 hours 100% ethanol, 24 hours 100% ethanol). Subsequently, specimen were embedded in Technovit 7100 (Heraus Kulzer, Wehrheim, Germany), following the protocol of the manufacturer. Finally, the

embedded tissue was cut into 2 μM thick slices using a microtome with glass blades (American Optical, Buffalo, USA).

Table II.1. : Name, sequence and description of the primers used for PCR genotyping of *atmrp3* mutants and cloning procedures of the present study. For the primers specific for the *AtMRP3* gene, the number given is the position of the 5' base of the primer relatively to the gene (position +1 is base A of the ATG). Restriction sites in the primers for cloning are indicated by colors in the sequences.

Name of the primer	Sequence (always 5'→3')	Description
3-1ver-up	AAAGCAAAGGATACAGATTGCAC	primer specific for the *AtMRP3* gene, sense (position 2307 bp)
3-2ver-up	AGATTGTCAAAGACCCGTGAAAGAGG	primer specific for the *AtMRP3* gene, sense (position -285 bp)
3-2ver-low	GCTGCGGAACATCTTCTAGATCAAGG	primer specific for the *AtMRP3* gene, antisense (position 838 bp)
3An-s	CATCTTTACTAGGAGAAGTACCCAAGG	primer specific for the *AtMRP3* gene, sense (position 2057 bp)
3C-s	TGCTGTGTTTCTCGGTTACGTGGCTGT	primer specific for the *AtMRP3* gene, sense (position 579 bp)
3C-α	GCAAAGAAGGCTGTCACTAGAATCTCCC	primer specific for the *AtMRP3* gene, antisense (position 995 bp)
3Cn-s	GCAACAGCAATGGAGTTTTGGAAGAG	primer specific for the *AtMRP3* gene, sense (position 623 bp)
3Cn-α	TTGAACGTGGTAACGCCACTTCTCTC	primer specific for the *AtMRP3* gene, antisense (position 935 bp)
AtMRP3-s	CCACTGCTTCTGTTGACACTG	primer specific for the *AtMRP3* gene, sense (position 4894 bp)

AtMRP3-as	GAGGTGTACTCAGCCACAAGC	primer specific for the *AtMRP3* gene, antisense (position 5207 bp)
atMRP3_NcoI_s	CATGCCATGGACTTTCTCGGTTCCAC	primer for amplification of the *AtMRP3* cDNA without stop codon, sense, extended with NcoI sites
atMRP3_NcoI_as	CATGCCATGGCATCGAAACTGGAACTAGATCTTGAG	primer for amplification of the *AtMRP3* cDNA without stop codon, antisense, extended with NcoI sites
Ds3-4	CCGTCCCGCAAGTTAAATATG	primer specific for the 3' end of the genetrap construct
Ds5-4	TACGATAACGGTCGGTACGG	primer specific for the 5' end of the genetrap construct
GFP5'_200R	GGCTGAAGCACTGCACGCCG	primer specific for the GFP5' gene in pCL60,antisense
GUSPacRev	CTGTTAATTAACAATTCACACGTGATGG	primer for amplification of the GUS reporter gene, extended with PacI site, antisens
LB2	GCTTCCTATTATATCTTCCCAAATTACCAATACA	primer specific for the left border of the pCSA110 T-DNA
LMRP3A_s	GATCTTCGGAAATCTGAGGAAGGATGGC	primer specific for the *AtMRP3* gene, sense (position 1588 bp)
LMRP3A_as	CTACTGCAAGAGCCTCCTGATGCGCACC	primer specific for the *AtMRP3* gene, antisense (position 2806 bp)
LUCPacRev	CTGTTAATTAATTACACGGCGATCTTTC	primer for amplification of the LUC reporter gene, extended with PacI site, antisens
MRP3_seq1	CTTTCTTTGCTGCTAAGATTGTGGAGTG	primer specific for the *AtMRP3* gene, sense (position 1106 bp)
MRP3_seq2	CTCAACTCTGGAACTGATTTCATGGAGC	primer specific for the *AtMRP3* gene, sense (position 2551 bp)

MRP3_seq3	GAGCTTCTACCGACCAATCCGCAGTAG	primer specific for the *AtMRP3* cDNA, sense (position 3149 bp)
MRP3_seq4	CCCAGTGAACCACCTCTTGTGATAGAATC	primer specific for the *AtMRP3* gene, sense (position 3739 bp)
NotGUSfwd	GTCGCGGCCGCATGGTAGATCTGAGGGT	primer for amplification of the GUS reporter gene, extended with NotI site, sense
NotLUCfwd	GTCGCGGCCGCATGGAAGACGCCAAAAAC	primer for amplification of the GUS reporter gene, extended with NotI site, sense
pCL60_35S	TCTCCACTGACGTAAGGGAT	primer specific for the CaMV 35 promoter in pCL60, sense
p745	AACGTCCGCAATGTGTTATTAAGTTGTC	primer specific for the left border of the pDs-lox T-DNA
Pr3fwd-Asc	CGTGGCGCGCCGTGATAACAATCGCACATAGAATA	primer for the amplification of the *AtMRP3* promoter, extended with AscI site, sense
Pr3rev-AKN	CGTGGCGCGCCGGTACCGCGGCCGCGGCTTTGAGCTCTCTGTTCTCTCTC	primer for the amplification of the *AtMRP3* promoter, extended with AscI, KpnI and NotI sites, antisense
QRB3	CGCCATGGCATATGCTAGCATGCATAATTC	primer specific for the right border of the pCSA110 T-DNA
S16-s	GGCGACTCAACCAGCTACTGA	sens primer specific for the At5g18380 mRNA
S16-as	CGGTAACTCTTCTGGTAACGA	antisens primer specific for the At5g18380 mRNA
SP6	TACGATTTAGGTGACACTATAG	sequencing primer
T7	TAATACGACTCACTATAGGG	sequencing primer

Ter3fwd-NP	CGTGCGGCCGCTTAATTAAAGCAAAGACTCTGCTATTTTCCTGC	primer for the amplification of the *AtMRP3* terminator, extended with NotI and PacI sites, sense
Ter3rev-Kpn	CGTGGTACCCATACCCATCATAAGAACCTGATA	primer for the amplification of the *AtMRP3* terminator, extended with KpnI site, antisense
TerNosfwd-NP	CGTGCGGCCGCTTAATTAAGCTAGAGTCAAGCAGATCG	primer for the amplification of the nos terminator, extended with NotI and PacI sites, sense
TerNosrev-Kpn	CGTGGTACCGATATCAGCTTGCATGCCG	primer for the amplification of the nos terminator, extended with KpnI site, antisense

III. Isolation of knockout mutants in the *AtMRP3* gene

To gain a better understanding of the role of AtMRP3 in *Arabidopsis thaliana*, various experiments have been performed in *Arabidopsis* plants lacking the functional *AtMRP3* gene. Mutant plants lacking *AtMRP3* expression also lack the function exerted by the protein and thus the differences between wild type and knockout mutants allows the analysis of the *in vivo* function of *AtMRP3*. Three different *atmrp3* mutant alleles have been isolated and subsequently used in these experiments, to ensure that the phenotype and physiological phenomena observed could be unequivocally related to the absence of *AtMRP3* in the mutants. In the following paragraphs the isolation and verification of the allelic mutants in *AtMRP3* is described with the aim to ensure the absence of a functional transporter.

III.1.1. Molecular characterisation of three mutant alleles of *AtMRP3*

All three mutant alleles in *AtMRP3* were found by searches in public mutant population databases, using either BLAST (Basic Local Alignment Search Tool) options with the genomic *AtMRP3* sequence as query or by searches using the AGI Code identifier At3g13080 in a public databases. The SAIL_351_B06 line was found by sequence comparison done at Syngenta Biotechnology with their own database ; the GT10839 line was found by sequence comparison in the Cold Spring Harbor Laboratory database (http://genetrap.cshl.edu/TrBLAST.html) and the WiscDsLox481-484C11 line was found with the AGI Code identifier in the "T-DNA Express" Arabidopsis Gene Mapping Tool (signal.salk.edu/cgi-bin/tdnaexpress). The first *AtMRP3* allele used in this study was a knockout mutant line obtained from the Syngenta SAIL large-scale insertional mutagenesis collection (Sessions et al., 2002). In this case, T-DNA mutagenesis was performed in the Columbia-0 (Col-0) wild-type background. We designated the name *mrp3-1* for the line with the SAIL identifier SAIL_351_B06. The vector used in the SAIL project to generate the T-DNA population in Arabidopsis was the binary pCSA110 plasmid (McElver et al., 2001).
A second line carrying a putative mutation in *AtMRP3* was obtained from the Cold Spring Harbor collection of gene trap transposon lines which contains a modified *Ds* transposon (Martienssen, 1998). GT lines were generated in the Landsberg erecta (Ler-0) background. This allele, termed *mrp3-2*, can be found in the Cold Spring Harbor collection (genetrap.cshl.org) with the identifier GT10839. It contains the genetrap *Ds* transposon.

The third line, named *mrp3-3*, is a knockout mutant line obtained by T-DNA insertional mutagenesis of Col-0 within the large-scale mutagenesis program of the Arabidopsis Knockout Facility of the University of Wisconsin (Krysan et al., 1996, 1999 ; Sussman et al., 2000). The identifier of *mrp3-3* in the Wisconsin collection is WiscDsLox481-484C11. It contains the pDs-Lox T-DNA. The *mrp3-1* and *mrp3-3* lines can be searched and found using the SIGnAL "T-DNA Express" Arabidopsis Gene Mapping Tool (signal.salk.edu/cgi-bin/tdnaexpress).

III.2.1. Genotyping of mutant alleles by PCR

We received seeds of the T2 generation of *mrp3-1* and *mrp3-3* and of the F3 generation of *mrp3-2* (third generation after crossing with the *Activator* (*Ac*) transposon followed by *Ac* outcrossing by counterselection – Martienssen, 1998). Sterilized seeds were germinated on growth media containing the appropriate selection chemical, depending on the dominant resistance gene which was part of the inserted T-DNA fragment to select for potential mutants. Resistant single plants were transferred to soil for further growth and PCR genotyping started from genomic DNA isolated from leaf material.

In order to determine the presence or absence of the inserted DNA fragment, its orientation, position and the genotype of each individual, a combination of PCR reactions with different primer pairs were performed using single plant genomic DNA as templates. For each mutant allele, a pair of primers amplifying a specific proportion of the *AtMRP3* gene and spanning the theoretical position of the insertion, was designed. PCR-reactions performed with gene-specific primers detected the presence of the wild-type *AtMRP3* allele in homozygous wild type or hemizygous plants while absence of an appropriate PCR product was interpreted as absence of a wild-type *AtMRP3* copy in homozygous mutants. In contrast, detection of the presence of either the T-DNA or the GT transposon in potential mutants was performed using PCR reactions containing a combination of one gene-specific primer with a second primer specific for either the left or right border of the T-DNA or the transposon. Thus, positive PCR reactions identified single plants which were either homo- or hemizygous for the insertion in *AtMRP3*. The relative orientation of the inserted DNA to the *AtMRP3* gene was scored by testing all possible combinations of gene-specific upper and lower primers together with

primers specific for the left and right borders of the inserted DNA (see Tables III.1.(a) and (b)). In order to define the exact position of the insertion in *AtMRP3*, PCR reactions positive for gene-specific and T-DNA/transposon-border primers were sequenced after cloning.

Six individual T2 plants of the *mrp3-1* allele were analysed for their genotype. PCR amplification in all of these plants with the combination of the primers LMRP3A_as (antisense primer specific for the *AtMRP3* gene) and LB2 (primer specific for the left border of the pCSA110 T-DNA) showed that they all contained the T-DNA insertion in the *AtMRP3* gene, with the right border of the insertion oriented towards the translational and transcriptional start site of the *AtMRP3* gene. The amplified fragment was around 600 base pairs long. It was cloned and sequenced. Alignment of the sequence of the fragment with that of *AtMRP3* showed that the insertion is located just before base pair +2343 of the *AtMRP3* gene (base pair +1 corresponds to the A of the translational start codon). Taking into account the position of the insertion, of the primers and the total length of the T-DNA, the amplified fragment should have been 887 base pairs long, but the observed length is shorter. An alignment of the sequenced border with the T-DNA sequence demonstrated that the left border of the T-DNA is partially deleted with a loss of around 290 base pairs of the pCSA110 sequence. Only two plants amplified a fragment with the combination of the primers LMRP3A_s (sense primer specific for the *AtMRP3* gene) and LMRP3A_as, corresponding to the predicted length of 1219 base pairs, sense, showing that they also contained an intact copy of the *AtMRP3* gene and thus were hemizygous. We were not able to identify the right border of the T-DNA. Any PCR amplifications with the combination of the primers LMRP3A_s and QRB3 (primer specific to the right border of the pCSA110 T-DNA) failed. This is probably due to a deletion of a fragment of DNA upon insertion, either at the right border of the insertion or in the *AtMRP3* gene (see Figures III.2.(a), (b) and (c)).

To ensure that the supposed deletion in the *mrp3-1* mutant did not extend to the genes neighbouring *AtMRP3*, we tried to amplify with specific primers a fragment of *AtMRP3* located at the beginning of the gene, before the insertion (primers 3Cn-s and 3Cn-α) and a fragment located at the end of the gene, after the insertion (primers AtMRP3-s and AtMRP3-as). Both amplifications were successful in all six analysed plants, producing fragments corresponding to the predicted lengths (313 base pairs for 3Cn-s and 3Cn-α, 314 base pairs for AtMRP3-s and AtMRP3-as) showing that the deletion, if it existed, was limited to a fragment near the insertion (see Figures III.1. and III.3.(a) and (b)).

Primer combination	Wild-type plant : two intact alleles	Hemizygous plant : one intact allele one mutated allele with insertion	Homozygous plant : two mutated alleles with insertion
AtMRP3 **sense primer -** ***AtMRP3*** **antisense primer**	+	+	-
AtMRP3 **specific primers – insertion specific primers**	-	+	+

Primer combination	Insertion in the same direction as the gene	Insertion in the reverse direction of the gene
AtMRP3 **sense primer – insertion left border primer**	+	-
AtMRP3 **antisense primer – insertion right border primer**	+	-
AtMRP3 **sense primer – insertion right border primer**	-	+
AtMRP3 **antisense primer – insertion left border primer**	-	+

Tables III.1.(a) (upper table) and (b) (lower table) : Scheme of the possible amplifications by PCR with different combinations of specific primers, depending on the genotype, the position and orientation of the T-DNA genome of the analysed plant.

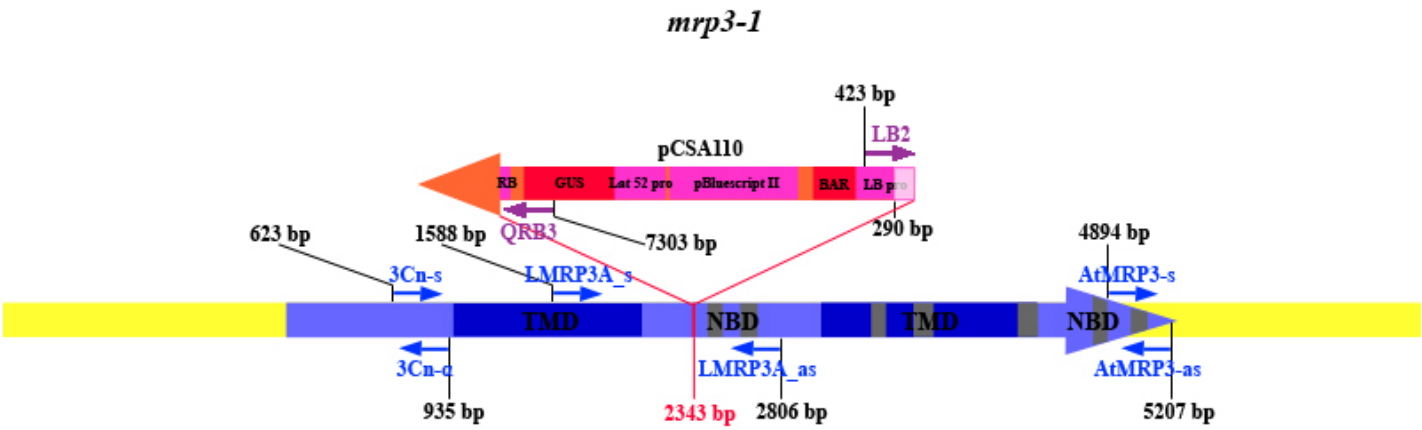

Figure III.1. : Schematic representation of the primer positions and T-DNA insertion of the *mrp3-1* mutant allele. The insertion is not presented to scale : the *AtMRP3* gene is 5232 bp long, pCSA110 is 7540 bp long.

Legends for pCSA110 : LB pro : left border of T-DNA, including a promoter ; RB : right border of T-DNA ; BAR : Basta resistance gene ; pBluescript II : cloning vector ; Lat 52 pro : promoter ; GUS : b-glucuronidase reporter gene. Lighter color at the left border represents the detected deletion.

AtMRP3 gene : dark blue : TMDs ; grey : introns.

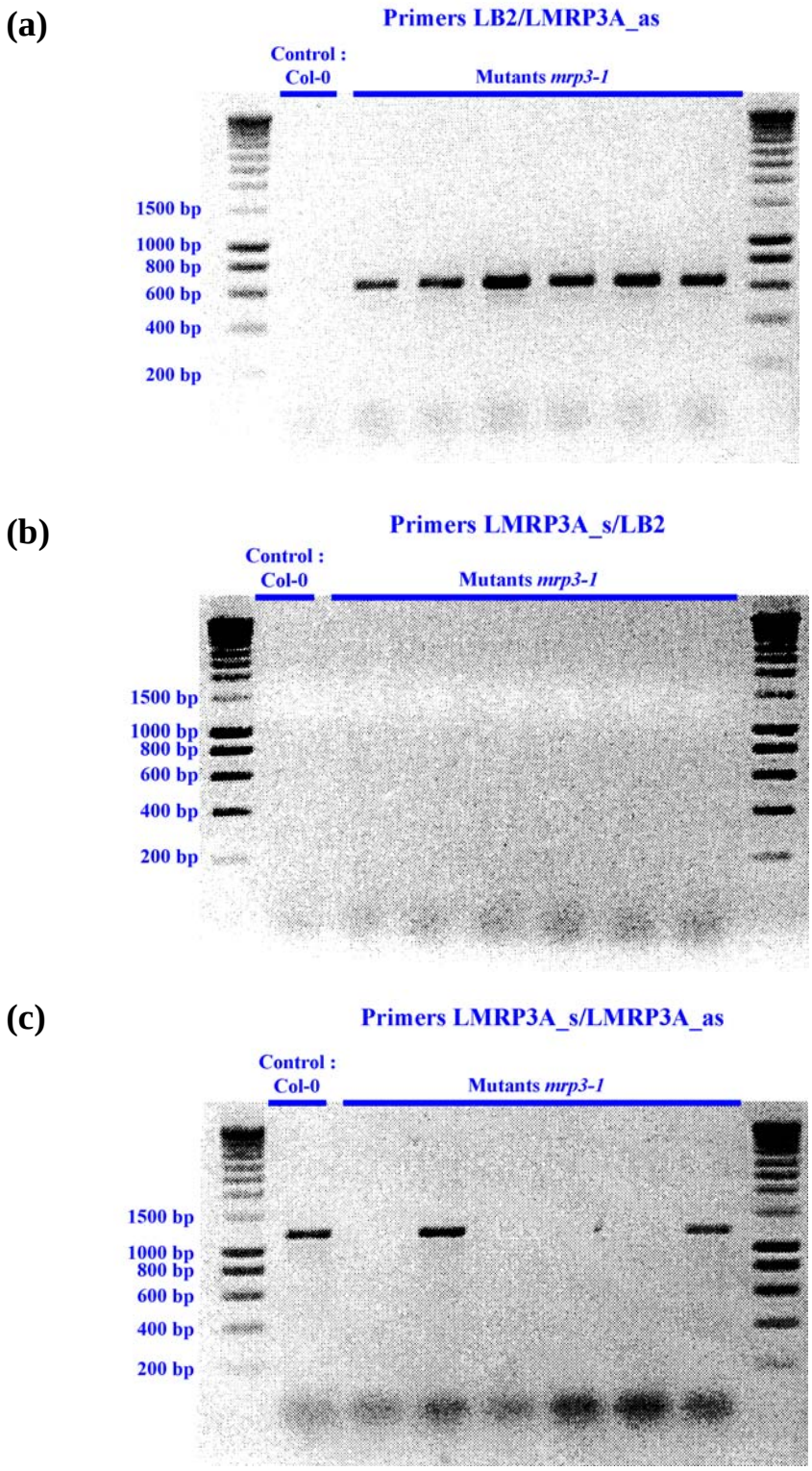

Figures III.2.(a), (b) and (c) : Results of PCR amplifications performed with the primer pairs LB2/LMRP3A_as, LMRP3A_s/LB2 and LMRP3A_s/LMRP3A_as. All plants contain the pCSA110 T-DNA. Lack of amplification with the pair LMRP3A_s/LB2 confirms the orientation of the insertion deduced by the amplification of a fragment with the pair LB2/LMRP3A_as.

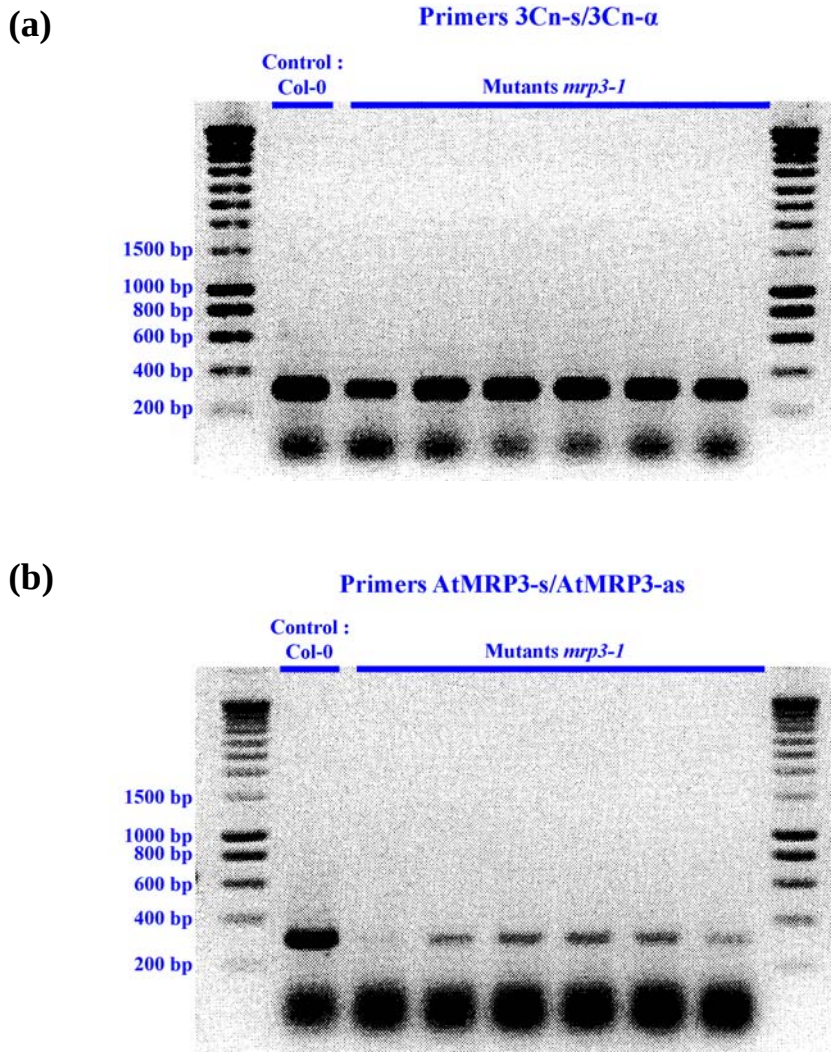

Figures III.3.(a) and (b) : The 5'- and 3'-ends of *AtMRP3* are still present in the *mrp3-1* allele and thus are not deleted during T-DNA integration. Depicted are the results of PCR amplifications performed with the primer pairs 3Cn-s/3Cn-α and AtMRP3-s/AtMRP3-as.

Twelve F3 plants of the *mrp3-2* allele were analysed with combinations of PCR reactions. Amplification in all of these plants with the combination of the primers 3-2ver-up (sense primer specific for the *AtMRP3* gene) and Ds3-4 (primer specific for the right border of the genetrap construct) produced a fragment demonstrating that all plants contained the Ds insertion in the *AtMRP3* gene and that the 3'-end of the *Ds* transposon designated by Martiennsen et al. (1998) faced the transcriptional and translational start of *AtMRPP3*. This

was confirmed by the successful amplification, also in all twelve plants, of a fragment with the primer-combination 3-2ver-low (antisense primer specific for the *AtMRP3* gene) and Ds5-4 (primer specific for the 5'-end of the genetrap construct). Both fragments 3-2ver-up/Ds3-4 and 3-2ver-low/Ds5-4 were cloned and sequenced. Sequence alignments performed with both sequences and the sequence of the *AtMRP3* gene demonstrated that the insertion lies exactly between the positions +119 and +120 of the *AtMRP3* gene. Taking into account the position of the insertion and of the primers and the length of the insertion, fragment 3-2ver-up/Ds3-4 should be 480 base pairs long and fragment 3-2ver-low/Ds5-4 should be 766 base pairs long. These predictions correspond to the sizes of PCR fragments obtained after electrophoretic separation on agarose gels. Nine plants amplified a fragment of the predicted length of 1123 base pairs with the combination of the primers 3-2ver-up and 3-2ver-low, showing that they contained an intact copy of the *AtMRP3* gene and were thus hemizygous (see Figures III.4. to III.6.) while all other plants were homozygous.

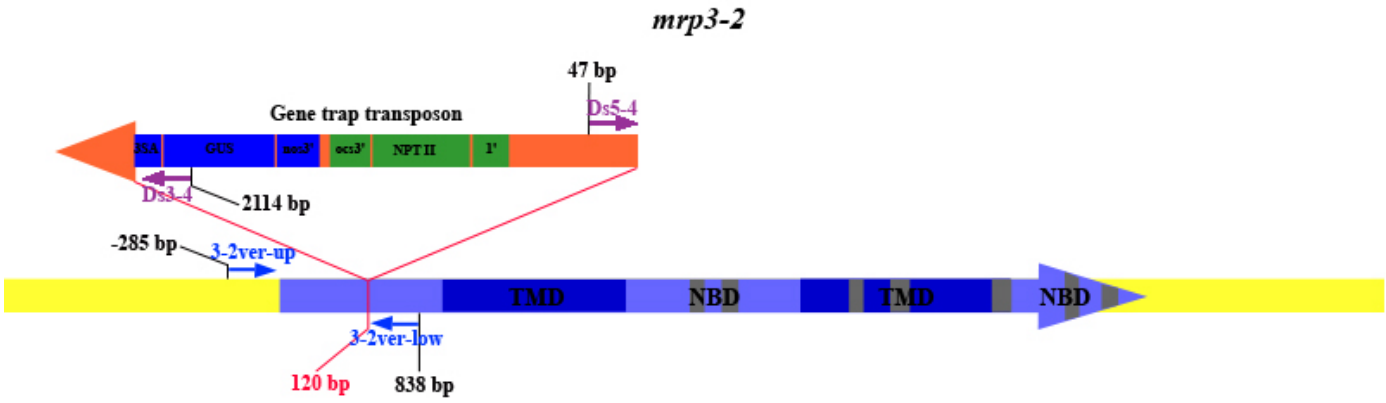

Figure III.4. : Schematic representation of the primers positions and transposon of the *mrp3-2* mutant allele. The insertion is not represented at the same scale as the gene : the *AtMRP3* gene is 5232 bp long, gene trap transposon is 2189 bp long.

Legends for gene trap transposon : 1' : promoter ; NPT II : neomycin phosphotransferase gene (confers resistance to kanamycin) ; oc3' : terminator ; nos3' : terminator ; GUS : β-glucuronidase reporter gene ; 3SA, triple splice acceptor.

(a)

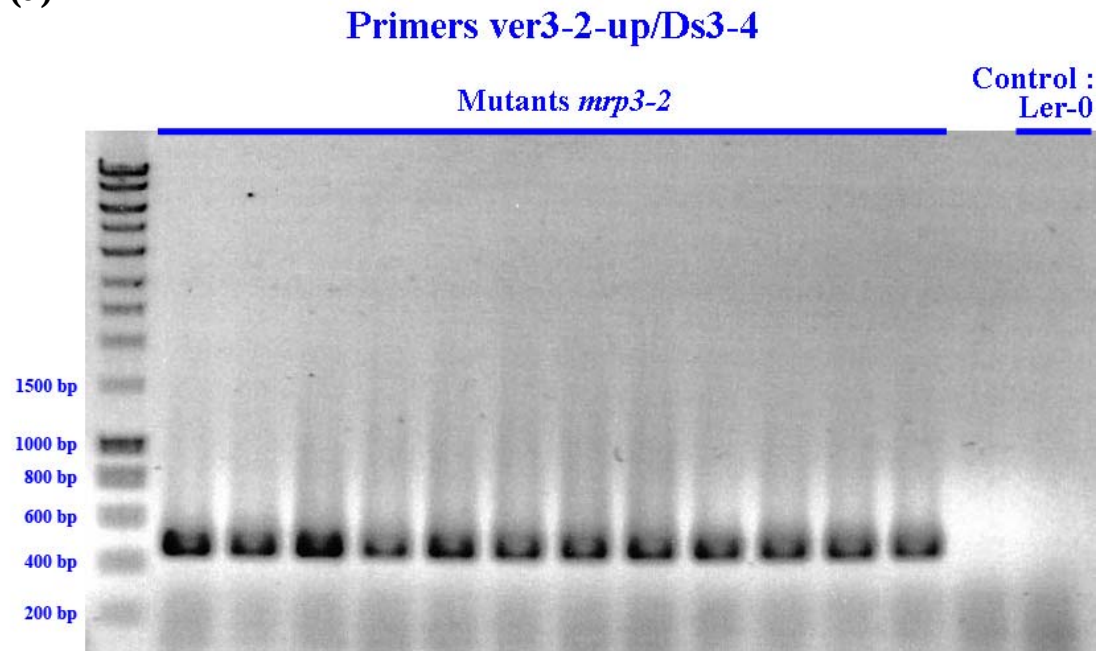

(b)

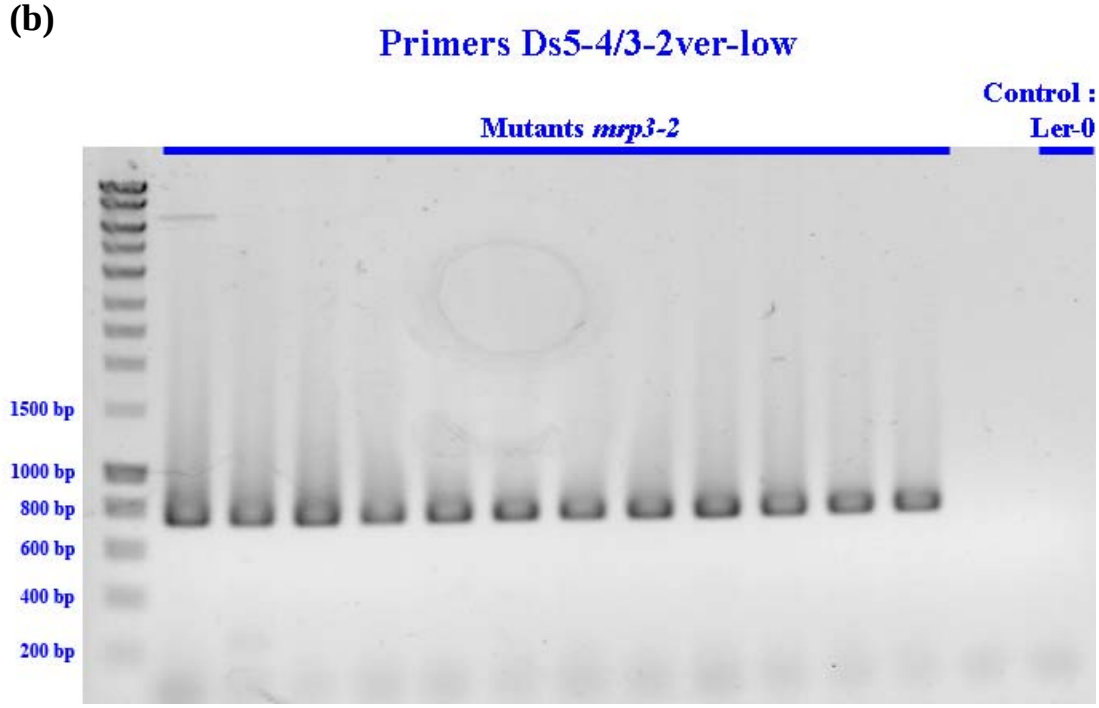

Figures III.5.(a) and (b) : Results of PCRs with the primer pairs ver3-2up/D3-4 and Ds5-4/3-2ver-low. All plants contain the genetrap transposon.

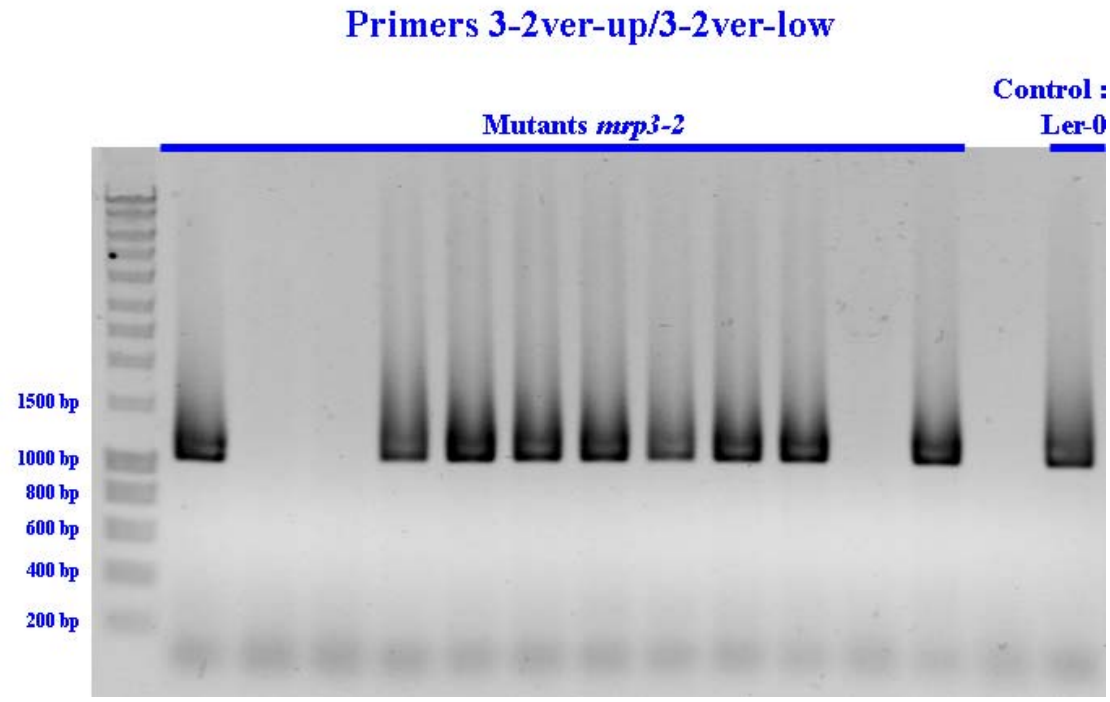

Figure III.6. : Results of PCRs with the primer pair 3-2ver-up/3-2ver-low. Nine plants contain an intact copy of the *AtMRP3* gene.

With the same rationale, the genotype of twelve T3 plants of the *mrp3-3* allele (offspring of one heterozygous T2 plant received from the Arabidopsis Knockout Facility of the University of Wisconsin ; see paragraph II.2.1.) was analysed with a combination of PCRs. In ten of the plants a successful PCR amplification with the primer combination 3-2ver-low (antisense primer specific for the *AtMRP3* gene) and p745 (primer specific for the left border of the pDs-Lox T-DNA) verified the presence of the T-DNA insertion in the *AtMRP3* gene. As predicted by the database searches, the left border of the inserted T-DNA faces the stop codon and 3'-UTR of *AtMRP3*. Lack of amplification with this combination in the two remaining plants could either be due to a problem in the extraction of the genomic DNA or to an error in the selection step (transfer of an antibiotic sensitive plant to soil). The amplified fragment was cloned and sequenced, and alignment with the sequence of the *AtMRP3* gene showed that T-DNA was inserted just after base pair –9 in the 5'UTR of *AtMRP3*. Taking into account the length of the T-DNA and the position of the primers, the amplified fragment was calculated to be 912 base pairs long which was also observed on agarose gels. In nine of the twelve plants, PCR amplification with the primer combination 3-2ver-up (sense primer specific for the *AtMRP3* gene) and 3-2ver-low was positive, suggesting that they contained an intact copy of

the *AtMRP3* gene and were thus hemizygous. The length of the amplified fragment corresponded to the predicted length of 1123 base pairs (see Figures III.7. to III.9.(a) and (b)). The right border of *mrp3-3* was not verified further.

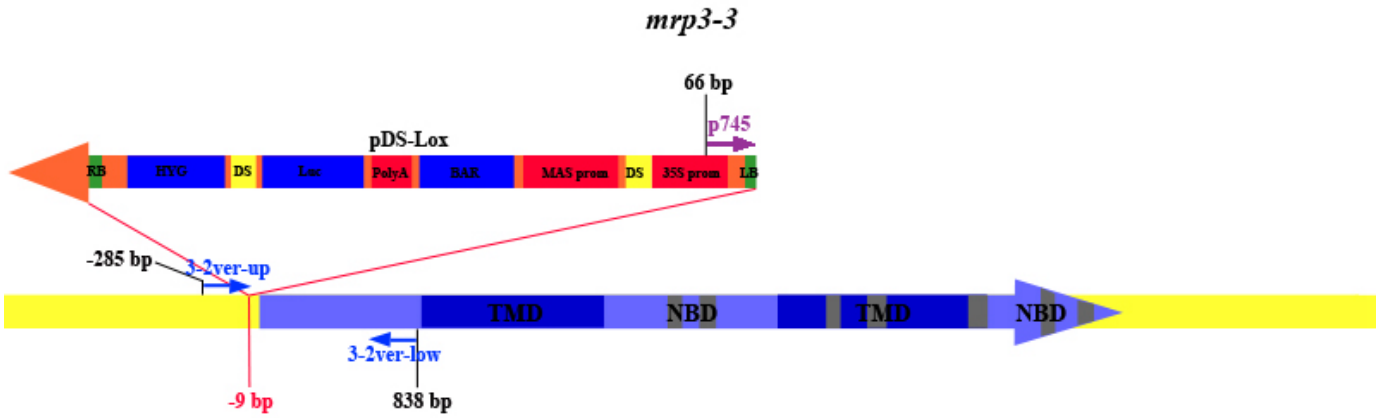

Figure III.7. : Schematic representation of the primer positions and T-DNA insertion of the *mrp3-3* mutant allele. The insertion is not represented at the same scale as the gene : the *AtMRP3* gene is 5232 bp long, pDS-Lox is 8954 bp long.

Legends for pDS-Lox : LB, RB : left and right borders of T-DNA ; 35S prom : promoter ; DS : Ds transposon border sequences ; MAS prom : promoter ; BAR : Basta resistance gene ; Luc : luciferase protein gene ; HYG : hygromycin resistance gene.

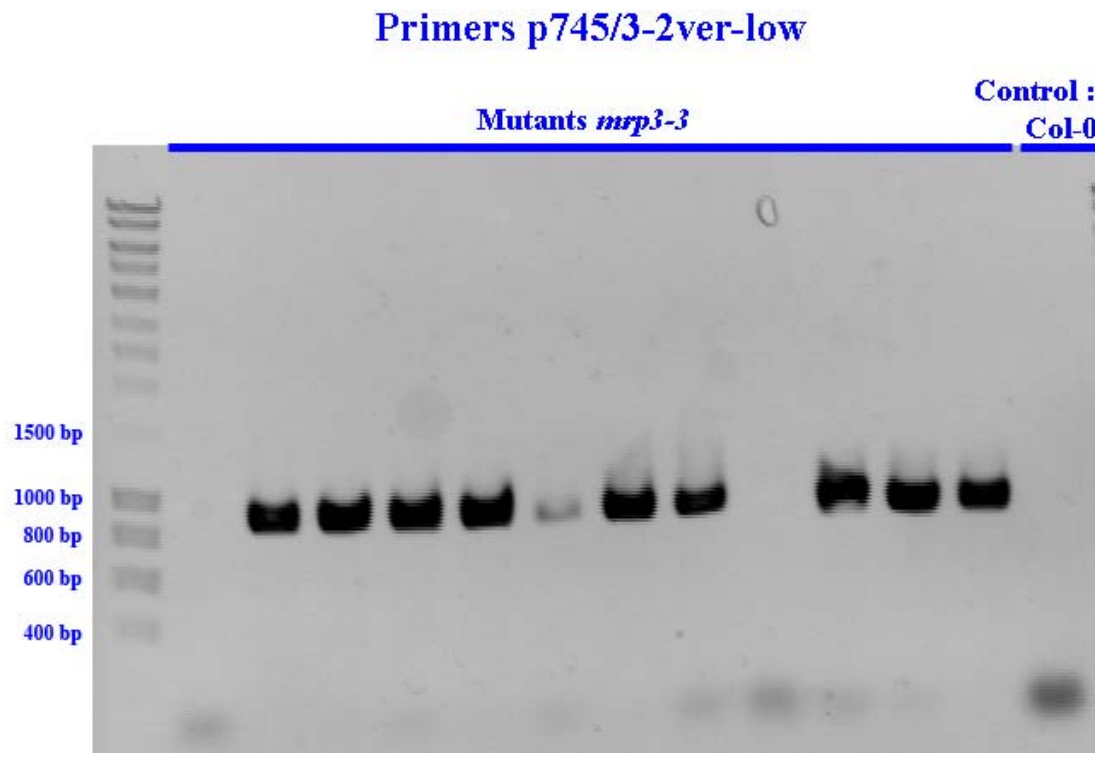

Figure III.8. : Results of PCRs with the primer pair p745/3-2ver-low. At least ten plants contain the pDS-Lox T-DNA.

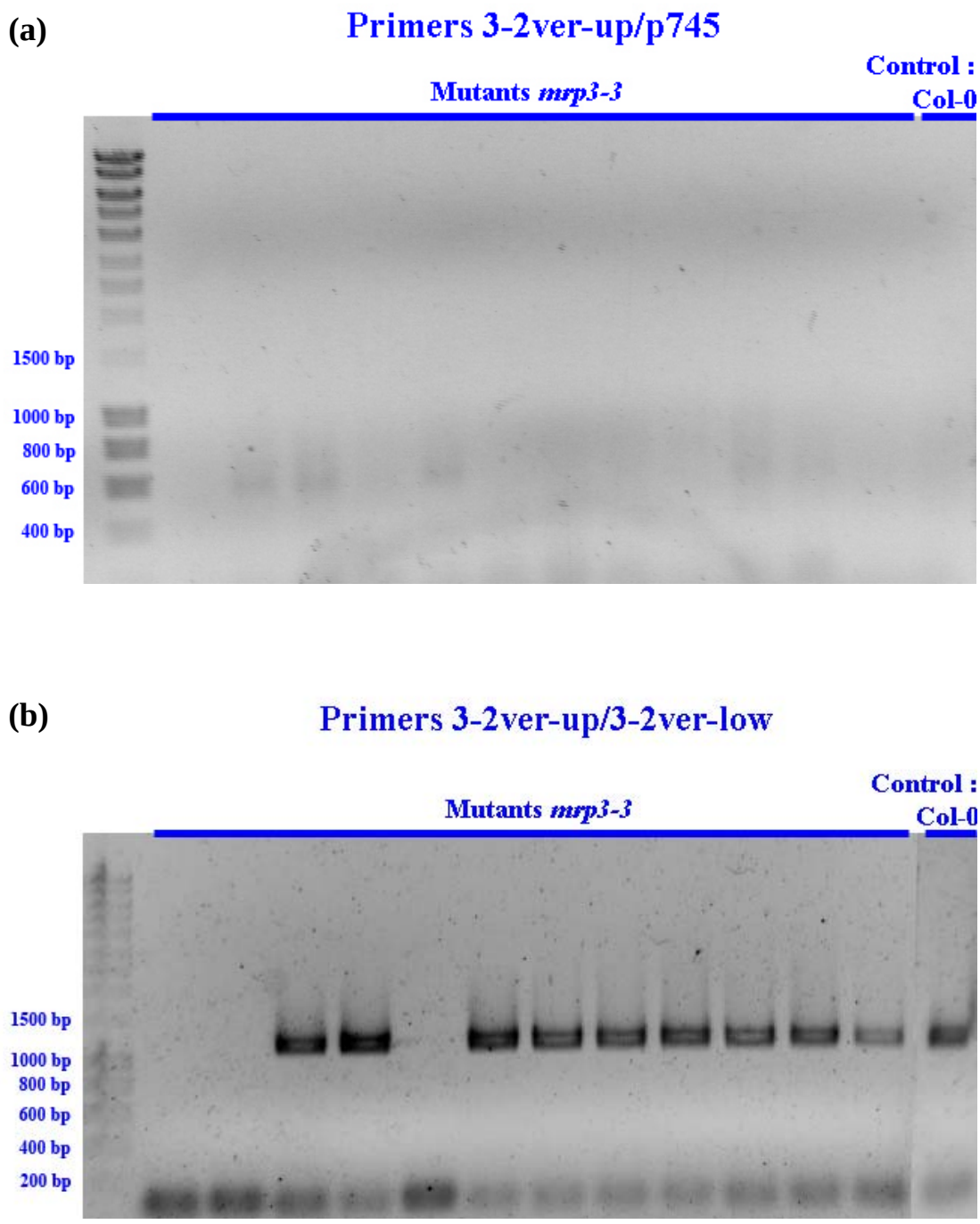

Figures III.9.(a) and (b) : Results of PCRs with with the primer pairs 3-2ver-up/p745 and 3-2ver-up/3-2ver-low. Lack of amplification with the pair 3-2ver-up/p745 confirms the orientation of the insertion deduced by the amplification of a fragment with the pair p745/3-2ver-low. Amplification with the combination 3-2ver-up/3-2ver-low reveals that nine plants contain an intact copy of the *AtMRP3* gene.

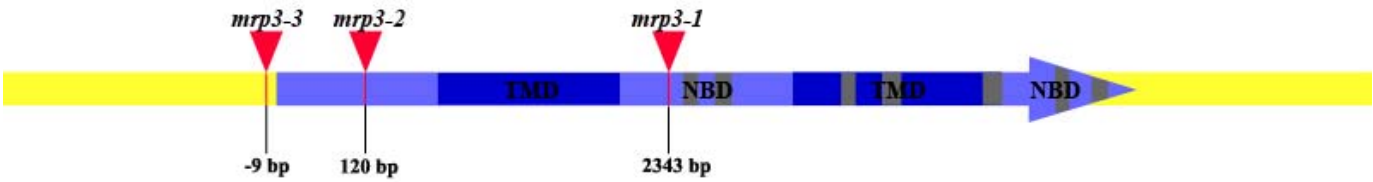

Figure III.10. : Summary of the positions of the insertions in the three mutant alleles of *AtMRP3*.

III.2.2. Additional assays to verify the position and number of the insertions

Segregation tests with the appropriate antibiotics were done on the offspring of the six *mrp3-1* mutants and the twelve *mrp3-2* mutants tested by PCR. 100% of the seeds of the mutants lines that were designated to be homozygous for the insertion by the PCR tests described above were resistant to the corresponding antibiotics. This confirms a homozygous presence of the T-DNA insertion in these two alleles. In contrast, about 75% of the offspring of the mutants that were demonstrated to be hemizygous for the insertion by genotyping PCR tests were resistant. 75% of resistance in the offspring of hemizygous plant is coherent with the Mendelian inheritance of a single T-DNA or transposon insertion each carrying one copy of the selectable marker. Thus, this is proof that *mrp3-1* mutants and *mrp3-2* mutant contain only a single insertion of the T-DNA or *Ds* transposon, respectively.

Another test for the homo- or hemizygosity of the six plants already examined by PCR, as well as a confirmation of the presence of the pCSA110 T-DNA in the *mrp3-1* mutants was obtained by DNA gel blot analysis. After digestion of the genomic DNAs with the restriction enzyme PstI, separate hybridisations of the digested DNA transferred to a nylon membrane with either ^{32}P-dCTP-labelled probe specific for the pCSA110 T-DNA, the GUS probe, or with a probe specific for the beginning of the *AtMRP3* gene was performed. The T-DNA-specific probe was generated by digestion of the vector pCambia 1305.1 with the restriction enzymes SpeI and NheI. The *AtMRP3*-specific probe, the 3C probe, corresponded to a DNA

fragment spanning the positions +579 to +995 of the *AtMRP3* gene and was generated by a PCR with the primers 3C-s/3C-as.

After hybridisation, the T-DNA-specific probe detected a single band corresponding to the predicted length (2790 base pairs) of the pCSA110 fragment that should hybridize with the GUS probe after digestion with PstI. This is a confirmation of the presence of the pCSA110 T-DNA in the *mrp3-1* mutants.

After hybridization with the *AtMRP3* specific probe (3Cn probe), a single band was detected in the T2 offspring that were PCR genotyped as homozygous *mrp3-1* mutant lines while two bands appeared in the lines identified as hemizygous offspring by PCR genotyping thus detecting the wild-type as well as the mutated *mrp3* allele. The slightly larger positively hybridising DNA fragment in the hemizygous lines corresponds in size to a fragment detected in the Col-0 wild-type and thus represents the wild-type allele. The length of this fragment corresponded to the predicted length (3312 base pairs) of the *AtMRP3* fragment that should hybridize with the 3C probe after digestion with PstI of the *AtMRP3* intact gene. Consequently, the lower migrating hybridisation signal detected in all *mrp3-1* lines but absent in the wild-type corresponds to the T-DNA allele. However, this lower band is much longer than the predicted length (2127 base pairs) of the fragment containing a piece of the *AtMRP3* gene and a piece of pCSA110 that should hybridize with the 3C probe after digestion with PstI of the mutated *mrp3* allele. We can hypothesize that some duplication phenomenon happened at the right border of the T-DNA upon insertion, which increases the size of the digested fragment. This hypothesis is supported by our lack of success to amplify a fragment by PCR with the right border specific primer (see previous paragraph).

Taken together, the DNA gel blot analysis confirms the results of the genotyping PCRs and the segregation tests for the *mrp3-1* mutant allele (see Figures III.11. and III.12.(a) and (b)).

Physiological and molecular investigations presented in this thesis were subsequently performed using homozygous offspring of the three *mrp3* alleles detected.

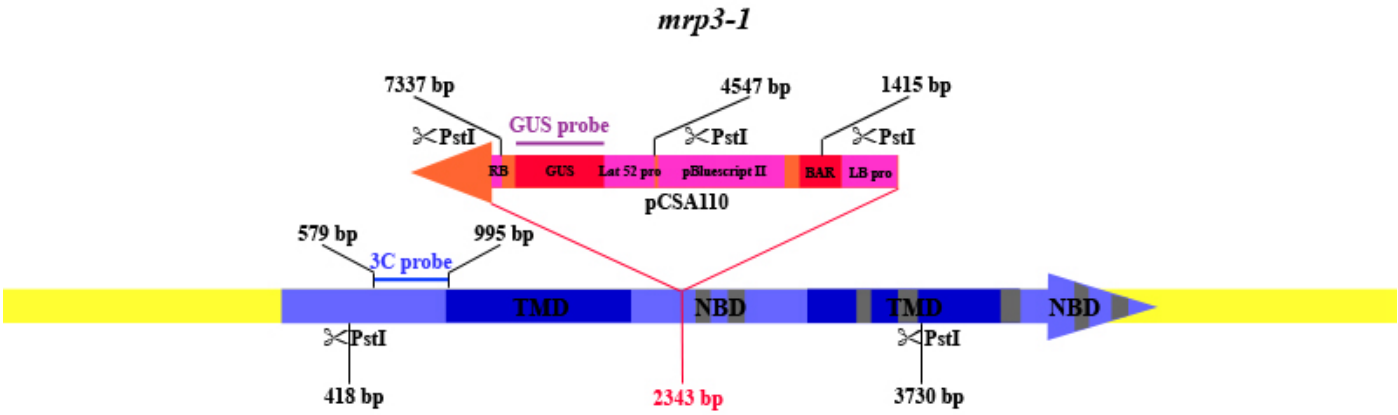

Figure III.11. : Scheme of the positions of the PstI restriction sites on the genomic *AtMRP3* gene and on the pCSA110 T-DNA. Hybridization probes used in DNA gel blot analysis (GUS and 3C probes) are indicated by thin lines. +1 corresponds to the A of the start codon for the positions indicated on the *AtMRP3* gene and to the first base of the left border for the positions indicated on the pCSA110 T-DNA.

(a)

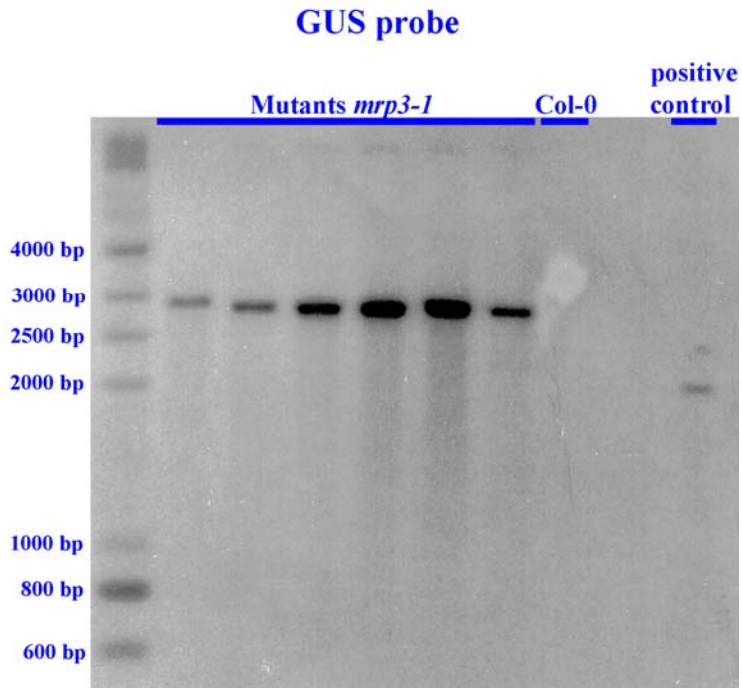

(b)

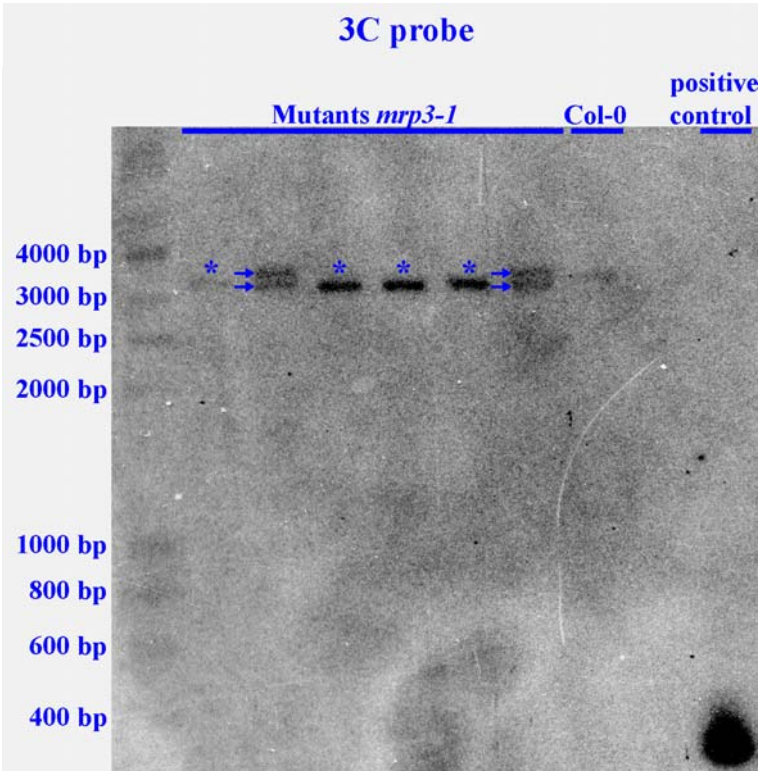

Figures III.12.(a) (upper panel) and (b) (lower panel) : Results of the DNA gel blot analysis with the labelled GUS probe (upper panel) and 3C probe (lower panel) indicating presence of the T-DNA and of the presence or absence of the *mrp3-1* allele, respectively. Positive controls : samples of unlabelled probes were either loaded on the gel (upper panel) or were spotted directly on the nylon membrane after transfer (lower panel). The untransformed Col-0 wild-type was added as a control indicating absence of the T-DNA in the upper panel and presence of the wild-type allele in the lower panel. Homozygous *mrp3-1* mutant lines are indicated with an asterisk. Hemizygous mutants are detected by the presence of two closely co-migrating hybridization signals indicated by arrows. The upper hybridization signal corresponds to the wild-type allele as it corresponds to the signal detected in Col-0.

III.3.1. Verification of the absence of transcription of *AtMRP3* in the mutant alleles

Subsequent to the genotypic investigation of the *mrp3* alleles, we sought to proof that all three mutants represented true null mutants by demonstrating absence of *AtMRP3* transcript. Due to the close homology between the *AtMRP* gene family which makes the application of hybridization probes for classical RNA gel blots doubtful, the presence and absence of *AtMRP3* transcripts was analyzed by the more sensitive reverse transcriptase PCR (RT-PCR method) performed on total RNA isolated from adult plants of the mutant alleles and the corresponding wild-types. By cloning and sequencing of the amplified fragment starting from wild-type RNAs, it was demonstrated before that the oligonucleotides AtMRP3-s and AtMRP3-as used for the PCR amplification specifically detected *AtMRP3* (Bovet et al., 2003).

In a first experiment, a two-step RT-PCR, RNA isolated from wild-types and mutants was reverse transcribed and the obtained cDNA was subsequently used in a PCR reaction containing the primers AtMRP3-s and AtMRP3-as, specifically detecting a 226 bp-fragment of the *AtMRP3* mRNA close to the translational stop codon (Bovet et al., 2003). As a control, a PCR reaction containing the primers S16-s and S16-as, specifically detecting a fragment of the At5g18380 mRNA (gene coding for a 40S ribosomal protein) (Bovet et al., 2003) was also carried out with this cDNA. After 35 cycles of the PCR reaction and electrophoretic separation on an agarose gel, a band of the correct size (226 base pairs) was apparent in both wild-types, Col-0 and Ler-0, while it was absent in *mrp3-2* and *mrp3-3* indicating presence and absence of *AtMRP3* transcript in total RNA isolated from wild-types and the two mutant alleles, respectively. However, a weak band of correct size was detected in the *mrp3-1* allele (Figure III.14.). Moreover, in the cDNAs of Col-O, Ler-0 and *mrp3-1* but not *mrp3-2* and *mrp3-3* a second fragment of around 400 base pairs was weakly amplified. This larger fragment neither corresponds to predicted fragment present in the mRNA of *AtMRP3*, nor to the length of the genomic fragment and thus does not represent genomic contamination.

In order to investigate in more detail presence or absence of *AtMRP3* transcript in the *mrp3-1* allele, a “one-step” RT-PCR was performed on RNA of all lines using the specific primers 3-1ver-up and LMRP3A_as (Figure III.13.), which amplifies a 305 bp fragment of the *AtMRP3* mRNA spanning the site of the T-DNA insertion in *mrp3-1*. In the one-step procedure, reverse transcription and subsequent amplification (40 cycles of amplification in

our case) took place in the same tube directly starting with *AtMRP3*-specific primers; thus reverse transcription only produced cDNA fragments corresponding to *AtMRP3*. In both wild-type RNAs, but not in the *mrp3-1* RNA one-step RT-PCR detected two fragments. The stronger band corresponded in size to the predicted fragment of the *AtMRP3* mRNA while the weaker, larger fragment could represent either contamination with genomic DNA or unspliced *AtMRP3* RNA. Since both fragments were lacking in the *mrp3-1* mutant, it was hypothesized that the integration of the T-DNA prevented synthesis of a functional *AtMRP3* transcript while the weak detection of transcript using the primer pair AtMRP3-s and AtMRP3-as amplifying a fragment downstream of the insertion site could be due to residual transcription of the 3'-region of the *AtMRP3* gene starting from a promoter within the T-DNA. In this case, we could still consider the *mrp3-1* allele as true null allele, since it would lack the first two TMDs and part of the first NBD of the full size protein and thus should be functionally inactive.

In contrast to the conventional two-step RT-PCR with the AtMRP3-s and AtMRP3-as primer pair, one-step RT-PCR detected the 500 and the 300bp-fragment in the RNAs isolated from the *mrp3-2* and *mrp3-3* mutants. However, in this case, the band corresponding to the *AtMRP3* mRNA was clearly weaker. We thus concluded that the *mrp3-2* and *mrp3-3* mutants could have some residual transcription of this region of the *AtMRP3* gene from internal promoters active in the inserted DNA fragments (transposon and T-DNA, respectively), but clearly to a lower level than in the wild types (see Figures III.13. and III.14.). However, since the AtMRP3-s and AtMRP3-as primer pair did not detect transcript in these alleles, *AtMRP3* transcription did not proceed to the end of the *AtMRP3* open reading frame.

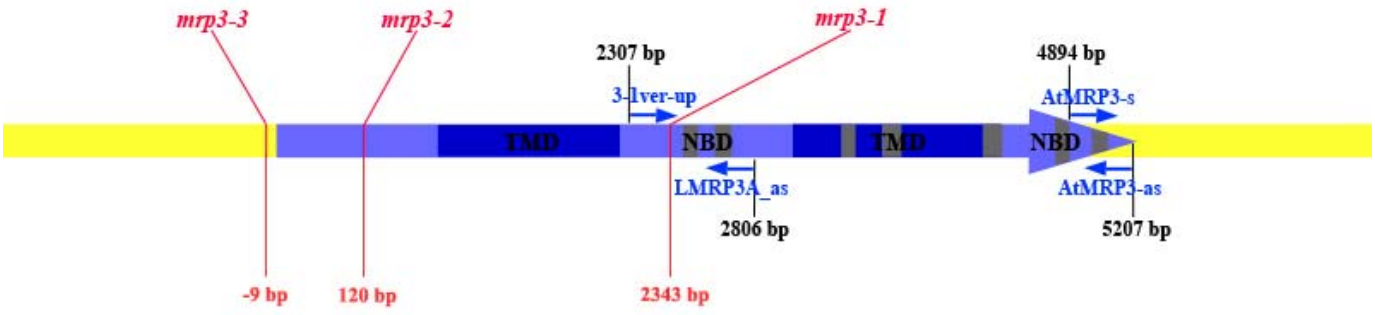

Figure III.13. : Schematic positions of the primers used to test the presence or absence of transcript in the AtMRP3 mutants.

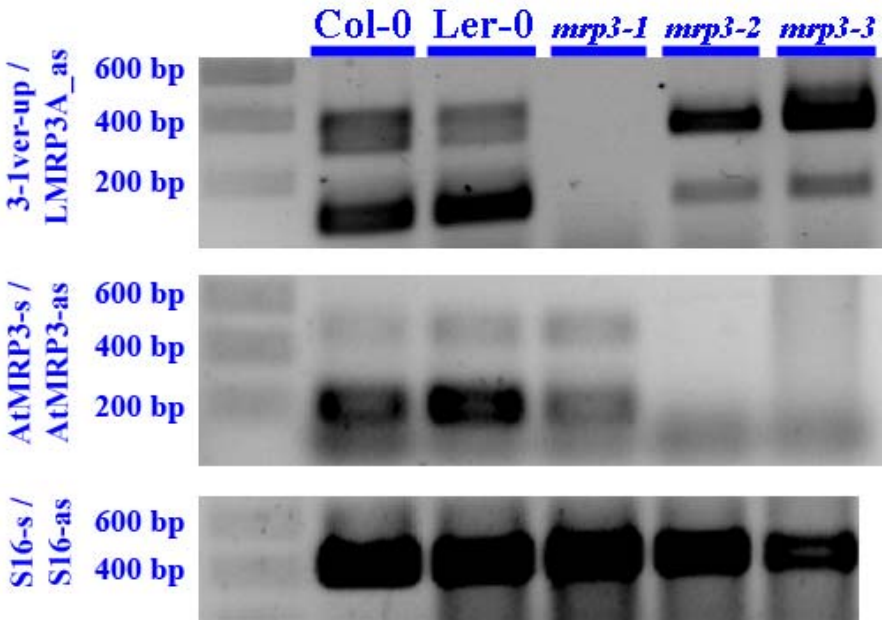

Figure III.14. : RT-PCR analysis demonstrates presence and absence of *AtMRP3* transcript in wild-type and mutant RNAs. Upper panel : results of the "one step" RT-PCRs carried out on wild-type and mutant RNAs with the primers 3-1ver-up and LMRP3A_as (40 amplification cycles). Middle panel : results of the RT-PCRs carried out on the cDNAs prepared from wild-type and mutant RNAs with the primers AtMRP3-s and AtMRP3-as (35 amplification cycles). Lower panel : control : results of the RT-PCRs carried on the cDNAs prepared from wild-type and mutant RNAs with the primers S16-s and S16-as (35 amplification cycles).

Taken together, it was concluded that no full-length *AtMRP3* transcript was present in the *mrp3-1*, *mrp3-2* and *mrp3-3* mutant alleles. However, since partial transcripts were detected, a RNA gel blot analysis with a probe uniquely detecting *AtMRP3* is necessary to unequivocally demonstrate the absence of a functional full-length *AtMRP3* transcript.

IV. Growth of wild-type and mutant plants submitted to cadmium or prosulfuron stress

Since there is no evident phenotype distinguishing the *AtMRP3* knockout alleles and their corresponding wild-types under normal growth conditions, and since the AtMRP3 protein is supposed to play a role in heavy metal and organic xenobiotic detoxification, series of growth experiments were performed with plants submitted to these two specific stresses. The basic hypothesis is that knockout plants will suffer more from these stresses than the corresponding wild-types.

Cadmium (in its ionic form Cd^{2+}) and prosulfuron were chosen as the stressors due to their well demonstrated property to induce *AtMRP3* transcription (Bovet et al., 2003 ; Glombitza et al., 2004). Furthermore, AtMRP3 is known to restore resistance to cadmium in sensitive yeast mutants (Tommasini et al. 1998). The majority of these growth experiments were performed using only the *mrp3-1* and *mrp3-3* mutant alleles and their corresponding wild-type, Col-0.

IV.1.1. Preliminary experiments

Several series of preliminary experiments were performed to establish the best conditions for growth experiments on plates, in order to highlight differences between mutants and wild-type plants. Different compositions of agarose media were tested, with several concentrations of sucrose and several concentrations of the toxic compounds. The transfer of seedlings, germinated in a first step on a medium without the toxic compounds, to the stressing media containing the chosen concentration of toxic compound was compared to the direct germination of the seedlings on the stressing media. Growth of the seedlings was monitored during two weeks, in order to spot the best time point to highlight a phenotype.

Some trends were observed in these preliminary experiments. First, concerning our basic hypothesis, it appeared that the *mrp3-1* and *mrp3-3* mutants were more sensitive to the chosen stresses than Col-0. Col-0 tended to have an overall “healthier” appearance than the mutants, when submitted to stress, producing more lateral roots and greener leaves. However the length of the main root was not much affected. The plants began to be clearly affected by the two agents at a concentration of 30 µM $CdCl_2$ and of 1,5 nM prosulfuron in media containing 0,5% sucrose. Furthermore, under these conditions, the differences between mutants and wild-type plants were apparent. Adding $CdCl_2$ and prosulfuron at concentrations of 60 µM and 6 nM respectively to media containing 0,5% sucrose, led to a disappearance of the difference in growth between the mutants and wild-type seedlings. The differences between

mutants and wild-type were more pronounced with prosulfuron stress than in the presence of cadmium. 45 µM $CdCl_2$ and 4 nM prosulfuron in media containing 0,5% sucrose were chosen as the best concentrations to repeat the experiments, since these conditions resulted in the most clear differences of phenotypes.

A second observation was the tendency of sucrose in the media to reduce the differences in phenotype : sucrose seemed to help the mutants to compensate their increased sensitivity to xenobiotic stresses. For example, a quite clear phenotype was observed on a medium without sucrose and with 30 µM Cd^{2+} and the phenotype almost completely disappeared when 1% sucrose was added to the medium. The same was observed with low concentrations of prosulfuron. This was quite problematic : seeds deposited on a medium without sucrose do not start to germinate all at the same time and this distorts the results of the growth experiments (see Figures IV.1.(a) to(c)). The strategy to germinate the seedlings on a medium with sucrose and without stress first and to transfer them to a medium without sucrose and with the chosen concentration of toxic compound three days later was tested but was not satisfactory : the difference in phenotype was very diminished under these conditions (see Figures IV.2.(a) to (e)). Finally the compromise to add only 0.5% sucrose in the media, resulting in even germination of seedlings but with a minimal compensation of the phenotype, was adopted.

A third observation, already experienced when seedlings were transferred from germination to stress medium, was the fact that the observed difference between wild-type and mutants tended to disappear with increasing development and growth of the seedlings : the phenotype was most pronounced in the early stages of growth. A time point of ten days of growth was finally chosen as the most appropriate to do the measurements.

The most evident observation in these preliminary experiments was that the phenotype of increased sensitivity against xenobiotics of the mutants was not very reproducible. Sometimes, in a series of plates the phenotype appeared clearly, and sometimes, using the same conditions, the mutants grew like wild-type plants. This is maybe due to a variability in the concentration of the toxic compound in the media available for absorption into the seedlings : the toxic compounds (especially cadmium) could be complexed to a certain extent by the agarose of the medium and hence a very small variation in the agarose concentration of the medium, which is nearly unavoidable, could result in a considerable variation of the concentration of free toxic compound which can affect growth. This variability could also be due to the differences in storage compound accumulation in seeds, despite the fact that we used comparable batches of seeds in all experiments. The effect of variable light exposure as a

cause for the phenotype was excluded : the variable phenotype was observed whatever position the seedling on the plates had relatively to the light. Furthermore, plates were regularly moved to ensure an equal light exposition.

In conclusion to this chapter, we can say that the reduced growth phenotype in the mutants was only visible when the stress of the xenobiotic was already high enough to affect the growth of wild-type plants and that the difference between wild-type and mutant is visible only in a small concentration "window".

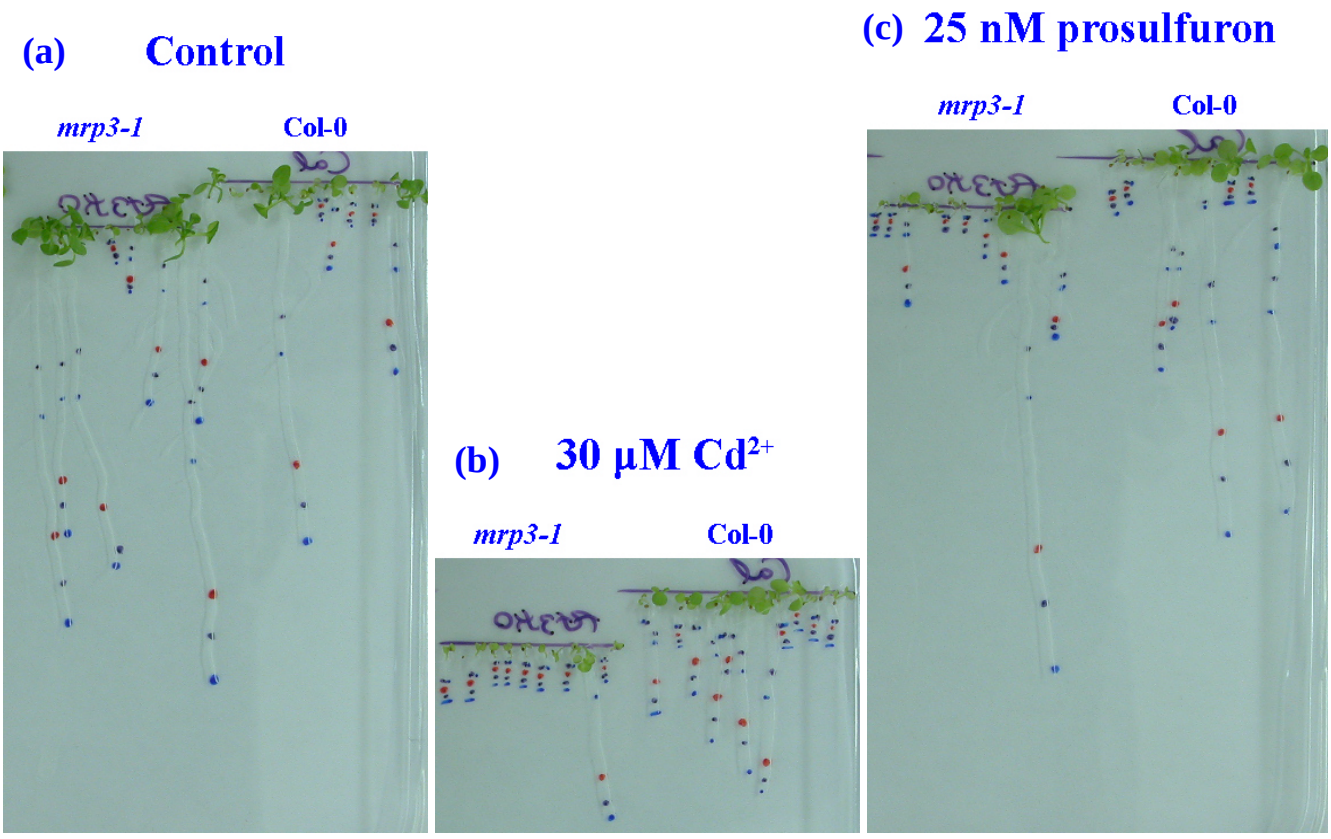

Figures IV.1.(a) to IV.1.(c) : Growth of mutant and wild-type seedlings on media containing no sucrose and variable concentrations of xenobiotics. 13 days of growth on media without sucrose and with the indicated concentrations of Cd^{2+} or prosulfuron. Colored dots were drawn regularly to visualize growth speed of the roots. The tendency to better growth and health of the wild-type seems clear (longer roots, larger leaves). But the controls show the very uneven germination time on a medium without sucrose for all alleles.

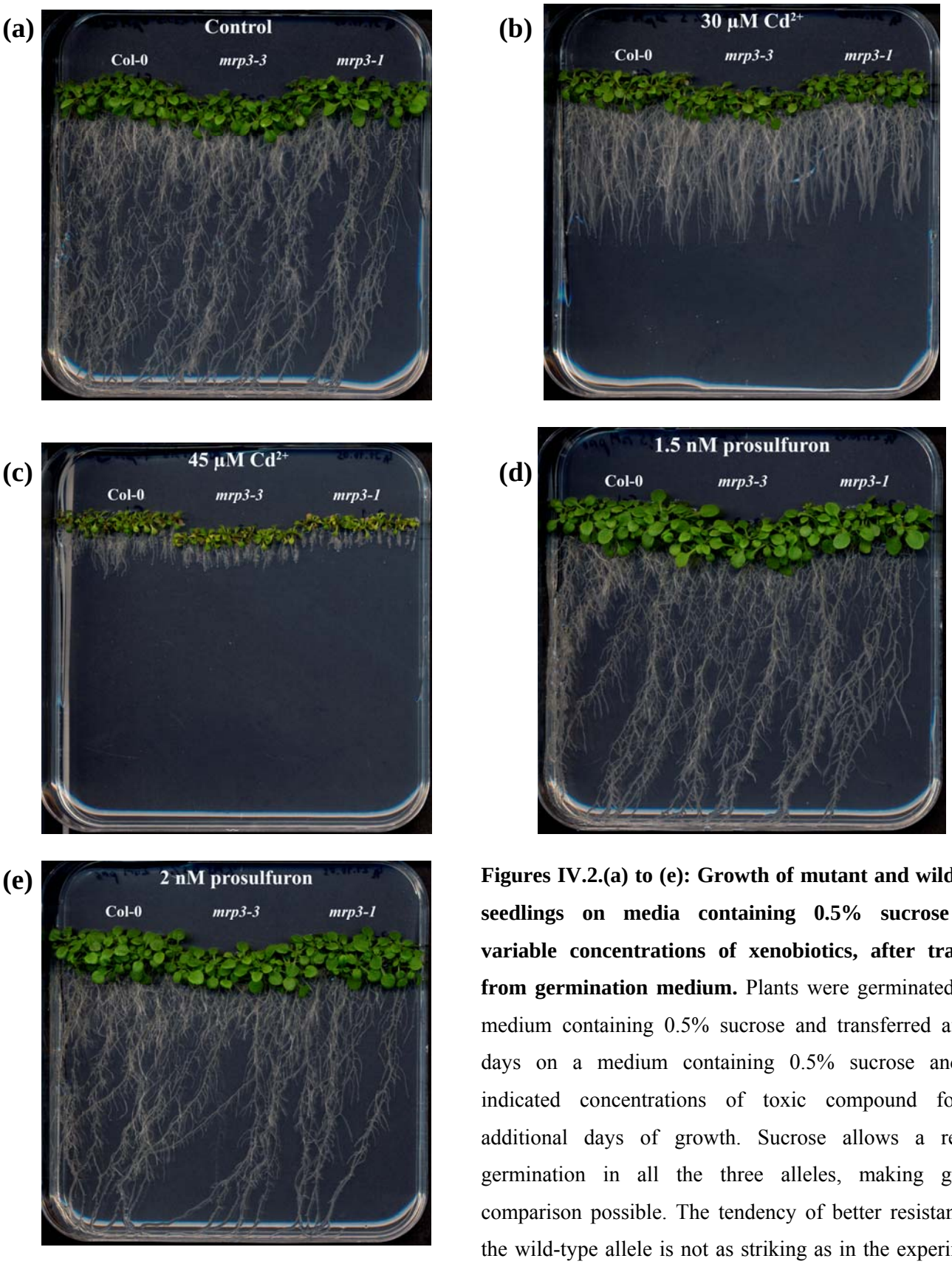

Figures IV.2.(a) to (e): Growth of mutant and wild-type seedlings on media containing 0.5% sucrose and variable concentrations of xenobiotics, after transfer from germination medium. Plants were germinated on a medium containing 0.5% sucrose and transferred after 3 days on a medium containing 0.5% sucrose and the indicated concentrations of toxic compound for 14 additional days of growth. Sucrose allows a regular germination in all the three alleles, making growth comparison possible. The tendency of better resistance of the wild-type allele is not as striking as in the experiments without sucrose, but is still visible. It manifests itself essentially by a greater "root density", meaning more lateral roots and root hairs in the wild-type seedlings. This better growth is verifiable visually but hard to quantify : primary root length is statistically the same in wild-type and mutant seedlings.

IV.2.1. Main experiments

Finally, for the main experiments, the following conditions were chosen : (i) for cadmium stress : 45 µM $CdCl_2$, 0,5% sucrose in the medium, ten days of growth (ii) for prosulfuron stress : 4 nM prosulfuron, 0,5% sucrose in the medium, ten days of growth. In both cases seeds were germinated directly in the presence of the toxic compound.

As a measure of global fitness, the chlorophyll content of each germinated seedling was determined.

As before, rather large differences were observed between the different experiments. Therefore we analysed the results of all series taken together, but also the results of each series of experiments separately. All series were carried out with the *mrp3-1* and *mrp3-3* alleles and their corresponding wild-type Col-0, except in a final series were the *mrp3-2* allele and its corresponding wild-type Ler-0 were included.

IV.2.2.Col-0, *mrp3-1* and *mrp3-3* in control condition

Looking at all series together, in the condition without stress, a statistically significant difference between the three alleles Col-0, *mrp3-1* and *mrp3-3* was observed. Col-0 had the highest overall chlorophyll content per seedling, while the chlorophyll content was lower in *mrp3-1* and *mrp3-3*. *mrp3-1* seedlings contained on average 16% less chlorophyll than Col-0 seedlings and *mrp3-3* seedlings containing on average 31% less than Col-0. When the series were analysed independently, a statistically significant difference was always observed between Col-0 and *mrp3-3*, in the condition without stress, but not always between Col-0 and *mrp3-1* or between *mrp3-1* and *mrp3-3* (see Figures IV.3. to IV.5.(b)).

IV.2.3.Effects of cadmium on Col-0, *mrp3-1* and *mrp3-3*

In the presence of 45 µM Cd^{2+}, no statistically significant difference was observed between these three alleles if all independent series of experiments were compared together. The same was true when we looked at the series independently, with only one exception in a series, where a statistically significant difference appeared, where Col-0 contained more chlorophyll than the *mrp3-3* allele. This was probably due to the fact that with 45 µM Cd^{2+} and 10 days of

growth we were no more in the "window" were the phenotype appears and all three alleles were too stressed (see Figures IV.3. to IV.4.(d) and IV.6.).

IV.2.4. Effects of prosulfuron on Col-0, *mrp3-1* and *mrp3-3*

In the presence of 4 nM prosulfuron, when all series were considered together, a statistically significant difference between the chlorophyll content of Col-0 and *mrp3-3* seedlings was observed, as well as between *mrp3-1* and *mrp3-3* seedlings, but not between Col-0 and *mrp3-1* seedlings. Here also, Col-0 had a higher chlorophyll content than the *mrp3-3* mutant allele, *mrp3-3* seedlings contained in average 66% less chlorophyll when compared to Col-0. This was much more than the difference observed in the condition without stress, confirming the previous results of diminished resistance to prosulfuron of *AtMRP3* mutants. However Col-0 and *mrp3-1* seedlings contained the same chlorophyll content. In contrast, the separate calculation of the averages in each series of experiments demonstrated a significant difference in chlorophyll content in three out of four series between Col-0 and *mrp3-3* and in one series out of four between Col-0 and *mrp3-1*. In that case the chlorophyll content of *mrp3-1* seedlings was about the same as that of *mrp3-3* seedlings, confirming the trend of *mrp3-1* seedlings to exhibit an intermediate chlorophyll content, which is between that of Col-0 seedlings and of *mrp3-3* seedlings (see Figures Figures IV.3. to IV.4.(d) and IV.7.(a) and (b)).

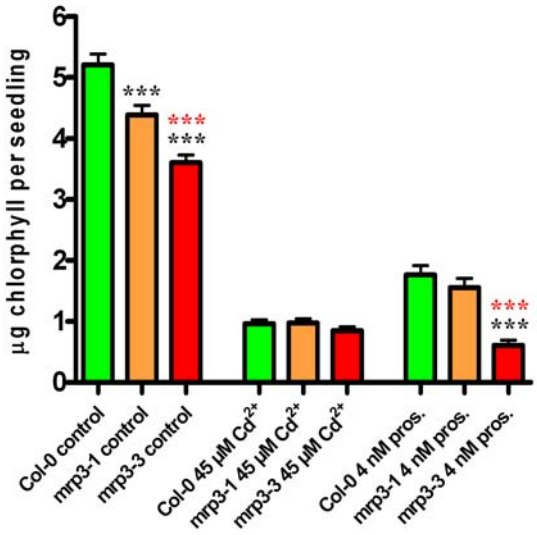

Figure IV.3. : Average chlorophyll content of the seedlings of Col-0, *mrp3-1* and *mrp3-3* alleles exposed to cadmium and prosulfuron, all series of experiments taken together. Averages are depicted together with their standard errors of the mean. Black stars indicate a statistically significant difference between Col-0 and a mutant, red stars indicate a statistically significant difference between

the two mutant alleles. Number of stars represent the "degree of significance" (one star : P value < 0.05 , two stars : P value < 0.01 , three stars : P value < 0.001 ; statistical test : Mann Whitney test).

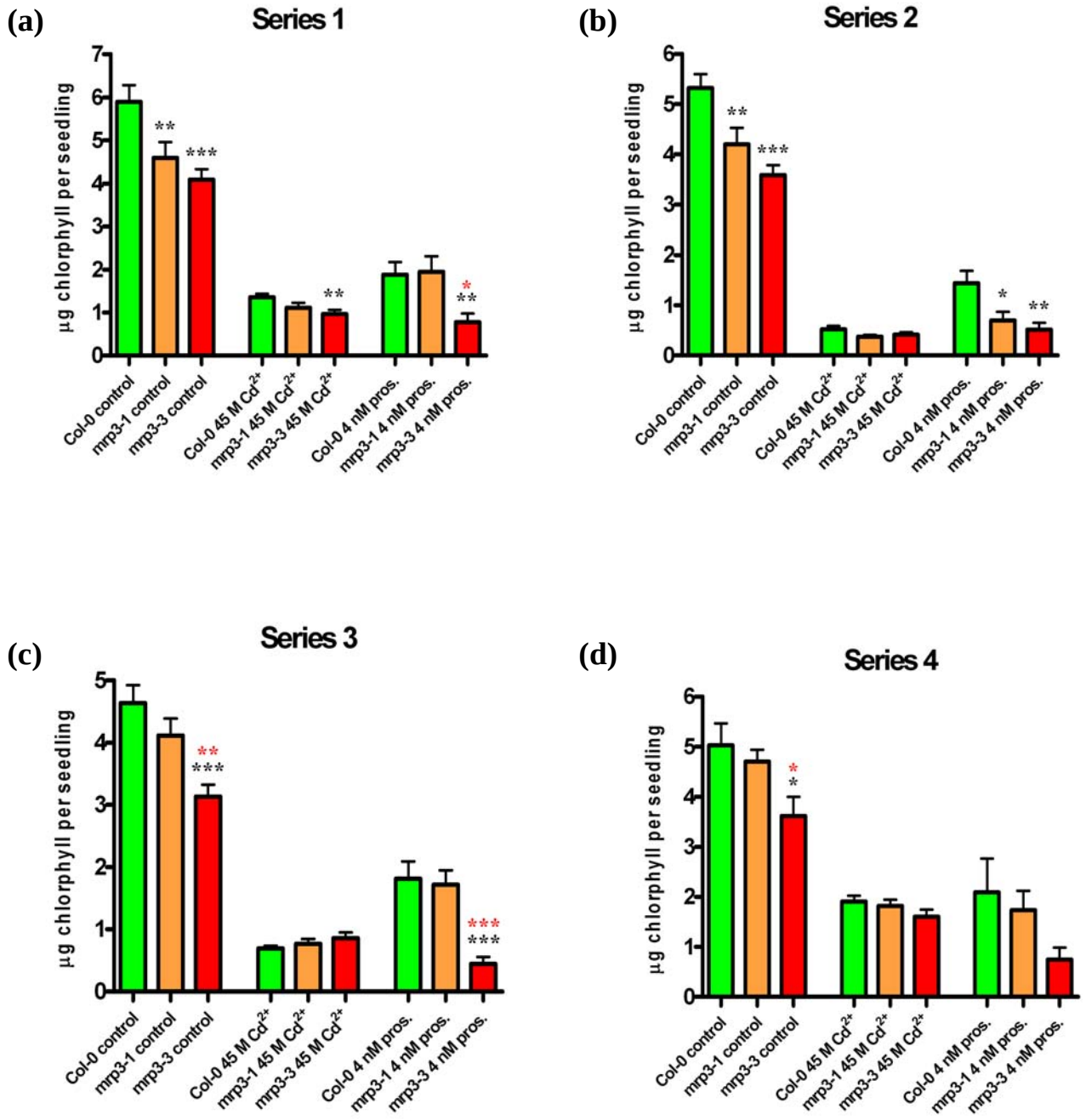

Figures IV.4.(a) to (d) : Average chlorophyll content of the seedlings of Col-0, *mrp3-1* and *mrp3-3* alleles exposed to cadmium and prosulfuron, all series of experiments analysed separately.

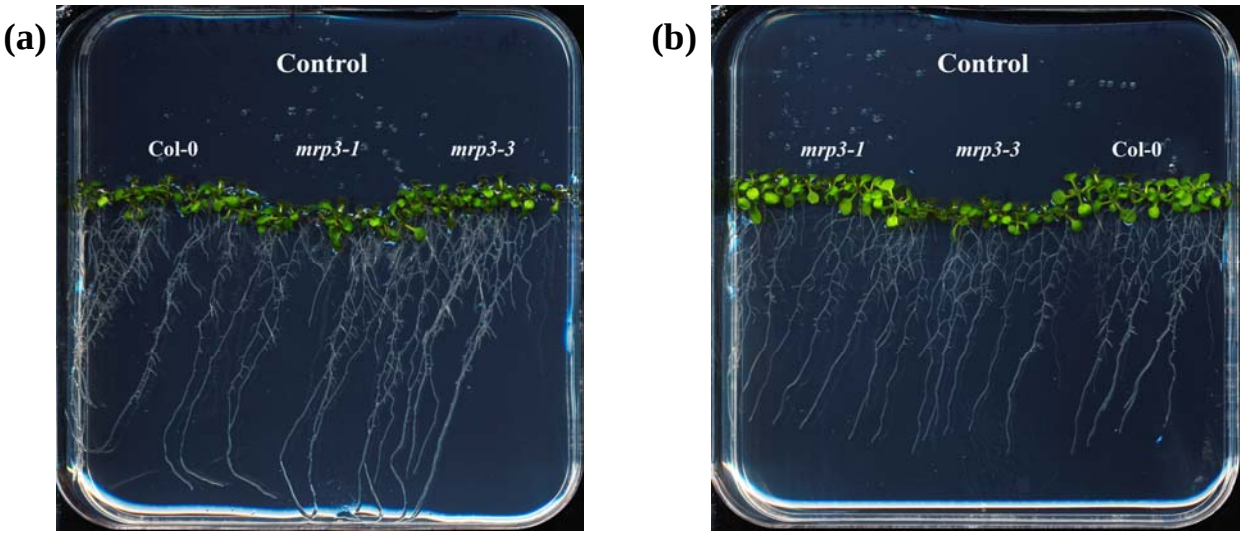

Figures IV.5.(a) and (b) : Control plates of the second series of experiments. Plants were directly germinated and grown 10 days on ½ MS / 1% (w/v) sucrose medium.

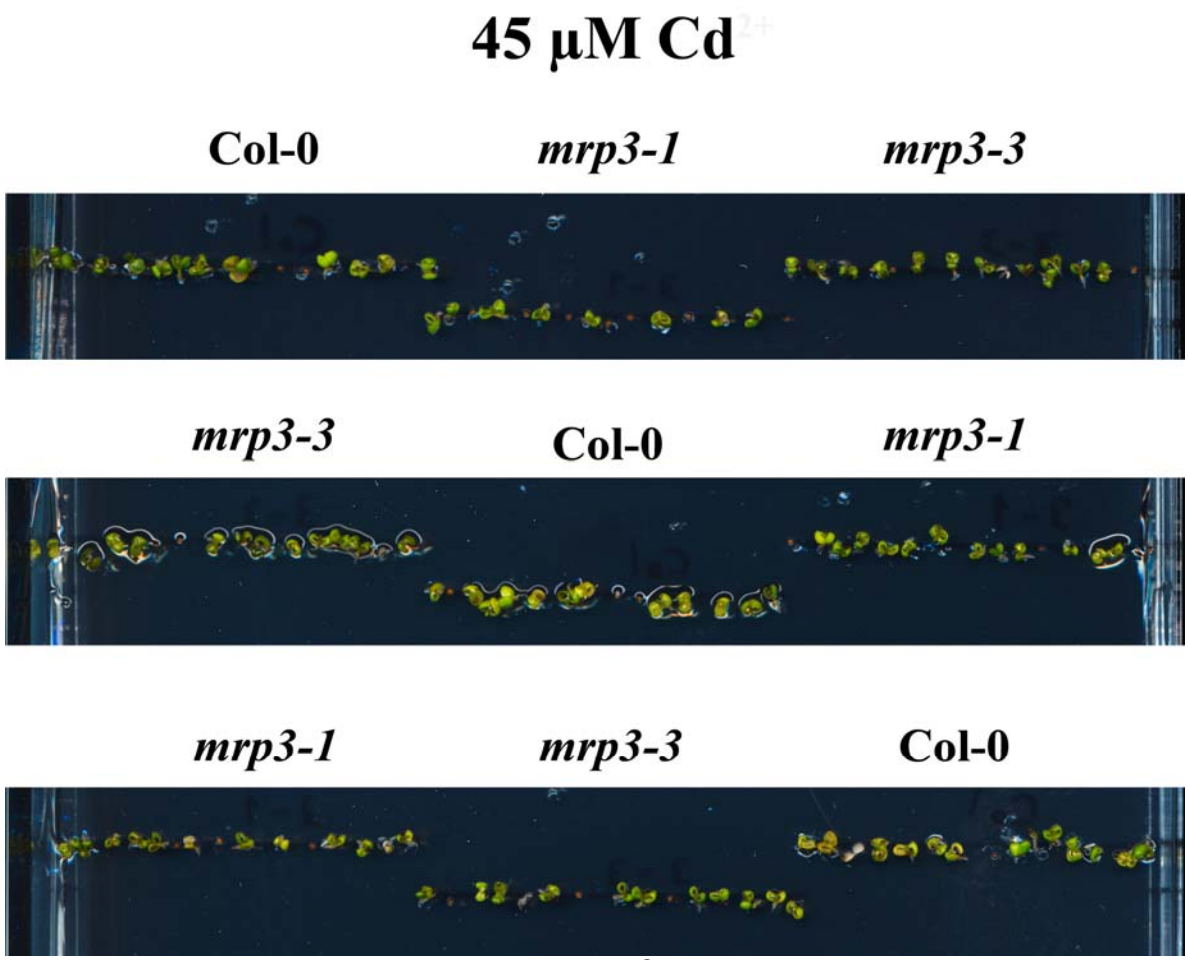

Figure IV.6. : Details of the plates with 45 µM Cd^{2+} of the second series of experiments. Each panel shows all the seedlings on one of the plates. Plants were directly germinated and grown 10 days on ½ MS / 1% (w/v) sucrose medium with 45 µM $CdCl_2$. The pictures are enlarged to allow to see the very small seedlings : their growth is drastically limited due to cadmium stress.

(a)

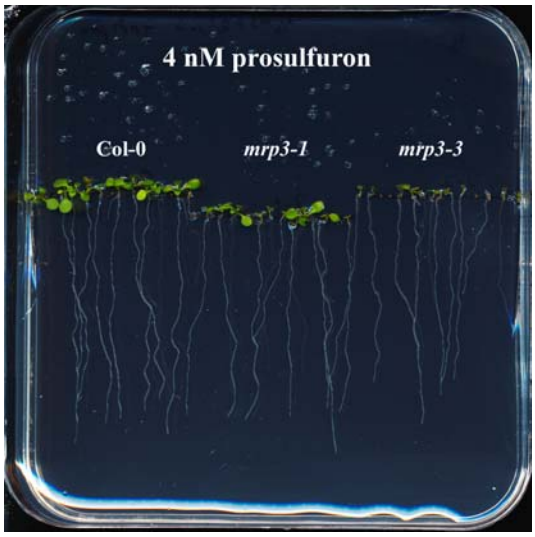

(b)

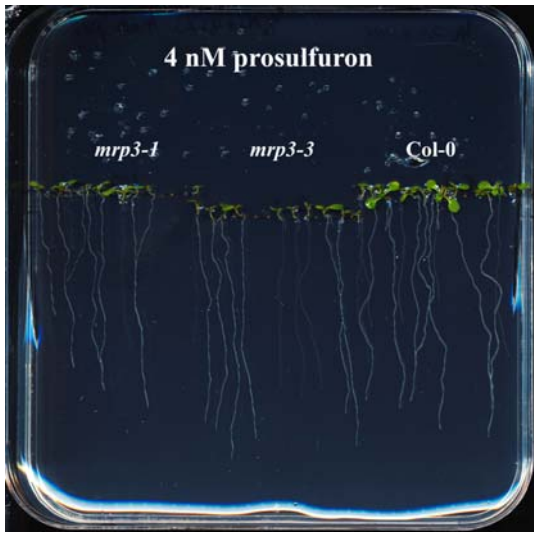

Figures IV.7.(a) and (b) : Plates with 4 nM prosulfuron of the second series of experiments. Plants were directly germinated and grown 10 days on ½ MS / 1% (w/v) sucrose medium with 4 nM prosulfuron.

IV.2.5. Ler-0 and *mrp3-2*

No significant difference in the average chlorophyll content of Ler-0 and *mrp3-2* seedlings was observed in the absence or presence of 4 nM prosulfuron. In contrast, a significant difference appeared in the presence of 45 µM $CdCl_2$. Paradoxically and in contrast to the hypothesis of higher sensitivity in *mrp3* mutants, the *mrp3-2* mutant allele contained more chlorophyll than wild-type plants when exposed to Cd^{2+} (see Figure IV.8.). This contradicts all previous observations made on *mrp3-1* and *mrp3-3* mutants when compared to their wild-type. However it should be considered that only one series of growth experiment was conducted with the *mrp3-2* mutants, which is probably not enough, taking into account the high variability observed between series. Furthermore the Ler-0 ecotype (and thus the mutants derived from this ecotype) reacts differently to cadmium and prosulfuron stress when compared to Col-0. This ecotype is evidently more resistant to cadmium stress and we may not be in the action "window" of stress, where a hypothetical hypersensitivity phenotype of the mutant could be observed. With prosulfuron, on the contrary, we may have applied a too severe stress to observe differences between Ler-0 and *mrp3-2*. There is also the possibility that the genetic differences between Col-0 and Ler-0 are the cause of what is observed with Ler-0 and *mrp3-2* seedlings when these are exposed to xenobiotic compounds. AtMRP3 could for example have different roles in Ler-0 and Col-0. Another series of preliminary

experiments with various concentrations of toxics, of sucrose and various growth times should be performed to see whether the conditions could be optimized.

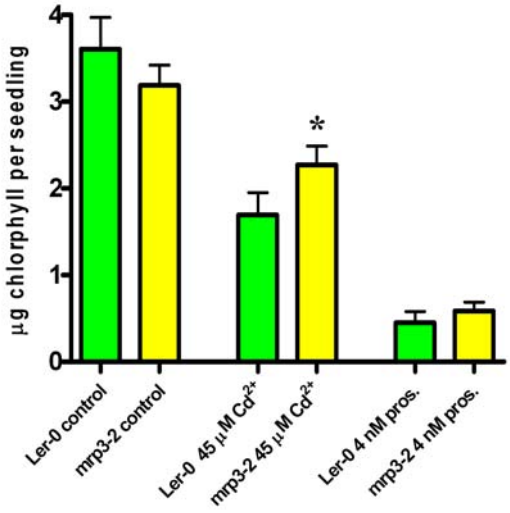

Figure IV.8. : Average chlorophyll content of the seedlings of Ler-0 and *mrp3-2* alleles exposed to cadmium and prosulfuron.

V. Transport and accumulation of cadmium in entire plants, comparison of mutants and wild-type

In the previous chapter, a trend to an increased cadmium resistance of the wild-type Col-0 when compared to the *AtMRP3* knock out mutants was visible. To gain further insight into the mechanisms underlying this process, we conducted a series of experiments designed to compare short and long term cadmium translocation and accumulation in the wild-type and mutants. These experiments were conducted on the level of entire plants, in conditions mimicking natural conditions, where cadmium enters the plants through the root system.

V.1.1. Short term accumulation of cadmium

To compare the short term transport and accumulation of cadmium in the wild-type and the mutants, experiments using radioactive cadmium were performed. A glassfiber filter imbedded in a solution containing 1mM $CaCl_2$, ⅛ MS and 10 µM $CdCl_2$ radiolabelled with $^{109}CdCl_2$ (final specific radioactivity : $3.7x10^7$ Bq/µmol) was deposited at the root tip of one week old Col-0 and *mrp3-1* seedlings which were grown under sterile conditions on square 12cm x 12cm plates in ½ MS medium containing 1% sucrose. After 2 hours, the filters were removed and the seedlings were incubated for a varying period of "recovery" : 2 hours, 8 hours or 24 hours. Subsequently, seedlings were exposed on screens for the "Cyclone Plus Storage Phosphor System" for autoradiographic detection of the radioactive cadmium absorbed by the seedlings. Afterwards, in order to quantify the amount of radioactivity in different plant parts, the seedlings were separated by cutting them into three segments : shoot and leaves, distal root (0 to 1 cm below the shoot) and proximal root including the $^{109}Cd^{2+}$ exposure zone at the root tip. Radioactivity in each part was quantified by liquid scintillation counting to analyse the distribution of radioactive cadmium.

In seedlings analysed 2 hours after contact with the filter, a very significant difference in the distribution of radioactive Cd^{2+} was observed when mutants were compared to the corresponding wild-type seedlings. This difference was striking when the autoradiographic imaging of the radioactivity in seedlings was considered and could be confirmed by radioactivity quantification. As seen in Figure V.1., Col-0 seedlings exhibited presence of radioactive Cd^{2+} in the shoot and especially in leaves. In contrast, *mrp3-1* seedlings contained very few $^{109}Cd^{2+}$ in the shoot : most of the radioactive ion remained in the proximal root, near the the contact point with the filters.

Liquid scintillation analysis of the $^{109}Cd^{2+}$ radioactivity in seedling segments and entire seedlings (see Figure V.2.) demonstrated that wild-type seedlings analysed 2 hours after of recovery accumulated around 3 times more cadmium in the root and shoot and 2 times more in the distal root segment than the mutants. Please note that under our experimental condition exposure of the distal root segment with the radioactivity-containing filter was carefully avoided suggesting that in this case, radioactivity in this segment is likely due to $^{109}Cd^{2+}$ translocation from the root tip upwards into the more distal regions of the root and into the shoot. Furthermore the overall cadmium accumulation was increased in wild-type seedlings. These seedlings contained 40% more radioactivity when compared to *mrp3-1* seedlings, while cadmium accumulation in the proximal root was not significantly different in wild-type and mutants. Strikingly, the root/shoot ratio of cadmium distribution is very different with a value of 5.3±0.8 for Col-0 and of 12.7±0.9 for *mrp3-1* (standard error : standard error of the mean ; see Figure V.2. and Table V.2.). This result suggests that in the absence of *AtMRP3*, cadmium is as well less efficiently absorbed as translocated into the upper plant parts.

Figure V.1. : Autoradiographic detection of $^{109}Cd^{2+}$ incorporated into wild-type and mutant seedlings after 2 hours of recovery. A clear difference in cadmium repartition was observed between mutants and wild-types : mutant translocated significantly less cadmium to their shoot, especially to the leaves ; a lower translocation to the distal root, below the shoot, in the mutants was also observable.

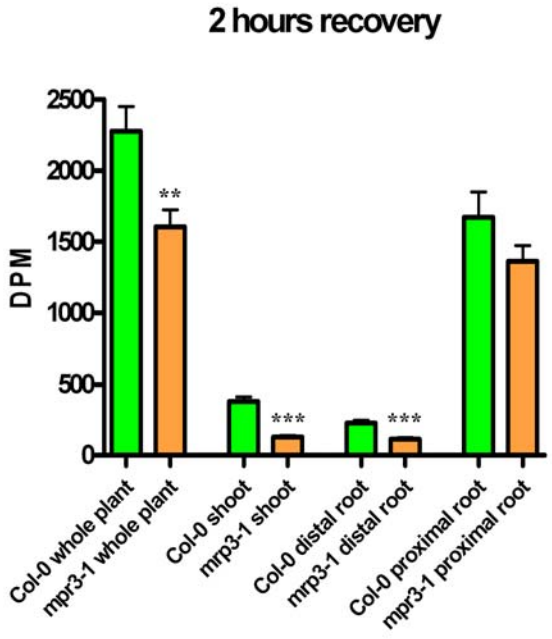

Figure V.2. : Quantification of the $^{109}Cd^{2+}$ radioactivity incorporated into wild-type and *mrp3-1* mutant seedlings 2 hours after exposure to radioactive Cd^{2+}. DPM= disintegrations per minute. Averages are depicted together with their standard errors of the mean. Black stars indicate a statistically significant difference between Col-0 and the mutant allele. The number of stars represents the "degree of significance" (one star : P value < 0.05 , two stars : P value < 0.01 , three stars : P value < 0.001 ; statistical test : Mann Whitney test). 30 seedlings per line were analysed.

Organ	Col-0	*mrp3-1*
Shoot	**17±1%**	**8±1%**
Distal root	**10±1%**	**7±1%**
Proximal root	**73±8%**	**85±7%**

Table V.1. : Proportion of cadmium in the different parts of the wild-types and the mutants with 2 hours of recovery. Average percentage in each segment of the seedlings with standard error of the mean. 100% = average of the total radioactive Cd^{2+} in one allele.

In contrast, 8 hours after exposure to the radioactive cadmium, no significant differences between wild-types and mutants in $^{109}Cd^{2+}$ distribution as well as quantity was observed. As expected, after a longer recovery period, the proportion of cadmium increased in the shoot

and leaves while it decreased in the root when compared to the 2 hours values reflecting a long-distance translocation of the heavy metal from the root to the shoot. This evolution in the $^{109}Cd^{2+}$ distribution was visible in the autoradiographic imaging and confirmed by radioactivity quantification (see Figures V.3. and V.4. and Table V.2.).

Figure V.3. : Autoradiographic detection of $^{109}Cd^{2+}$ incorporated into wild-type and mutant seedlings after 8 hours of recovery. No significant difference in cadmium repartion is visible between mutants and wild-types.

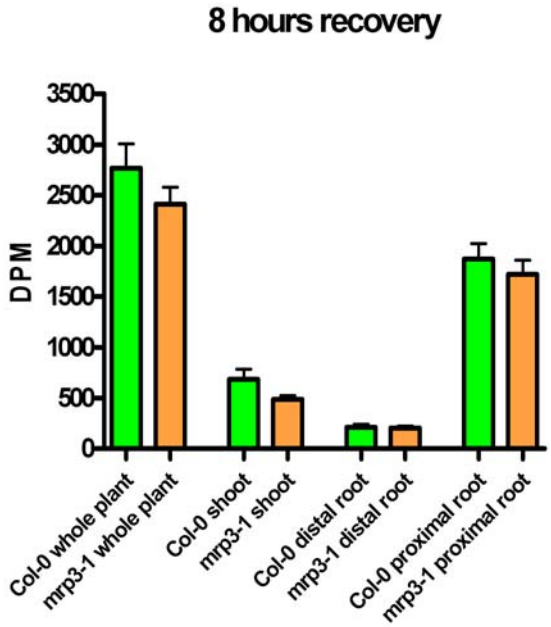

Figure V.4. : Quantification of the $^{109}Cd^{2+}$ radioactivity incorporated into wild-type and *mrp3-1* mutant seedlings after 8 hours of recovery. 15 seedlings per line were analysed.

Organ	Col-0	*mrp3-1*
Shoot	25±4%	20±1%
Distal root	8±1%	9±1%
Proximal root	68±5%	71±6%

Table V.2. : Proportion of cadmium in the different parts of the wild-types and the mutants with 8 hours of recovery.

24 hours after exposure to radioactive cadmium, the proportion of cadmium in the leaves of both mutants and wild-types increases even more, with a parallele decrease in the lower root, confirming the phenomenon of root to shoot translocation over time. A small significant difference is visible between the quantity of $^{109}Cd^{2+}$ in the *mrp3-1* proximal root and the quantity of $^{109}Cd^{2+}$ in the wild-type proximal root, due probably to a slightly higher fixation of cadmium at the site of absorption in the mutants (see Figures V.5. and V.6. and Table V.3.).

Figure V.5. : Autoradiographic detection of $^{109}Cd^{2+}$ incorporated into wild-type and mutant seedlings after 24 hours of recovery. A significantly higher quantity of radioactive cadmium is visible in the proximal root of the mutants, when compared to the wild-types.

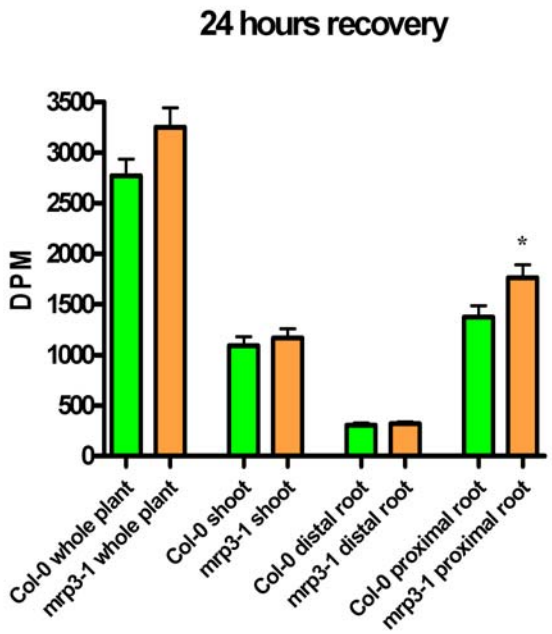

Figure V.6. : Quantification of the $^{109}Cd^{2+}$ radioactivity incorporated into wild-type and *mrp3-1* mutant seedlings after 24 hours of recovery. 30 seedlings per line were analysed.

Organ	Col-0	*mrp3-1*
Shoot	**39±3%**	**36±3%**
Distal root	**11±1%**	**10±1%**
Proximal root	**50±4%**	**54±4%**

Table V.3. : Proportion of cadmium in the different parts of the wild-types and the mutants with 24 hours of recovery.

V.2.1. Long term accumulation of cadmium

In order to compare long term accumulation of cadmium in the wild-type and the knock out mutants, experiments using plants grown in hydroponic cultures were performed. The experiments were carried out with the Col-0 and the *mrp3-1* allele, and, in some instances, also with the *mrp3-3* allele. Cadmium accumulation in the leaves and shoot was measured after harvesting by inductively coupled plasma-mass spectrometry (ICP-MS).

In a preliminary experiment only Col-0 and *mrp3-1* were analysed, with only one sample of six plants analysed by line and condition. The experiment was performed with 39 or 46 days old plants, the plants were first germinated under sterile conditions on plates and, after 13 days, transferred to hydroponic cultures with ½ MAMI medium. The plants were grown for 19 additional days in the ½ MAMI medium before they were either incubated with normal ½ MAMI medium (control condition) or supplied with medium containing 1 µM Cd^{2+}. Subsequently, plants were kept under these conditions for one or two weeks. Then, they were harvested, and cadmium concentrations in the leaves and shoots were measured by ICP-MS, each measurement being carried out on a pool of six plants. The *mrp3-1* plants supplied one or two weeks with a medium containg Cd^{2+} accumulated less cadmium than the wild-type plants exposed to the same conditions. Interestingly, cadmium concentration, both in *mrp3-1* mutants and in Col-0 plants, decreased with the longer exposure time to Cd^{2+}. Maybe this was due to the higher biomass of these plants : since they had one additional week to grow when compared to the plants exposed only one week to the medium containing Cd^{2+}, the cadmium could be distributed in more biomass and the additional cadmium absorbed in one additional week of exposure was not enough to compensate for the enhanced biomass (see Figure V.7.).

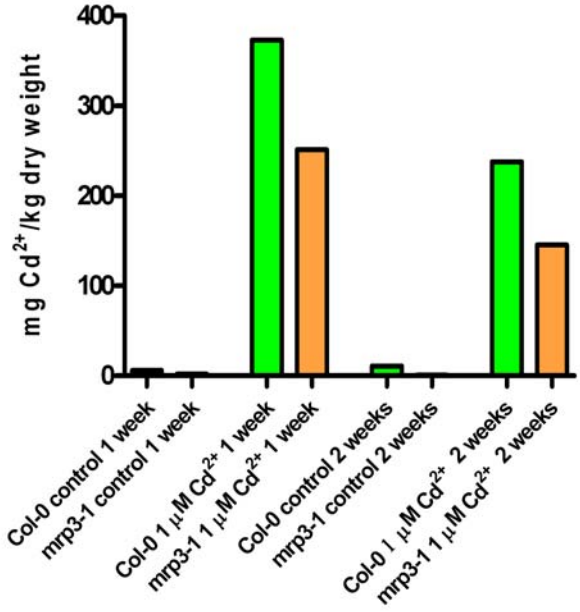

Figure V.7. : Quantification of cadmium in the shoots and leaves of plants cultivated in hydroponic culture : comparison between wild-type and mutant plants, preliminary experiment. Only one pool of plants per allele and condition was analysed.

On the basis of the preliminary experiment, we decided to determine cadmium accumulation after one week of exposure to the metal. Since growth experiments and short term cadmium transport experiments were done using the MS medium and since a protocol for using MS in hydroponic cultures was finally devised, we decided to use MS as a basis for the long term cadmium accumulation experiments. Plants of the Col-0 and *mrp3-1* alleles were used in these experiments, as well as plants of the *mrp3-3* allele for the low concentrations of cadmium.

The plants were first germinated under sterile conditions on plates and, after one week, transferred to hydroponic cultures with ⅓ MS medium. The plants were grown for 18 additional days in the ⅓ MS medium. The medium was then exchanged by ½ MS medium (older plants necessiting a more concentrated medium) and the plants were grown for 15 additional days. Finally, they were either incubated with normal ½ MS medium (control condition) or supplied with medium containing various concentration of cadmium : 0.5 µM Cd^{2+}, 1 µM Cd^{2+} or 2 µM Cd^{2+}. Subsequently, plants were kept under these conditions for one additional week. Then, these 47 days old plants were harvested, and cadmium concentrations in the leaves and shoots were measured by ICP-MS. Each measurement was carried out on a

pool of plants, to have enough material for the ICP-MS. Each pool was constituted either of four or of eight plants of the same line submitted to the same conditions.

In this experiment, a very interesting phenomenon was observed : the mutants accumulated indeed less cadmium in the leaves and shoots than the wild-types, but the difference was depending on the cadmium concentration supplied to the medium and appeared at concentrations above the threshold of 1 µM Cd^{2+}. Furthermore, raising the cadmium concentration from 1 to 2 µM increased the difference in cadmium in the aerial parts between Col-0 and *mrp3-1* (see Figure V.8.). This is perfectly consistent with the observations of the growth experiments presented in chapter IV., where the differences between wild-type and mutant plants could only be detected in a certain "window" of conditions, also above a given minimal concentration of Cd^{2+} in the medium.

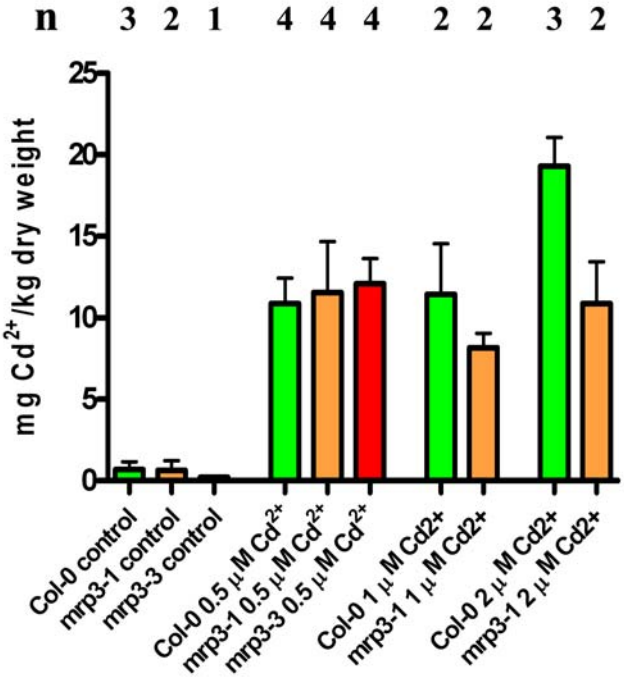

Figure V.8. : Quantification of cadmium in the shoots and leaves of plants cultivated in hydroponic cultures : comparison betwen wild-type and mutant plants, main experiments. Averages with standard deviations are given. A difference is observed between Col-0 and *mrp3-1* with 1 µM Cd^{2+} in the medium which is not statistically significant. The difference increases with 2 µM Cd^{2+} in the medium and is statistically significant. n = number of independent samples analysed for each condition. Each sample constituted of 4 or 8 plants.

Interestingly and in contrast to Cd^{2+}, the ICP-MS revealed no significant difference in the accumulation of any other metal between wild-type and mutants, with the exception of calcium : the mutants accumulated less calcium than the wild-type in the presence of 1 µM Cd^{2+} in the medium and raising cadmium concentration in the medium to 2 µM Cd^{2+} also increased this difference (see Figure V.9.).

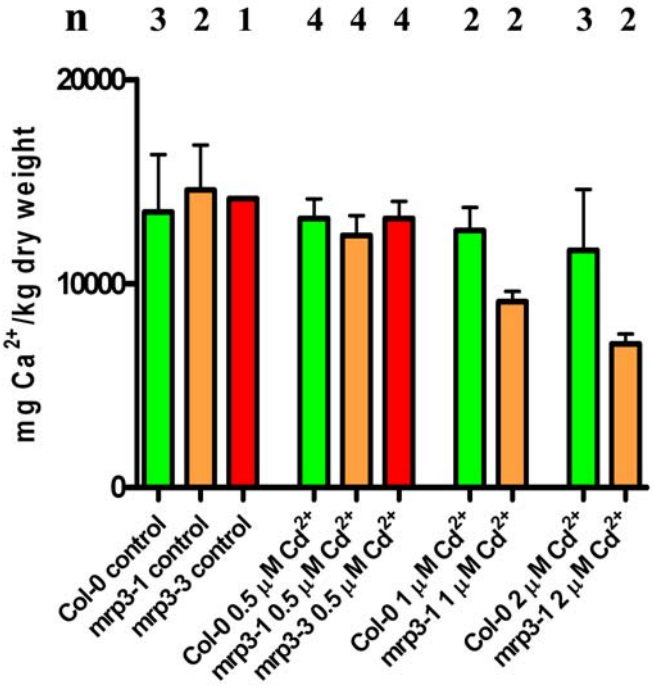

Table V.9. : quantification of calcium in the shoots and leaves of plants cultivated in hydroponic cultures : comparison betwen wild-type and mutant plants, main experiments. Averages with standard deviations are given. A statistically significant difference is observed between Col-0 and *mrp3-1* with 1 µM Cd^{2+} in the medium. The difference increases with 2 µM Cd^{2+} in the medium and is also significant. n = number of independent samples analysed for each condition. Each sample constituted of 4 or 8 plants.

VI. Cadmium transport in mutant and wild-type protoplasts

Based on the hypothesis that AtMRP3 mediates cadmium transport and since the protein is known to be expressed also in leaves, transport experiments with Col-0 and *mrp3-1* mesophyll protoplasts were carried out.

Protoplasts were incubated in a medium containing radioactive cadmium – $^{109}Cd^{2+}$ –, in the light, to provide energy to the protoplasts through photosynthesis. At defined time points, samples of protoplasts were taken and separated from the media through silicon oil centrifugation. Radioactivity in the protoplasts was then measured and the amount of Cd^{2+} taken up was calculated by dividing the radioactivity in the protoplasts by the specific radioactivity of Cd^{2+} in the protoplast suspension and by the volume of protoplasts in the suspension. The volume of protoplasts in the protoplast suspensions was measured by taking aliquots of the preparations and incubating them with tritiated water, which diffuses freely across the plasma membrane. Hence the radioactivity inside the protoplasts allows to calculate their volume.

A difference between wild-type and mutant was expected. If AtMRP3 represented a major Cd^{2+} transporter, a lower Cd^{2+} accumulation in *mrp3-1* protoplasts, when compared to wild-type protoplasts, would be an indication that AtMRP3 acts as a cadmium importer – in this case AtMRP3 could be located in the plasma membrane or in any other cellular membrane, the tonoplast being the most likely candidate. A higher accumulation in *mrp3-1* protoplasts would be an indication that AtMRP3 acts as a cadmium exporter – in that case AtMRP3 would most likely be located in the plasma membrane.

VI.1. Results

Four independent transport experiments with protoplasts were carried out. Time dependent Cd^{2+} uptake into protoplasts could be observed. However, no significant differences between mutant and wild type protoplast were recognised : at most time points concentrations of Cd^{2+} inside the protoplasts were identical in the two types of protoplasts. In a few experiments a significant difference in cadmium accumulation was detectable at certain time points, however, depending on the experiment, either wild-type or the mutant accumulated more of this heavy metal (see Figures VI.1 to VI.4.).

To summarize, no difference between wild-type and mutant was found for cadmium transport in intact protoplasts. Thus, AtMRP3 does not seem to act as a cadmium transporter in the

plasma membrane of mesophyll cells, neither as an importer nor as an exporter. Alternatively, the contribution of AtMRP3 in the overall Cd^{2+} into protoplasts is only marginal. Furthermore, these results suggest that AtMRP3 does not create a strong Cd^{2+} sink within the cell since such a sink could increase Cd^{2+} flux across the plasma membrane.

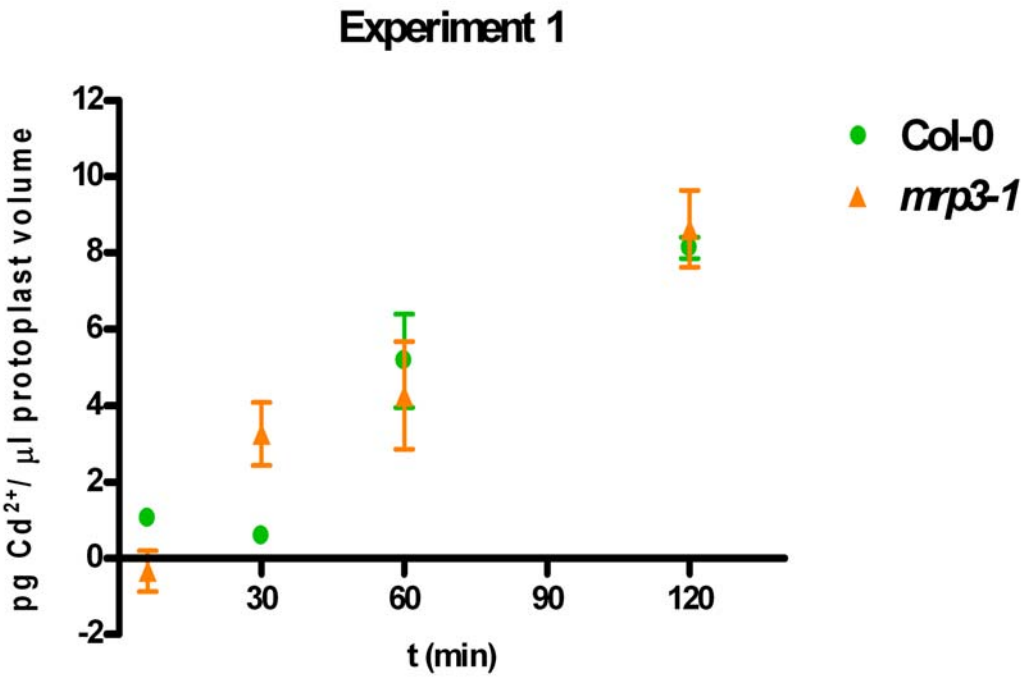

Figure VI.1. : Uptake of cadmium into wild-type and atmrp3-1 knockout mesophyll protoplasts, first experiment. Uptake of Cd^{2+} was stopped by a centrifugation through silicone oil 6, 30, 60 and 120 minutes after addition of $^{109}Cd^{2+}$ to the medium. Five aliquots were taken for each allele at each time point ; measurements diverging completely from the others were not taken into account. Averages are depicted with their standard deviation. The unspecific binding of cadmium to the protoplasts has been eliminated by correction for the y-axis intercept at time zero of a linear regression analysis of the original data of the early time points.

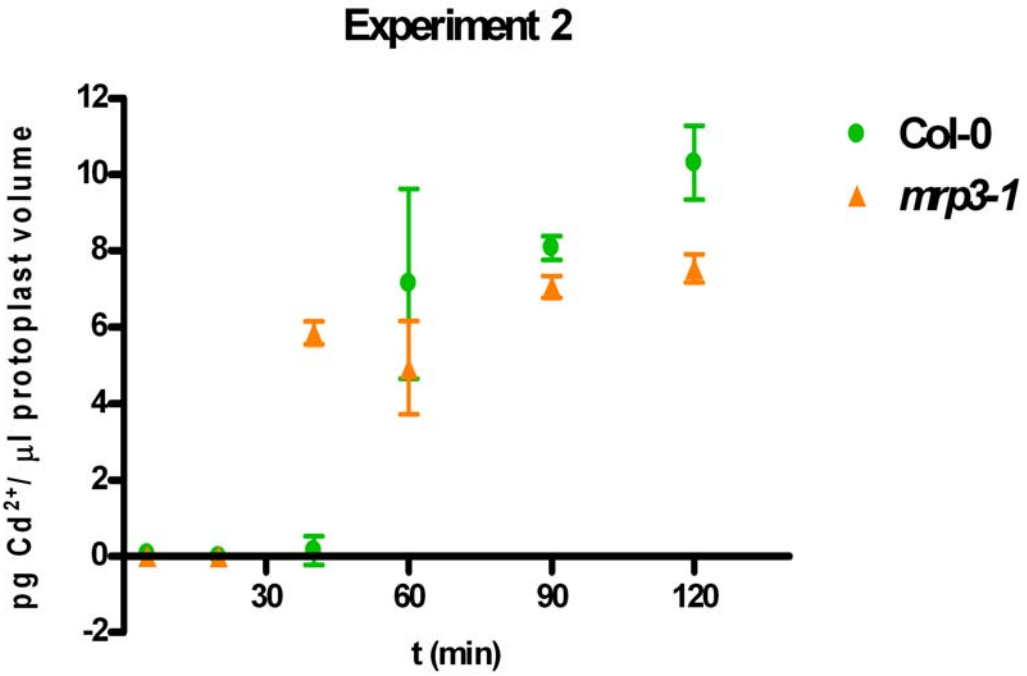

Figure VI.2. : Uptake of cadmium into wild-type and atmrp3-1 knockout mesophyll protoplasts, second experiment. Uptake of Cd^{2+} was stopped by a centrifugation through silicone oil 5, 20, 40, 60, 90 and 120 minutes after addition of $^{109}Cd^{2+}$ to the medium.

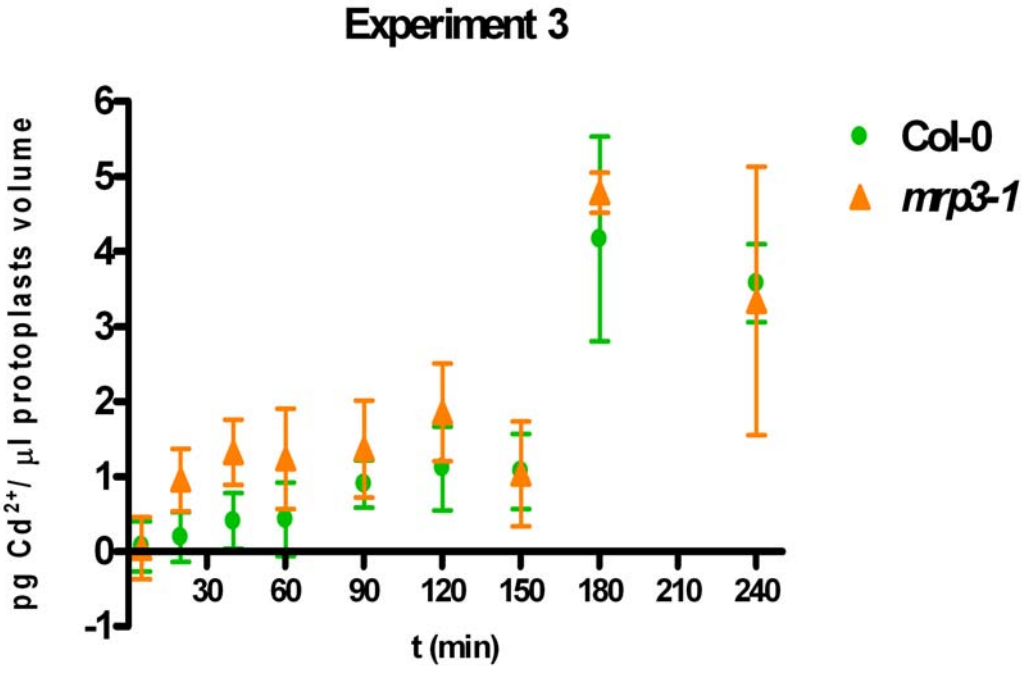

Figure VI.3. : Uptake of cadmium into wild-type and atmrp3-1 knockout mesophyll protoplasts, third experiment. Uptake of Cd^{2+} was stopped by a centrifugation through silicone oil 5, 20, 40, 60, 90, 120, 150, 180 and 240 minutes after addition of $^{109}Cd^{2+}$ to the medium.

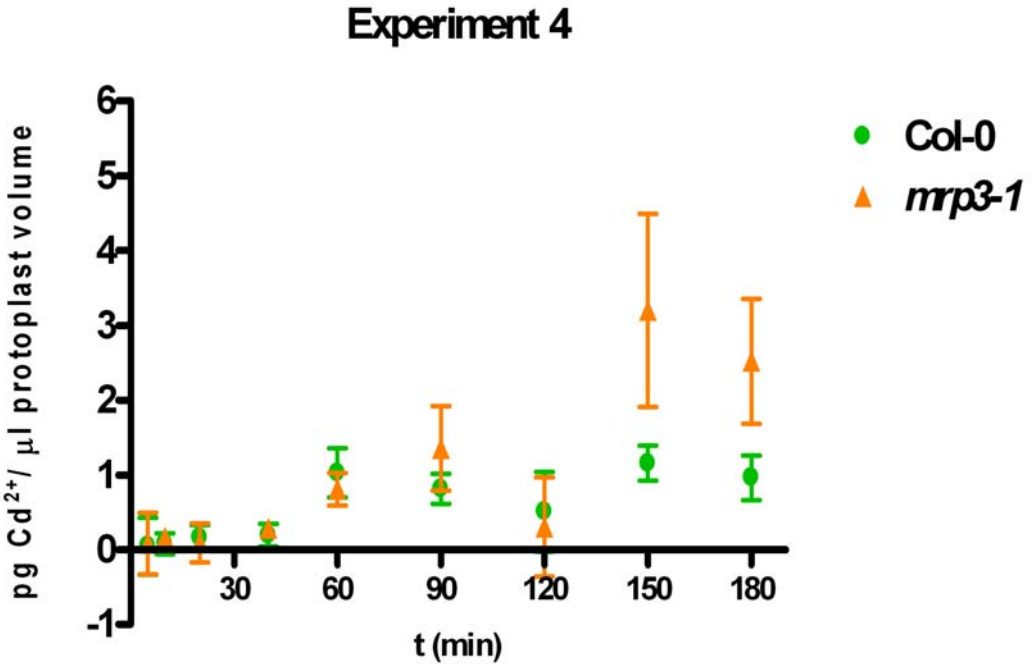

Figure VI.4. : Uptake of cadmium into wild-type and atmrp3-1 knockout mesophyll protoplasts, fourth experiment. Uptake of Cd^{2+} was stopped by a centrifugation through silicone oil 5, 10, 20, 40, 60, 90, 120, 150 and 180 minutes after addition of $^{109}Cd^{2+}$ to the medium.

VII.Subcellular localization of AtMRP3

In order to establish a hypothesis with regard to the role AtMRP3 plays in cadmium and prosulfuron resistance, and to be able to design more specifically further experiments (such as transport experiments with specific organelles), the subcellular localization of the protein must be known. In the present study, two different approaches have been used to reach this goal. First, using a peptide-specific antibody ; secondly, using a genetic fusion including the full length AtMRP3 protein fused to the green fluorescent protein GFP, a fluorescent marker protein.

VII.1.1. Use of a specific antibody to localise AtMRP3

To obtain an AtMRP3-specific antibody, the first step was to construct genetically a fusion protein between a polypeptide coding for an *AtMRP3* specific sequence and a gene encoding a glutathione transferase enzyme (*GST*). The construct was expressed in *E. coli*, the soluble proteins extracted from the bacterial culture and the fusion protein recovered by affinity chromatography on a glutathione affinity matrix. The purified fusion protein was injected into a rabbit and the serum of the rabbit was recovered. The serum was controlled by western blot and the antibodies hybridized indeed with the fusion peptide.

In a first step, Western blots were made, using the crude serum as marker for the detection of AtMRP3. Various protein extracts were charged on these Western : total protein extracts of Col-0 leaves, fractions of a two-phase partitioning experiment performed with Col-0 leaves (one phase is enriched in plasma membranes proteins, the other in all the other membrane proteins). However, in Western blots the unpurified serum was not specific enough.

In a subsequent step, the raw serum was purified by column affinity chromatography. In the first step of the purification, the serum was passed through a column containing an affinity matrix onto which antigens of a soluble protein phase were bound which was obtained from an *E.coli* culture expressing a soluble GST. In this step, all the antibodies in the serum that recognized *E.coli* proteins or the GST alone were retained on the column, and the flowthrough, still containing the antibodies specific for the fusion protein, was recovered. This fraction was further purified in a second affinity chromatography step. Here, the purified GST fusion protein that was used to immunize the rabbits was bound to the affinity matrix. In this case, only the antibodies specific for the fusion protein were retained on the column which. These antibodies were then eluted by passing through the column a buffer of low pH

(50 mM glycine/HCl pH 2.3, 0.15 M NaCl), the pH of the recovered fraction being neutralized after the elution. Tested by western blot, this fraction demonstrated a strong hybridization to the fusion protein and the disappearance of non-specific hybridization to other proteins coming from *E.coli* cultures expressing a *GST* (this non-specific hybridization was important in the raw serum).

The purified antibodies were then tested to detect AtMRP3 in various Western blots using crude protein extracts of Col-0 or *mrp3-1* leaves and membrane fractions of an aqueous two-phase partitioning of the same lines. Unfortunately, all these western blots did not highlight a band and the antibody did not crossreact with any protein. It was concluded that either expression of AtMRP3 in the leaves was too low to be detected by Western blot, or the purified antibodies, despite their affinity to the fusion peptide, have a too low affinity towards the native AtMRP3 protein.

VII.2.1. Use of a AtMRP3-GFP fusion to localize AtMRP3

Since immunolocalization of AtMRP3 using an antibody proved to be impossible within the framework of this thesis, another strategy was designed : the use of a genetic construct coding for a fusion protein consisting of the complete AtMRP3 protein and a C-terminally added GFP5 fluorescent marker protein expressed under the transcriptional control of the strong, constitutive Cauliflower Mosaic Virus 35S promoter.

AtMRP3 cDNA was cloned and fused to the coding sequence of a *GFP5* resulting in a protein fusion at its C-terminus in the transient expression vector pCL60 (Bauer et al., 2002). Plasmid DNA of this construct was delivered by biolistic bombardment to epidermial onion cells either alone or together with pA7 vector containing the 35S::*DsRed2-KCO1* construct. *KCO1* encodes a potassium channel and the protein is an established marker for the tonoplast (Czempinski et al., 2002).

One day after particle delivery of *AtMRP3-GFP5*, single onion cells depicted the characteristic fluorescence of the green fluorescent protein. In all cases, the fluorescence was restricted to membranous structures (Figures VII.1.(a) to VII.3.(a) and Figures VII.4.(a) and (b)). Furthermore, fluorescence appeared restricted to the tonoplast based on the following arguments:

The labelled membrane delimited a structure filling most of the internal cell space, but it surrounded the nucleus (Figures VII.1.(a) to VII.3.(a) and Figures VII.4.(a) and (b)). The delimited structure thus matches the well-known description of the vacuole : the vacuole is

the most voluminous organelle in plant cells, occupying up to 90% of the cell space and the cytosol is mainly restricted to the space occupied by the nucleus.

Labelled transvacuolar strands were also observed in our localization experiments (Figures VII.1.(a) and (b)). The transvacuolar strands are pipe-like structures traversing the vacuole, delimited by the tonoplast and allowing the passage of the cytoplasm through this organelle. Thus the fact that our fusion protein labelled these structures further confirms its tonoplast localization.

No small organelle, like the nucleus, mitochondria or chloroplasts for example, showed any green fluorescent labelling (Figures VII.1.(a) to VII.3.(a) and Figures VII.4.(a) and (b)).

Finally tonoplast localization was confirmed by cobombardment of the *AtMRP3-GFP5* fusion protein with the tonoplast marker *DsRed2-KCO1* : DsRed2-KCO1 and AtMRP3-GFP5 labelled identical membranous structures : a membrane delimiting an organelle occupying most of the cell space and circumventing the nucleus (Figures VII.3.(a) to VII.4.(b)). DsRed2-KCO1 labelled also small round structures clearly not pertaining to the tonoplast (Figures VII.3.(b) to VII.4.(b)). These structures may be artefacts caused by DsRed2-KCO1 , which is an obligate tetramer and may thus form protein clumps. This can also be explained by the hypothesis that DsRed2-KCO1 was more slowly delivered to the tonoplast than AtMRP3-GFP5 after protein synthesis, or it was more slowly synthetized than AtMRP3-GFP5 : these red labelled structures possibly belonged to the Golgi apparatus or to the prevacuolar compartment or were vesicles coming from one of these organelles, on their way to the vacuole. This hypothesis is confirmed by the size and the shape of these small structures labelled by red fluorescence. Furthermore, our observations of the differences in the time of appearance of the two different fluorescences in onion cells also confirmed this hypothesis : the maximum of the green fluorescence, representing AtMRP3-GFP5, was observed one day after the bombardment and then it quickly decreased afterwards, whereas the maximum of red fluorescence, due to DsRed2-KCO1, was observed two or three days after the bombardment.

In conclusion, we can say that the tonoplast localisation of the AtMRP3-GFP5 construct is a strong indication that *in planta* AtMRP3 is located on the vacuolar membrane. Thus, AtMRP3 should be involved in vacuolar transport of solutes from the cytosol.

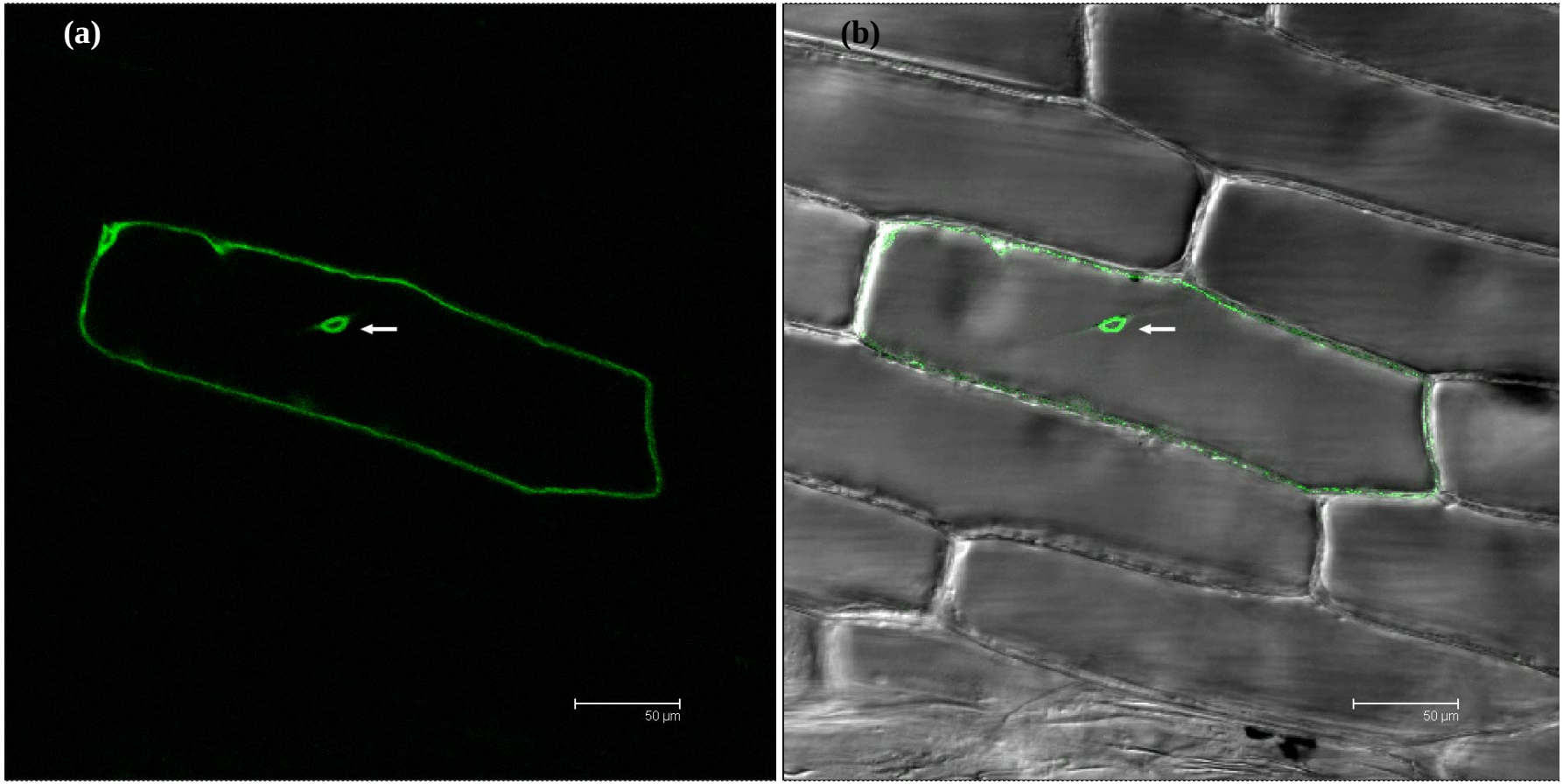

Figures VII.1.(a) and (b) : Green fluorescence specific for GFP of an onion cell expressing AtMRP3-GFP5 (left panel) and overlay with the differential interference contrast transmission picture (DIC) of the same cell (right panel). Fluorescence is clearly located on the membrane of an organelle contained inside the cell, occupying most of the intracellular space, which is the tonoplast. Furthermore, fluorescence occurs within the cell on membranes of transvacuolar strands (white arrow).

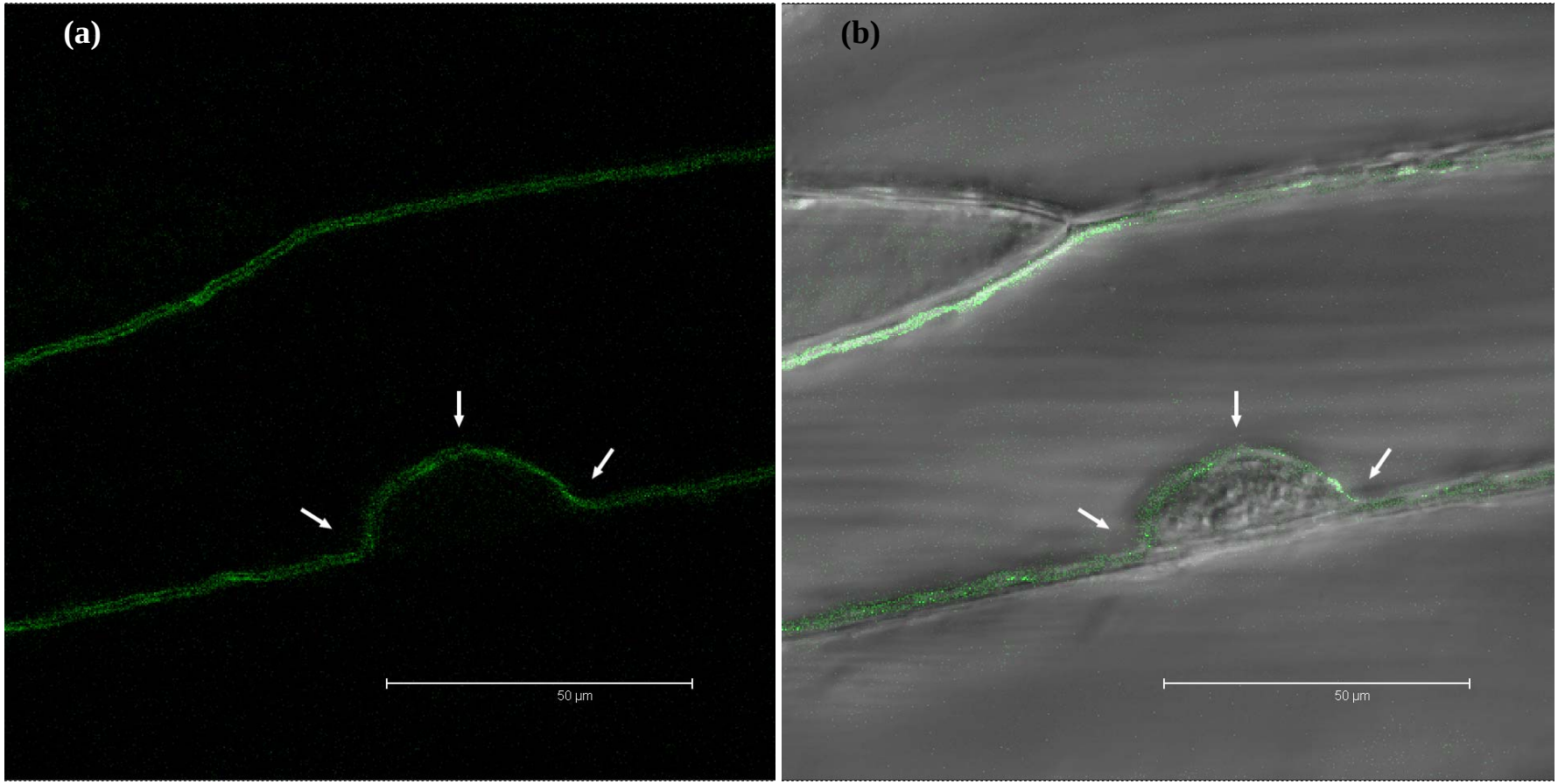

Figures VII.2.(a) and (b) : Green fluorescence specific for GFP of another onion cell expressing AtMRP3-GFP5 (left panel) and overlay with the differential interference contrast transmission picture (DIC) of the same cell (right panel). The labelled membrane circumvents the nucleus (white arrows), another evidence of the tonoplast localization of our fusion protein.

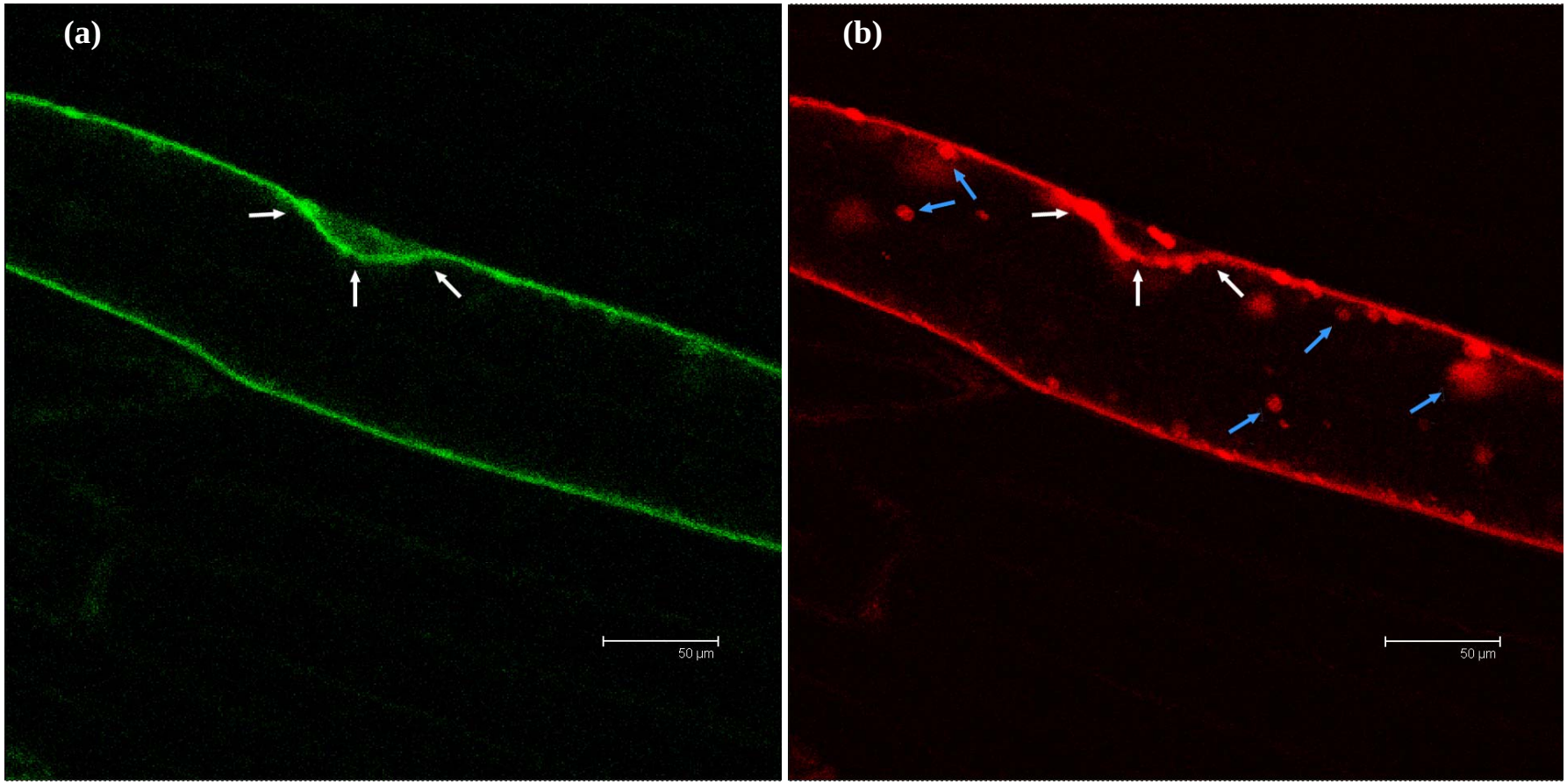

Figures VII.3.(a) and (b) : Green fluorescence specific for GFP (left panel) and red fluorescence specific for DsRed (right panel) of the same onion cell, cotransformed with AtMRP3-GFP5 and DsRed2-KCO1. In most places, AtMRP3-GFP5 and DsRed2-KCO1 are colocalized : they both label a membrane that occupies most of the cell space and circumvents the nucleus (white arrows) : the tonoplast. But DsRed2-KCO1 also labels small round structures not labelled by AtMRP3-GFP5 (blue arrows) ; these structures probably pertain to the golgi apparatus or to the prevacuolar compartment.

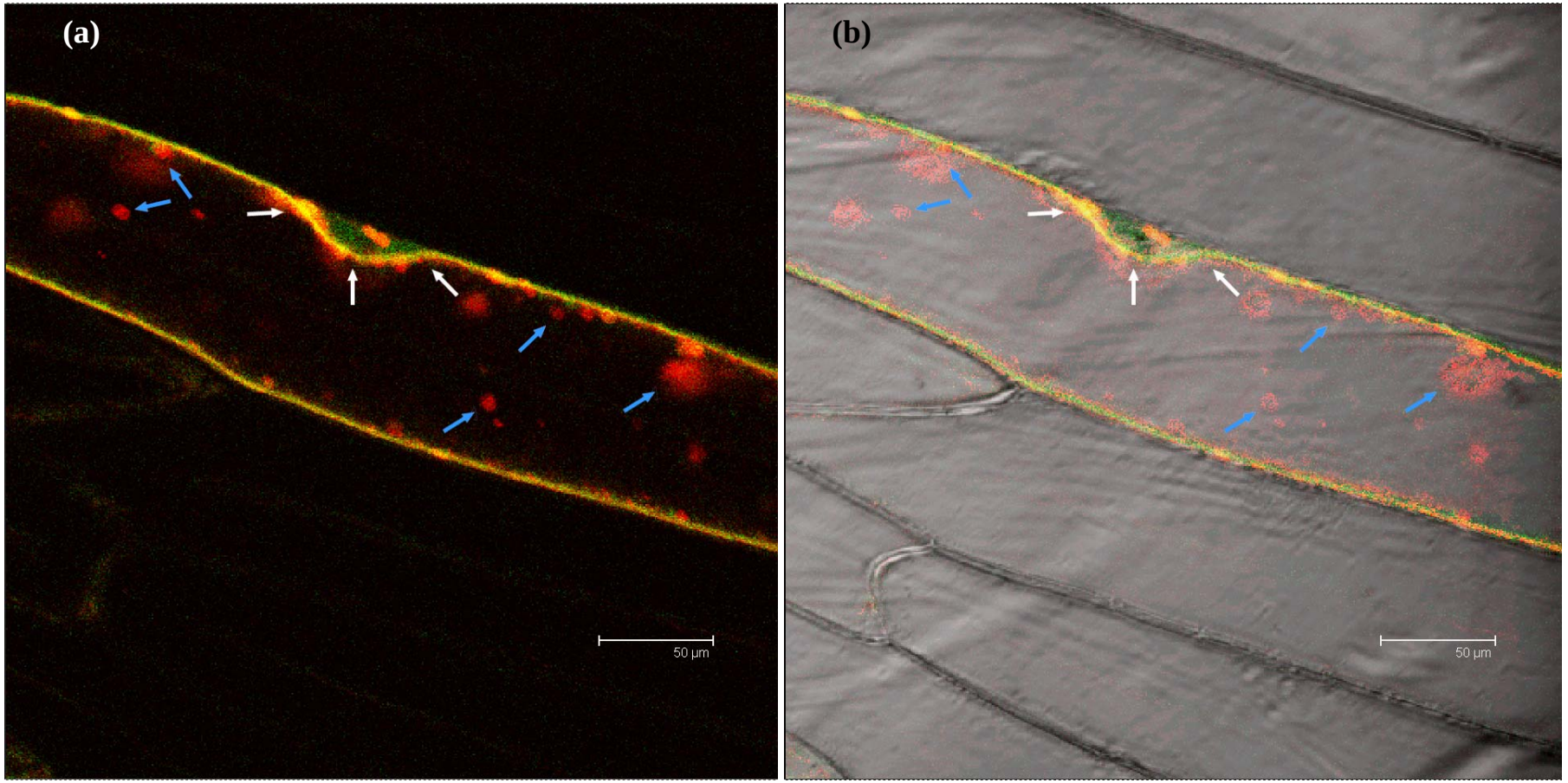

Figures VII.4.(a) and (b) : Overlay of the two previous figures (left panel) and overlay with DIC image of the same cell. Overlay of AtMRP3-GFP5 (green channel) and DsRed2-KCO1 (red channel) appears here in yellow proving colocalisation of both proteins on the tonoplast. Structures were DsRed2-KCO1 is localized alone appear in red (blue arrows). The tonoplast, circumventing the nucleus (white arrows) shows clearly that it contains both AtMRP3-GFP5 and DsRed2-KCO1.

VIII. Glutathione import in wild-type and mutant vacuoles

Based on our experiments we have localizing AtMRP3 to the tonoplast, its specific activity should be detectable in isolated vacuoles of wild type plants, but not in isolated vacuoles of any of the knockout mutant alleles. As a result it ws hypothesized that *in planta* AtMRP3 functions as a vacuolar importer of glutathione conjugates and especially of glutathione-cadmium complexes, as shown for glutathione conjugate transport and increased Cd^{2+} resitance after heterologous expression in yeast (Tommasini et al., 1998). Thus, if our hypothesis is right, a higher import of glutathione-cadmium complexes should be detected in wild type vacuoles when compared to mutant vacuoles.

VIII.1.1. Results

Three independent transport experiments were performed with mesophyll vacuoles isolated from wild type and mutant *Arabidopsis*. After isolation, vacuoles were incubated in different media containing 200 µM glutathione (radiolabelled with ^{3}H-glutathione, $3.7x10^{5}$ Bq/µmol) to allow the quantification of the glutathione imported. At the end of the incubation time, vacuoles were separated from the incubation media by centrifugation through a layer of silicone oil.

In the first experiment, vacuoles of Col-0 and *mrp3-1* were extracted and incubated for 18 minutes in four different media :

- The first medium contained 5m M ATP and was used to follow the ATP-dependent vacuolar import of unconjugated glutathione.
- The second medium contained 200 µM $CdCl_2$ and 5 mM ATP and allowed to follow the ATP-dependent vacuolar import of glutathione and glutathione-cadium complexes.
- The third medium contained 200 µM $CdCl_2$, 5 mM ATP and 1 mM vanadate. Vanadate is a strong inhibitor of the transport activity of ABC transporters by blocking their capacity to hydrolise ATP, but vanadate does not inhibit the tonoplaste H^{+}-ATPases and thus does not disturb transport activities driven by the pH gradient between the inside and the outside of vacuoles. Therefore the transport activity (of glutathione and glutathione-cadium complexes) observed in the third condition can be attributed to secondary energized transporters.

In this first experiment, the vacuolar volume in the two vacuole preparations was measured by incubating samples of the two vacuole preparations and incubating them with tritiated water.

Tritiated water diffuses freely across the tonoplast and hence the radioactivity inside the vacuoles allows to calculate their volume. This means that the vacuolar volume was not measured in the same samples as those taken to measure glutathione accumulation but separatly, since tritiated water can not be distinguished from ^{3}H-glutathione. This can be a source of error, since the quantity of vacuoles in each sample may vary. Results : see Tables VII.1.(a) and (b).

In the second import experiment, vacuoles of Col-0 and *mrp3-3* were isolated and transport was measured after a 20 minutes incubation in four different media :

- The first medium contained and 5m M ATP and was used to follow the ATP-dependent vacuolar import of unconjugated glutathione, as in the first experiment.
- The second medium contained 200 μM $CdCl_2$ and 5 mM ATP and allowed to detect the ATP-dependent vacuolar import of glutathione and glutathione-cadium complexes, as in the first experiment.
- The third medium contained no ATP and was to used to reveal whether an ATP-independent vacuolar import of unconjugated glutathione exists.
- The fourth medium contained 200 μM $CdCl_2$ but no ATP and allowed to observe an possible ATP-independent vacuolar import of glutathione and glutathione-cadium complexes.

In contrast to the first experiment, there was no condition containing vanadate and the vacuolar volume was measured together with glutathione in each vacuole sample. In these cases, ^{14}C-glycerol instead of $^{3}H_2O$ was added to the media : ^{14}C-glycerol diffuses freely across the tonoplast and can be quantified at the same time as ^{3}H-glutathione. Thus, calculations of the concentration of glutathione inside the vacuoles should be more accurate since the quantity of vacuoles in each sample may vary, which is a source of error. Results : see Table VII.2.

In the third import experiment, vacuoles of Col-0 , *mrp3-1* and *mrp3-3* were isolated and incubated for 20 minutes in four different media. The conditions used were the same as in the second experiment. Vacuolar volumes were also measured using ^{14}C-glycerol. Results : see Table VII.3.

Condition	Concentration of GSH in Col-0 vacuoles after 18' (μM)	(n)	Concentration of GSH in *mrp3-1* vacuoles after 18' (μM)	(n)
GSH + 5 mM ATP	**259 ± 69**	**(3)**	**56 ± 1**	**(2)**
GSH + 200 μM Cd^{2+} + 5 mM ATP	**1892 ± 462**	**(3)**	**288 ± 202**	**(4)**
GSH + 200 μM Cd^{2+} + 5 mM ATP + 1 mM vanadate	**10659 ± 8976**	**(5)**	**125 ± 52**	**(4)**

	Col-0 vacuoles	(n)	*mrp3-1* vacuoles	(n)
Vacuolar volume (μl)	**0.076 ± 0.006**	**(3)**	**0.418 ± 0.044**	**(4)**

Tables VIII.1.(a) (upper table) and (b) (lower table) : First experiment. Concentration of glutathione inside wild type and mutant vacuoles after 18 minutes of incubation in media containing 200 μM glutathione. Values are calculated based on the volume calculated from ^3H_2O volume. Averages of the samples with standard deviations. Five samples taken for each allele and condition, measurements diverging completely from the others were not taken into account in the calculations. Number n in brackets is the number of measurements kept.

Condition	Concentration of GSH in Col-0 vacuoles after 20' (μM)	(n)	Concentration of GSH in *mrp3-3* vacuoles after 20' (μM)	(n)
GSH + 5 mM ATP	**85 ± 3**	**(4)**	**91 ± 6**	**(4)**
GSH + 200 μM Cd^{2+} + 5mM ATP	**116 ± 9**	**(2)**	**128 ± 20**	**(3)**
GSH without ATP	**86 ± 8**	**(4)**	**86 ± 4**	**(3)**
GSH + 200 μM Cd^{2+} without ATP	**147 ± 22**	**(2)**	**105 ± 11**	**(2)**

Table VIII.2. : Second experiment. Concentration of glutathione inside wild type and mutant vacuoles after 20 minutes of incubation in media containing 200 μM glutathione. Averages of the samples with standard deviations. Five samples taken for each allele and condition, measurements diverging completely from the others were not taken into acount in the calculations. Number n in brackets is the number of measurements kept.

Condition	Concentration of GSH in Col-0 vacuoles after 20' (μM)	(n)	Concentration of GSH in *mrp3-1* vacuoles after 20' (μM)	(n)	Concentration of GSH in *mrp3-3* vacuoles after 20' (μM)	(n)
GSH + 5 mM ATP	**178 ± 10**	**(4)**	**170 ± 13**	**(5)**	**168 ± 17**	**(3)**
GSH + 200 μM Cd^{2+} + 5mM ATP	**157 ± 17**	**(3)**	**164 ± 10**	**(3)**	**180 ± 9**	**(3)**
GSH without ATP	**144 ± 13**	**(3)**	**109 ± 16**	**(4)**	**155 ± 13**	**(3)**
GSH + 200 μM Cd^{2+} without ATP	**45**	**(1)**	**53 ± 0**	**(2)**	**x**	**(0)**

Table VIII.3. : Third experiment. Concentration of glutathione inside wild type and mutant vacuoles after 20 minutes of incubation in media containing 200 μM glutathione. Averages of the samples with standard deviations. Five samples taken for each allele and condition, measurements diverging completely from the others were not taken into acount in the calculations. Number n in brackets is the number of measurements kept.

The first experiment showed large differences between wild type and mutant vacuoles, with the wild types importing more glutathione than the mutants in the presence and absence of Cd^{2+}. Cd^{2+} in the media seemed also to enhance glutathione import. Most likely this increased glutathione uptake was due to the fact that both, glutathione as well as glutathione-cadmium complexes were transported into the vacuole. However, it can not be excluded that in the presence of Cd^{2+} transport of free glutathione is more efficient. However, in our opinion, all the results of the first experiments should be considered as artefacts. Indeed, glutathione accumulation in this experiment, was much higher than what was observed in any condition of the other experiments, except in the *mrp3-1* vacuoles in presence of 5 mM ATP medium and in presence of 200 μM Cd^{2+}, 5 mM ATP and 1 mM vanadate. And this despite a shorter incubation time than in the other experiments. This accumulation would also imply a higher accumulation rate of glutathione in *Arabidopsi*s vacuoles than what was observed in past studies (Song et al., 2003). In the presence of vanadate, which is an inhibitor of ABC

transporters, glutathione accumulation was even higher in Col-0 vacuoles. Failure to obtain accurate measures in this experiment is very probably due to inaccurate vacuolar volume determination. The ^3H_2O counts were very low and ^3H_2O could not be included in the samples containing the glutathione. Thus a small variation in the quantity of vacuoles of a sample measured for glutathione accumulation would lead to a big variation of the calculated concentration of glutathione inside the vacuoles. The same is true if even a very small amount of the media goes through the silicon oil layer upon centrifugation and contaminates the vacuoles.

In experiments two and three, the volume of vacuoles in each vacuole preparation was clearly larger than in the first experiment and the volume of vacuoles was measured together with glutathione accumulation in each sample. Thus errors due to variation in the vacuolar volume in the samples are reduced. The last serie of measurements of the third experiment – those in the medium with glutathione and Cd^{2+} but no ATP – should in our opinion be discarded because of problems in the centrifugation step.

In all conditions of experiments two and three, no significant differences were observed between wild type and knockout mutants, except in two cases. A small difference was visible between Col-0 and *mrp3-3* vacuoles in the presence of Cd^{2+} and absence of ATP in experiment two and also between Col-0 and *mrp3-1* vacuoles in the absence of ATP in experiment three. However, no difference was observed between Col-0 and *mrp3-3* mutants in experiment three. We can thus conclude that there was neither significant difference in vacuolar glutathione import between *Arabidposis* wild-type and knockout mutants in the *AtMRP3* gene, nor a significant difference in vacuolar import of glutathione-cadmium complexes. Thus, *AtMRP3* does not seem to function as a vacuolar importer of glutathione or of glutathione-cadmium complexe, at least not in mesophyll vacuoles.

In experiment two, addition of Cd^{2+} in the medium seemed to enhance slightly glutathione import. However this observation was not confirmed in experiment three. Thus, a specific mechanism for glutathione-cadmium complexes vacuolar import might exist, but if it exist it seems only marginal when compared to the total amount of imported glutathione. This point needs further investigation. Another interesting observation is that in experiments two and three absence or presence of ATP had only a small impact on glutathione import. A small difference was only observed in experiment three between the medium with glutathione and ATP and the medium with glutathione and without ATP. We can thus conclude that vacuolar import of glutathione is primarily based on an ATP independent mechanism such as an H^+ antiport or a diffusion faciliator protein.

IX. Tissue distribution of *AtMRP3* expression by reporter gene analysis

In order to investigate in which tissues the AtMRP3 protein is expressed, plants transformed with a reporter gene construct were studied : five independent transgenic lines of *Arabidopsis thaliana* transformed with a GUS reporter gene flanked by 2 kb of the promoter and 5'UTR region of the *AtMRP3* gene and by 1 kb of the 3'UTR and terminator region of the *AtMRP3* gene were isolated. The five lines were termed MTER B to MTER F.

The GT transposon inserted in the *AtMRP3* gene of the *mrp3-2* mutants contains a β-glucoronidase (GUS) reporter gene flanked downstream by a nos terminator (see Figure III.6. in chapter II). Due to the position of insertion and the orientation of the GT transposon in the *mrp3-2* mutants, the included GUS reporter gene is in the same orientation as the *AtMRP3* gene and is flanked upstream by the *AtMRP3* promoter – the ATG of the GUS gene is located only 460 base pairs after the ATG of the *AtMRP3* gene – and downstream by the nos terminator (see Figure III.6. in chapter II). As a consequence, the GUS reporter gene is under the control of the *AtMRP3* promoter in *mrp3-2* mutants and the *mrp3-2* mutants are suitable transgenes for the reporter gene analysis of AtMRP3 expression. Consequently we used also this line for expression analysis.

Furthermore, we have transformed *Arabidopsis* plants by floral dipping with *Agrobacterium tumefasciens*, in order to obtain stable transformants carrying four different reporter gene cassettes : (i) plants with a GUS reporter gene flanked by 2030 bp of the promoter and 5'UTR region of the *AtMRP3* gene and by 918 bp of the terminator and 3'UTR region of the *AtMRP3* gene – termed *promM3-GUS-terM3* (ii) plants with the luciferase reporter gene flanked by 2030 bp of the promoter and 5'UTR region of the *AtMRP3* gene and by 918 bp of the terminator and 3'UTR region of the *AtMRP3* gene – termed *promM3-LUC-terM3* (iii) plants with the GUS reporter gene flanked by 2030 bp of the promoter and 5'UTR region of the *AtMRP3* gene and by the nos terminator – termed *promM3-GUS-ternos* (iv) plants with the luciferase reporter gene flanked by 2030 bp of the promoter and 5'UTR region of the *AtMRP3* gene and by the nos terminator – termed *promM3-LUC-ternos*. After selection on ½ MS / 1% (w/v) sucrose plates containing hygromycin B, one T1 *promM3-LUC-terM3* transformant and two T1 *promM3-GUS-ternos* transformants were obtained. Leaves of the two T1 *promM3-GUS-ternos* transformants were also analysed to investigate the distribution of AtMRP3 expression.

IX.1.1. Observed tissue localisation

GUS activity of the MTER lines was analysed in 11 day and 8 week old plants. The overall blue coloration due to GUS enzymatic activity was stronger in the aerial parts than in the roots. This observation is in accordance with previously published data obtained by RT-PCR (Bovet et al., 2003).

GUS staining was maximal in the vascular system of shoots, leaves and roots. Shoot and leaf staining of the vascular system was observed in all five independent lines. GUS activity in the vascular system of roots was observed in three out of the five independent lines (see Figures IX.1. to IX.4.).

In roots GUS activity was observed in four lines in root tips and, in two lines, in certain zones of the root in all root tissues, including root hairs (see Figures IX.3. to IX.5.).

In leaves, GUS activity was always observed in the mesophyll, but its intensity was variable. Furthermore, GUS activity was always detected in hydathodes, it was detected in four lines in the trichomes and in one line in stomata (see Figures IX.1., IX.2. and IX.6. to IX.8.).

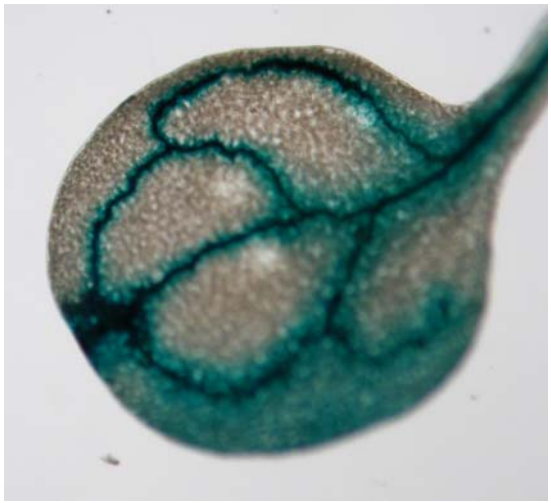

Figure IX.1. : Cotyledon of an 11 days old MTER seedling. GUS activity is strong in the vascular system, but also clearly present in the mesophyll. This pattern of GUS activity was observed in all five MTER lines.

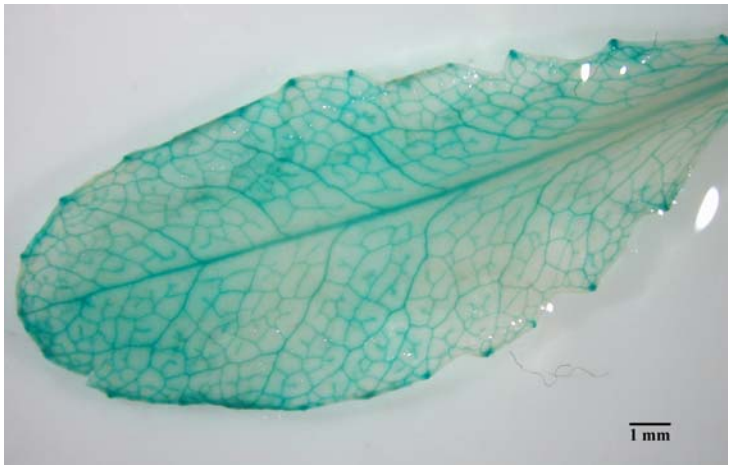

Figure IX.2. : Rosette leaf of an 8 weeks old MTER plant. GUS activity is strong in the whole vascular system and in the hydathodes ; it is weaker, but present, in the mesophyll. This pattern of GUS activity was observed in all five MTER lines.

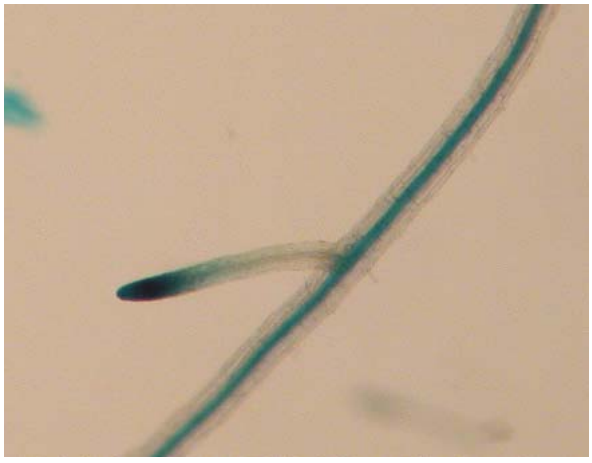

Figures IX.3. (left panel) and IX.4. (right panel) : GUS activity in roots of 11 days old MTER seedlings. GUS activity is visible all along the root, but limited to the vascular system and the root tips. This pattern of GUS activity was observed in three out of the five MTER lines.

Figure IX.5. : Root of an 11 days old MTER seedling. In certain zones of the root, GUS activity is present in all root tissues, including root hair. This pattern of GUS activity was observed in two out of the five MTER lines. In one of these two, GUS activity was also visible in root tips.

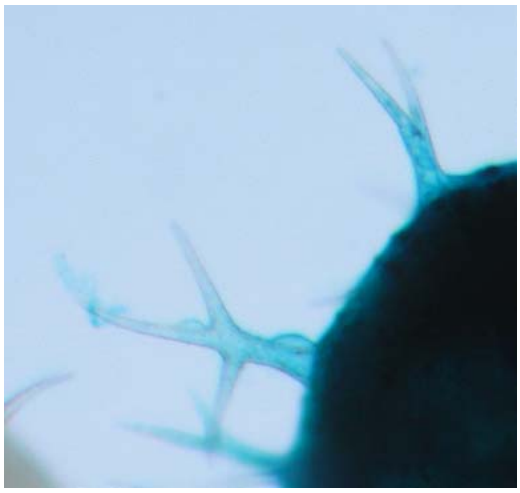

Figure IX.6. : GUS activity in trichomes of an 11 days old MTER seedling. This pattern of GUS activity was observed in four out of the five MTER lines.

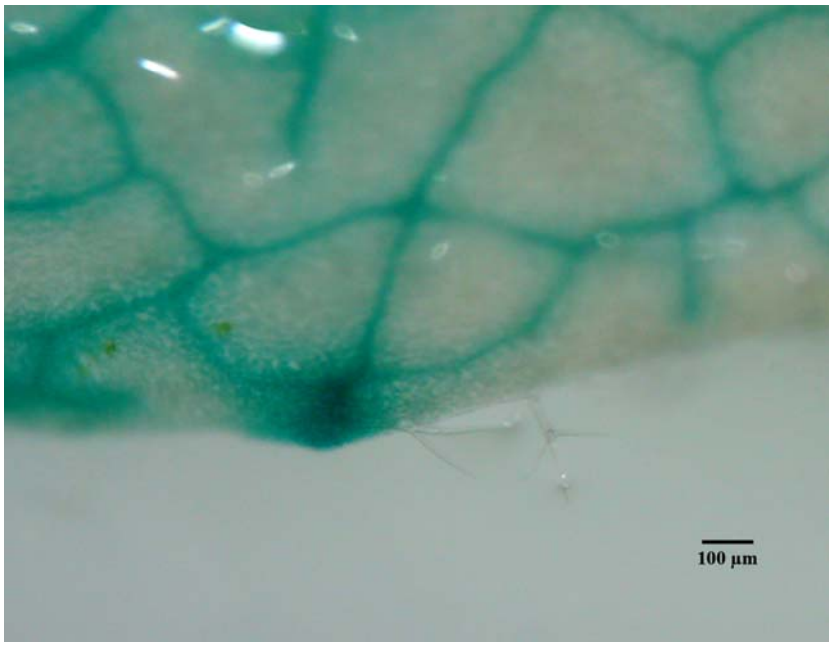

Figure IX.7. : Hydathode of an 8 weeks old MTER plant. GUS activity is stronger in the hydathodes than in the mesophyll. This pattern of GUS activity was observed in all five MTER lines.

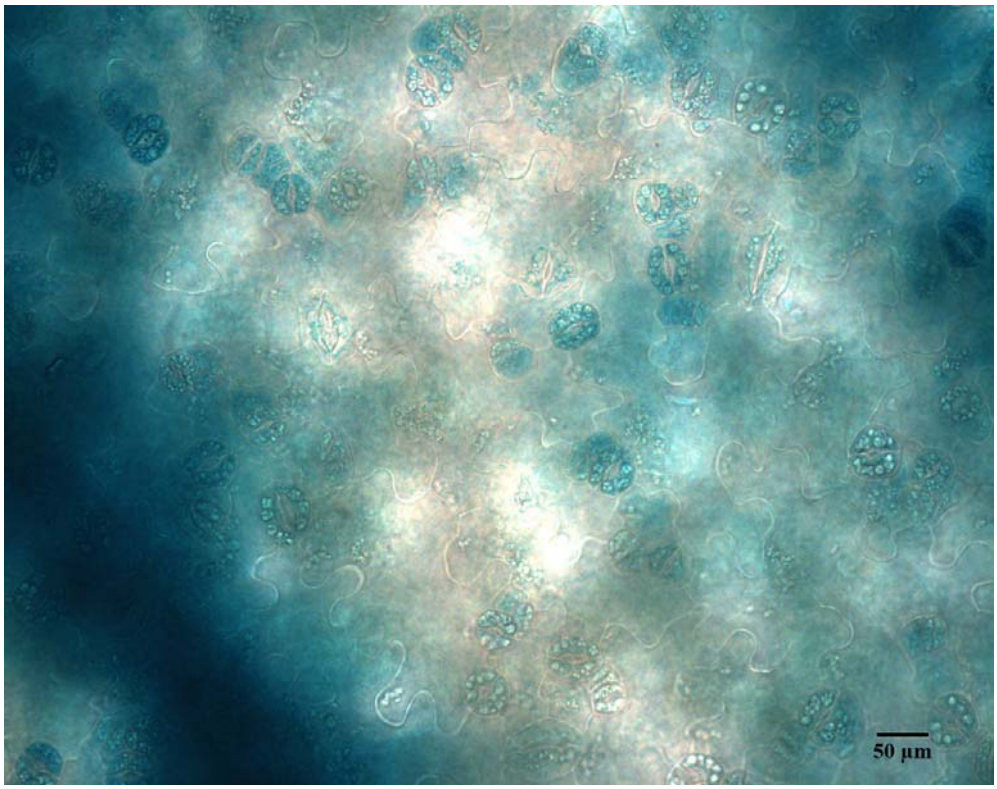

Figure IX.8. : Epidermal surface of a leaf of an 11 days old MTER seedling. GUS activity is visible in the guard cells of stomata. This pattern of GUS activity was observed in one out of the five MTER lines.

In the *mrp3-2* allele, GUS expression, obtained by insertion of gene trap Ds element in the *AtMRP3* gene, was observed in the vascular system of root, shoots and leaves, in the mesophyll, in the hydathodes and at the root tip. Thus the GUS staining pattern in the *mrp3-2* allele is coherent with the pattern obtained in the transformed MTER lines.

The *promM3-GUS-ternos* transgenic plants showed GUS activity in the vascular system of leaves, in the mesophyll, in hydathodes and in the trichomes. Again this verifies the observations obtained with the MTER lines. Strong GUS activity – stronger than that of the surrounding mesophyll and that of the trichomes – was also observed in the basal cells supporting the trichomes (see Figure IX.9.). GUS colorations with the roots of these three lines have not been performed.

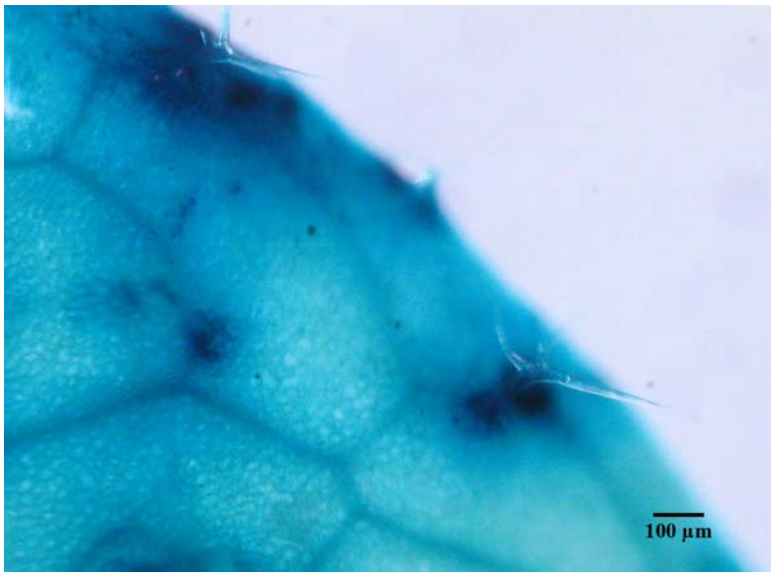

Figure IX.9. : GUS activity in a leaf of a *promM3-GUS-ternos plant.* GUS activity is present in the vascular system, in the mesophyll, in the trichomes, but is also very strong in the basal cells supporting the trichomes.

IX.1.2. Association of GUS activity with the vascular system

Microscopic observations of GUS-stained sections prepared from leaves and stems of MTER plants showed that the high GUS activity in the vascular system is present in the entire vascular bundle, including the xylem, phloem and all surrounding cells of the bundle sheet (see Figures IX.10. to IX.12.).

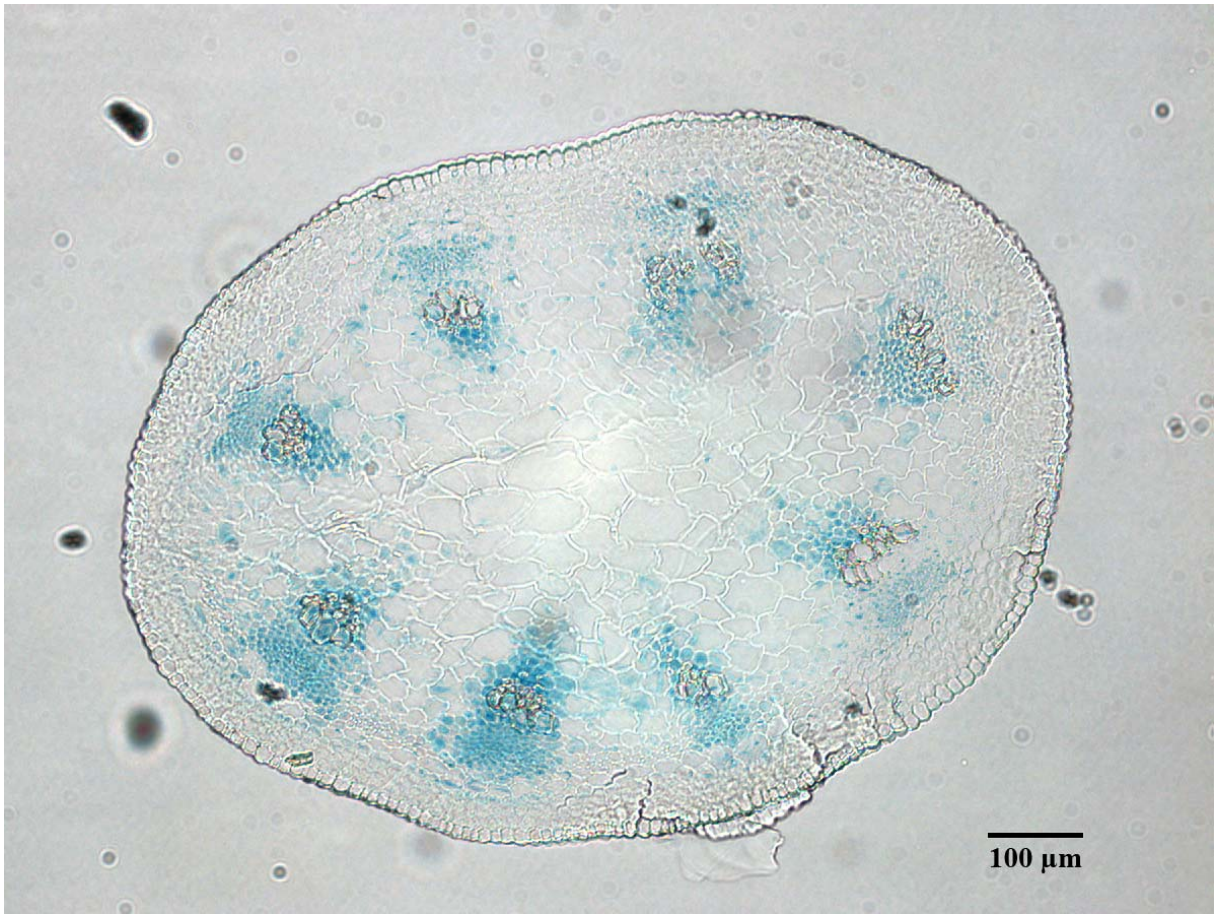

Figure IX.10. : GUS activity in a transversal section of a transgenic MTER stem. In the stem tissue, GUS activity is clearly limited to the vascular bundles.

Figure IX.11. Detail of a transversal section of a transgenic MTER stem. GUS activity is present in the entire vascular bundle, including phloem, xylem and surrounding cells of the bundle sheet.

Figure IX.12. : Detail of a transversal section of a transgenic MTER leaf. GUS activity is visible in the mesophyll, but is stronger in the vascular bundle, including phloem and xylem.

IX.1.3. Induction of GUS activity by xenobiotic stresses

In RT-PCR and microarray experiments, it had been demonstrated that AtMRP3 expression is induced when *Arabidopsis* plants are submitted to Cd^{2+} or prosulfuron stress (Bovet et al., 2003 ; Glombitza et al., 2004). Consequently, it was attempted to verify the induction by the same stresses of the reporter gene activity in our transgenic lines carrying the GUS reporter gene under the control of the *AtMRP3* promoter and terminator. Seedlings of the MTER lines were grown 11 days on ½ MS / 1% (w/v) sucrose medium in presence or absence of 10 µM $CdCl_2$ before staining. A third treatment consisted in 11 days of growth on ½ MS / 1% (w/v) sucrose medium and spraying of the seedlings with an aqueous solution of 500 nM prosulfuron six hours before GUS staining. In both stress conditions, with Cd^{2+} and with prosulfuron, GUS activity was clearly enhanced in aerial parts. Interestingly, GUS activity in the mesophyll cells increased strongly (see figures IX.13 and IX.14.). Furthermore, the blue

staining of trichomes and stomata was also enhanced, but to a lesser extent. This is in line with the observations made in the studies cited above. Although less obvious when compared to leaves, GUS activity was also enhanced in the roots of seedlings submitted to cadmium or prosulfuron stress : in the regions where GUS activity was already detected without stress (vascular system, root tip, zones with GUS activity in all root tissues) activity increased with exposure to Cd^{2+} or prosulfuron. Increased *AtMRP3* transcription in the roots under cadmium stress has already been documented by Bovet et al. (2003). Glombitza et al. (2004) have only investigated *AtMRP3* transcription under prosulfuron stress in the leaves and whether this transcription was also enhanced in the roots after treatment with the herbicide was not documented until now. However, we have to remember that in our experiments with prosulfuron treatment not only the leaves, but also the roots of the seedlings were directly in contact with the herbicide after the plates were sprayed.

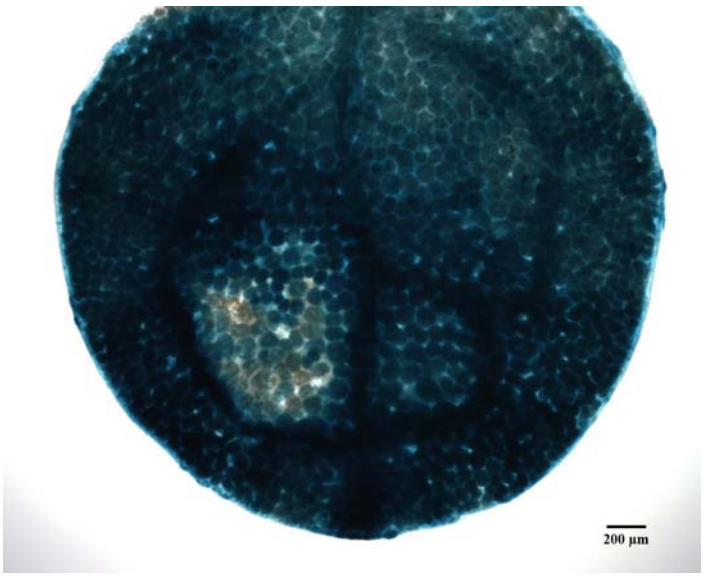

Figure IX.13. : Leaf of a MTER seedling grown on 10 µM $CdCl_2$. GUS activity in the mesophyll has increased, when compared to unstressed seedlings (see figure IX.1.). This induction of GUS activity by cadmium was observed in all five MTER lines.

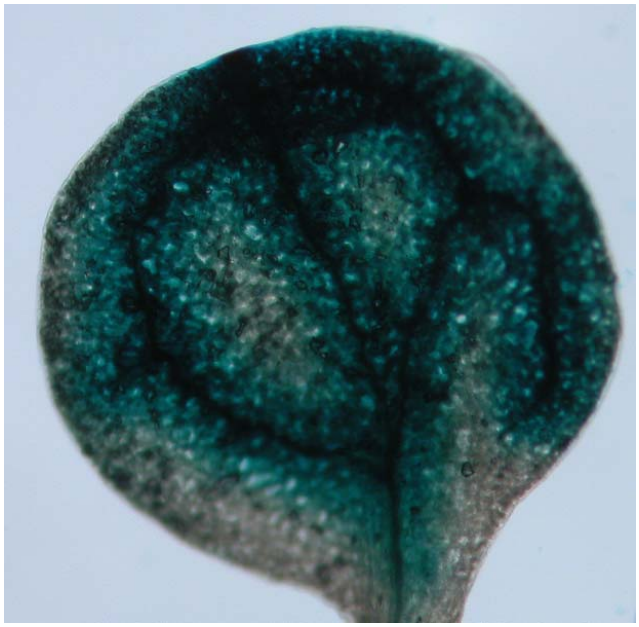

Figure IX.14. : Leaf of a MTER plantlet treated with prosulfuron. GUS activity in the mesophyll has increased, when compared to unstressed seedlings (see figure IX.1.). This induction of GUS activity by prosulfuron was observed in all five MTER lines.

X. Discussion

The *Arabidopsis* ABC transporter AtMRP3 has been investigated in some detail with respect to its function by heterologous expression in yeast and to its transcriptional activation in response to heavy metal stress and herbicide treatment (Tommasini et al. 1998 ; Bovet et al., 2003, 2005 ; Glombitza et al., 2004). In consequence, several pieces of evidence have been reported that support the hypothesis of a role of AtMRP3 in detoxification of heavy metals and of organic xenobiotic compounds. (i) AtMRP3 is able to restore resistance to Cd^{2+} in the hypersensitive yeast strain Δycf1 suggesting that it acts as a glutathione conjugate-pump when expressed in yeast (Tommasini et al. 1998). (ii) *AtMRP3* transcription is induced *in planta* if plants are exposed to xenobiotic stress (Bovet et al., 2003, 2005 ; Glombitza et al., 2004). However, these are indirect pieces of evidence : restoration of Cd^{2+} resistance and transport activity were observed in a heterologous expression system and one could argue that AtMRP3 does not function the same way *in planta*. Despite the fact that induction of *AtMRP3* transcription is only activated by some specific stresses *in planta* (Bovet et al., 2003 ; Glombitza et al., 2004), this protein could play a role in a physiological mechanism linked to stress but not specifically in transporting toxic compounds. Thus, direct proof demonstrating that AtMRP3 is an integral part of a physiological mechanism allowing plant resistance to toxic xenobiotic compounds is missing. In the present study, mutants in *AtMRP3* were isolated. The analysis of phenotypical differences in response to herbicide treatment or cadmium exposure as well as experiments aiming at changes in long-distance and subcellular cadmium transport using these mutants allow an analysis of the *in vivo* contribution of transport processes mediated by AtMRP3 to overall detoxification. Furthermore, the discovery of the subcellular localization of AtMRP3, by means of the expression of a fluorescent fusion protein, seems to confirm the classical hypothesis that AtMRP3 functions as a vacuolar importer of conjugated toxic compounds *in planta*. Finally, analysis of Pro_{AtMRP3}*::GUS::*Ter_{AtMRP3} and Pro_{AtMRP3}*::GUS::*Ter_{nos} allows a spatially resolved analysis of *AtMRP3* expression in contrast to RNA-based experiments which integrate over all cell types in a tissue. The observed differences in cadmium accumulation in wild-type and mutant plants and the changes in expression patterns of a reporter gene under the control of the *AtMRP3* promoter and terminator lead us to hypothetisize that AtMRP3 is part of a mechanism of resistance to xenobiotics.

X.1.1. Growth experiments reveal phenotypes in *AtMRP3* knockout mutants

When grown in ½ MS medium containing 0.5% sucrose, in the absence of xenobiotic compounds, the *mrp3-1* and *mrp3-3* seedlings exhibited a reduced growth when compared to the Col-0 wild-types. The difference in growth was quantified by chlorophyll measurements but could also be observed visually as reduced leaf size and decreased number of lateral roots in the mutants. When 4 nM prosulfuron were added to the medium, the difference between the *mrp3-3* and Col-0 became more pronounced. Thus, the *mrp3-3* mutant plants are more sensitive to the herbicide than the wild-type and displayed reduced growth when compared to Col-0. *mrp3-1* mutants exhibited a tendency a slightly higher sensitivity towards prosulfuron when compared to Col-0. However, the difference was not statistically significant. If 45 µM Cd^{2+} was added to the medium, no statiscally significant difference in growth was observed between *mrp3-1*, *mrp3-3* and Col-0. However, observations made during preliminary experiments preparing media without sucrose convinced us that the mutant alleles are more sensitive to cadmium than Col-0. Interestingly, *mrp3-1* mutants exhibited a phenotype intermediate between *mrp3-3* and Col-0. This may be explained by the hypothesis of the expression in the *mrp3-1* of a truncated AtMRP3 protein, sufficient to partially restore the function of the complete protein : the insertion of the T-DNA in the *mrp3-1* allele is located in the first NBD and the RT-PCRs tests have demonstrated that there is a residual transcription of the final part of the *AtMRP3* mRNA. Perhaps an artificial "half-size" transporter is synthesized from this mutant mRNA, comprising the second TMD and the second NBD of AtMRP3, and perhaps this "half-size" transporter, alone or by dimerisation, retains some of the original activity of the normal protein.

The overall conclusion that can be drawn from these observations is that AtMRP3 plays indeed a role in plant fitness, even under normal growth conditions, without xenobiotic stress, since the seedlings lacking expression of the protein showed a reduced growth phenotype. Furthermore, this reduced growth phenotype is dramatically increased under prosulfuron stress in the *mrp3-3* mutants : in control conditions the chlorophyll content of *mrp3-3* seedlings was 69% of the content of the Col-0 seedlings. When 4 nM prosulfuron were added to the medium the chlorophyll content of *mrp3-3* seedlings was only 34% of the content of Col-0 seedlings. Even if the quantity of chlorophyll in *mrp3-1* seedlings is not statistically different from that of the Col-0 seedlings in the presence of 4 nM prosulfuron, a tendency to a lower fitness of these mutants seems nevertheless present. It may thus be concluded that the function filled by AtMRP3 is much more critical for the plant in cases of exposure to

prosulfuron. This is also an evidence for one of our basic assumption : AtMRP3 has a function in a mechanism that allows the plant to cope with prosulfuron stress. Our observations in growth experiments in presence or absence of prosulfuron fit also very well with the reported pattern of *AtMRP3* transcription (Bovet et al., 2003, 2005 ; Glombitza et al., 2004) : the basal expression of *AtMRP3* in observed unstressed control conditions is strongly increased in case of xenobiotic stress, when its role becomes critical, its transcription is enhanced.

No statistically significant difference in chlorophyll content between mutant and wild-type seedlings was observed under cadmium stress in our main experiments, but the observations made during the preliminary experiments are indications that the knockout mutants have also an enhanced sensitivity when compared to the wild-type plants submitted to cadmium stress. Thus, no clear cut conclusion about our hypothesis that AtMRP3 contributes to cadmium resistance in *Arabidopsis* can be drawn from these observations. Further growth experiments with different concentrations of cadmium and sucrose in the medium should be carried out to confirm or invalidate this hypothesis. However, since the previously published data showed an increased transcription of *AtMRP3* also in case of cadmium stress (Bovet et al., 2003, 2005), it seems obvious to suppose that the role played by AtMRP3 in the detoxification mechanisms *in planta* is not limited to prosulfuron detoxification, but also concerns cadmium detoxification.

If we consider AtMRP3 as an integral component of a detoxification mechanism for xenobiotics what could be its role in normal conditions? We can suppose that in normal conditions, AtMRP3 contributes to the detoxification of endogenous toxic compounds ; plants lacking the protein would be more affected by the byproducts of their own metabolism and this would explain the phenotype observed in control conditions. This hypothesis is supported by the fact that, in yeast, AtMRP3 is able to transport the chlorophyll catabolite *Bn*-NCC-1 (Tommasini et al., 1998) and is thus suspected to play a role in chlorophyll catabolite import into the vacuole *in planta*. Interestingly, another *Arabidopsis* MRP, AtMRP2, that has also been demonstrated to transport *Bn*-NCC-1 when expressed in yeast (Lu et al., 1998) and which is also localized to the tonoplast (Liu et al., 2001), is involved in chlorophyll degradation *in planta* : knockout mutants lacking AtMRP3 showed a delay in chlorophyll degradation (Frelet et al., 2006). We can thus hypothesize that AtMRP3 has a function in chlorophyll catabolism analogous to that of AtMRP2 – the transport of chlorophyll catabolites into the vacuole – and that its absence could disturb this catabolytic pathway

enough to impair the normal growth of the plants, resulting in the differences observed between Col-0 and the mutants *mrp3-1* and *mrp3-3* on plates without xenobiotic compounds.
Another hypothesis is that in conditions where no artificial stress is imposed on plants, AtMRP3 contributes to the detoxification of trace amounts of xenobiotics or of allelochemicals present in the plant environment. With respect to our artificial growth conditions on plates, it seems difficult to believe that there is enough of these trace toxic compounds in the culture media we used that would result in such a reduced growth of the mutants. However, the analysis of the *Aberrant Lateral Formation5 (ALF5)* gene which encodes a multidrug and toxic extrusion transporter controlling the number of lateral roots formed by seedlings on artificial media suggested that a contamination in an impure commercial agar led to a clear reduction in lateral root number in *alf5* mutants which suddenly disappeared if a purified phytoagar was used (Diener et al., 2001).
Alternatively, we can hypothesize that AtMRP3 has a double function, one linked to xenobiotic detoxification and the other function in an unrelated physiological mechanism, such as for example the transport of a non-toxic metabolites essential for the plant. The analysis of the metal composition in wild-type and mutant plants demonstrates that in the absence of AtMRP3 and in the presence of a sublethal cadmium dose (1 µM) hydroponically grown *atmrp3-1* plants accumulate less Ca^{2+}. Thus, AtMRP3 could have a role in calcium homeostasis. If AtMRP3 is directly or indirectly involved in Ca^{2+} transport, the absence of AtMRP3 could result in reduced transport of this essential ion and thus lead to a reduced fitness of the plant, explaining the reduced growth phenotype in control conditions.
The finding that AtMRP3 seems to be even more important for prosulfuron detoxification than for cadmium detoxification is puzzling. Prosulfuron is known to be detoxified in a pathway implying its conjugation to glucose in barley (Klein et al., 1996). In yeast, AtMRP3 has been demonstrated to transport glutathione conjugates instead (Tommasini et al., 1998). If we suppose that AtMRP3 participates to prosulfuron detoxification by transport of a phase II conjugated hydroxyprosulfuron product into the vacuole, two models are possible : (i) AtMRP3 is able to transport glucosides as well as glutathione conjugates. This is plausible since several ABC transporters, including AtMRP2 and AtMRP3, have been demonstrated to have multispecific substrate affinity (Lu et al., 1998 ; Tommasini et al., 1998 ; Liu et al. 2001), and it has been demonstrated in barley that hydroxyprimisulfurin-glucoside, a close homolog of prosulfuron-glucoside is imported into the vacuole by an ABC-type transporter (Klein et al., 1996). Furthermore, AtMRP2, which is comparable to AtMRP3, since it also exhibits chlorophyll catabolites and glutathione conjugates transport activity when expressed

in yeast (Lu et al., 1998), has been demonstrated to have a transport activity for glucuronate conjugates when expressed in yeast (Liu et al., 2001) as well as *in planta* (Frelet et al., 2006). Since glucuronate and glucose are closely related molecules, this is a further indication of the plausibility of a plant MRP transporting simultaneously glucose conjugates, glutathione conjugates and chlorophyll catabolites. (ii) An alternative but yet unknown pathway to detoxify prosulfuron exists in *Arabidopsis*, implying its conjugation to glutathione.

The observations made during the preliminary growth experiment seem to indicate that addition of sucrose in the culture medium allowed the mutants to partially compensate their reduced growth phenotype, in control conditions as well as under xenobiotic stress : the more sucrose was added to the medium, the more mutant seedlings appeared to compensate their reduced growth phenotype and the more they seemed tolerant to toxic stresses. It would be interesting to confirm these observations by a series of growth experiments comparing the chlorophyll content of mutant and wild-type plants grown on media containing various concentration of sucrose, in the presence or absence of cadmium or prosulfuron. If we believe that the supposedly observed compensation phenomenon is real, we can suppose that other mechanisms exist in the plant, overlapping the functions of AtMRP3. The plants could use these mechanisms to compensate the absence of AtMRP3 but it would cost the plant more energy or more carbon. Thus the use of these alternative mechanisms would be more active in the presence of sucrose in the medium. This hypothesis could also explain why xenobiotic stress has a much more dramatic impact on the knockout mutant in the early stages of development than at later stages : when the seedling has just germinated, its photosynthesis capacity is very reduced and growth mainly depends on the storage compounds of the seeds as energy and carbon source . Thus the capacity of a seedling to spend a lot of energy on detoxification may be very limited.

The hypothesis of the existence of alternative parallel mechanisms filling the same functions as AtMRP3 is also supported by the fact that the phenotype of increased sensitivity to xenobiotics is only visible in a precise concentration “window” of the toxic compounds. Mutants and wild type exhibit no clear phenotypical differences at concentrations lower than within the “window”, while concentrations exceeding the damage threshold lead to irreparable impairment which is identical in wild types and mutants. Thus, below this range of concentrations the alternative mechanisms could be sufficiently active to compensate the absence of AtMRP3, while above this range all mechanisms of xenobiotic resistance, including the one implying AtMRP3, would be overloaded. Other transporters of the AtMRP family, and especially AtMRP4 and AtMRP7, which have been demonstrated to have Cd^{2+}

transport activity in yeast and to play a role in the root-shoot distribution of Cd^{2+} *in planta* (Plaza et al., 2005), could be part of such alternative mechanisms. Transporters such as *AtHMA2*, *AtHMA4* (Eren and Arguello, 2004 ; Verret et al., 2005 ; Mills et al., 2005) or antiporters of the CAX family (Hirschi et al., 2000 ; Shigaki et al., 2005 ; Koren'kov et al., 2006) are also likely candidates for such a function.

X.2.1. Analysis of short and long term cadmium accumulation and distribution in plants reveals differences between wild-type and knockout mutants

In order to evaluate directly the contribution of AtMRP3 to cadmium accumulation and long-distance distribution of Cd^{2+}, wild-type and mutant plants were incubated with $^{109}CdCl_2$ and the allocation of $^{109}Cd^{2+}$ was analyzed.

Experiments investigating the short term cadmium accumulation revealed a reduced root to shoot transfer of $^{109}Cd^{2+}$ in *atmrp3* mutant seedlings when compared to Col-0. Furthermore, overall accumulation of $^{109}Cd^{2+}$ was reduced in the mutants. If seedlings were given enough time after exposure to $^{109}CdCl_2$, the distribution of $^{109}Cd^{2+}$ in *mrp3-1* was comparable to the root/shoot-ratio found in Col-0 seedlings and finally *mrp3-1* accumulated as much cadmium in the shoot and in the whole plant as Col-0 (with some retention of cadmium in the root). In the long term cadmium accumulation experiments, the knockout mutant alleles *mpr3-1* and *mrp3-3* did not show a difference when compared to the wild-type below a threshold of 1 µM of Cd^{2+} in the medium. But above this threshold values the observed difference was similar as in the short term cadmium accumulation experiments : a reduced accumulation of cadmium in the shoots of the mutants. With 1 µM of Cd^{2+} in the medium, the shoot concentration of Cd^{2+} in *mrp3-1* mutants was only 71 % of the cadmium concentration found in the shoots of Col-0 but this difference was not statistically significant ; with 2 µM of Cd^{2+} in the medium, the shoot concentration of Cd^{2+} in *mrp3-1* mutants was only 56 % of the cadmium concentration found in the shoots of Col-0 and this difference was statistically significant.

These experiments prove unequivocally that AtMRP3 plays a role in the transport of cadmium across the plant. The hypothesis that the observed differences are due to a lower transpiration in *AtMRP3* could be excluded : *mrp3-1*, *mrp3-2* and *mrp3-3* did not show any difference in their sensitivity to drought stress when compared to their corresponding wild-types (results not shown). The differences in metal content between Col-0 and the mutants tested by ICP-MS were present only if at least 1 µM Cd^{2+} was present in the culture medium, and these differences concerned only cadmium and, to a lesser extent, calcium. These results

further support the hypothesis that AtMRP3 is involved in cadmium translocation : plants that do not have a functional AtMRP3 protein do not transport cadmium from root to shoot as efficiently and do not accumulate as much cadmium in their leaves as plant expressing the protein. Interestingly these experiments add something new to our understanding of the mechanisms in which AtMRP3 functions : based on the results obtained by heterologous expression of AtMRP3 in yeast (Tommasini et al., 1998), it was supposed that the action of the transporter lead to different partitioning of cadmium in the cells. This has not been demonstrated *in planta* until now. Our experiments prove that the action of AtMRP3 leads to a different distribution of cadmium in the entire plant. Furthermore, the difference observed between wild-type and mutants is analogous to the difference between hyperaccumulator plants and non-accumulator plants : one of the mechanisms that plants hyperaccumulating heavy metals use to resist to these toxic ions is their enhanced capacity to transfer them from root to shoot (Lassat et al., 1996, 2000 ; Bert et al., 2003).

The observation that after a prolonged recovery time *mrp3-1* seedlings are able to translocate as much cadmium to the shoot as Col-0 seedling in the short term exposition experiment demonstrates again that AtMRP3 is only one component involved in heavy metal transport and that several alternative long-distance transport mechanisms exist. The fact that a difference between mutants and wild-type in long term accumulation of cadmium is only visible above a given threshold of Cd^{2+} concentration in the medium fits well with the fact that in growth experiments the hypersensitivity phenotype was only visible in a certain range of concentrations. Thus, when the concentration of Cd^{2+} in the hydroponic medium is too low, the alternative mechanisms can compensate the absence of *AtMRP3* in a satisfactory way.

ICP-MS analysis of the long term accumulation experiment proves also the specificity for cadmium and maybe also to a lesser extent for calcium because it allows to quantify the amount of many elements of the periodic system in the same sample. Consequently, the transport process catalyzed by AtMRP3 should be specific for Cd^{2+}(-complexes) and probably Ca^{2+}(-complexes), since apart from these two metals no other significant differences in the elemental composition was observed between *mrp3-1*, *mrp3-3* and Col-0.

Two hypothesises can explain the reduced shoot accumulation of calcium in the mutants when cadmium in the culture medium is high : (i) AtMRP3 also has a role in Ca^{2+} transfer from root to shoot beside its role in Cd^{2+} transfer. The fact that Ca^{2+} ions are very similar to Cd^{2+} ions – both have the same charge and almost the same ion radius : 0.99 Å for Ca^{2+} ions and 0.97 Å for Cd^{2+} ions – supports this hypothesis. Additionally we performed a single experiment for short term accumulation of Ca^{2+} which showed that *mrp3-1* seedlings

exhibited a slight reduction of root to shoot transfer of this ion when compared to Col-0 seedlings (results not shown). (ii) The retention of Cd^{2+} ions in the roots of the mutants lacking AtMRP3 disturbs normal absorption and xylem loading of Ca^{2+} ions, an hypothesis supported by the fact that diminished calcium accumulation only occurs if the culture medium contains at least 1 μM Cd^{2+}. Previous studies have also proven that Cd^{2+} ions can pass Ca^{2+} channels and thus disturb normal metabolism (Perfus-Barbeoch et al., 2002).

X.3.1. AtMRP3 localizes to the vacuolar membrane

Our transient expression experiments investigating the subcellular localisation of an AtMRP3-GFP fusion protein in onion cells showed that AtMRP3-GFP was targeted to the vacuolar membrane and largely co-localizes with the known tonoplast marker TPK1-DsRed (Czempinski et al., 2002). As a consequence, it must be concluded that perturbations observed in mutants with regard to detoxification efficiencies and long-term distribution of toxic compounds are a result of a missing or reduced vacuolar storage of these compounds or of their derivatives synthesized during cellular detoxification.

However, we were unable to demonstrate either differences in cadmium import between *mrp3-1* and Col-0 protoplasts isolated from leaf mesophyll or a difference in Cd^{2+}-induced glutathione import between *mrp3-1*, *mrp3-3* and Col-0 vacuoles isolated from leaf mesophyll cells. If tonoplast-bound AtMRP3 was involved in the accumulation of Cd-glutathione complexes into the vacuole, it was expected that vacuolar uptake of Cd-GSH complexes would be reduced. As a consequence protoplast import would also be decreased to a certain degree since in this case the cytosolic cadmium would increase, changing the concentration gradients between the outer space and the cytosol. Thus, unfortunately a direct demonstration of the transport activity of AtMRP3 is missing.

Nevertheless, the absence of differences observed in our transport experiments is not sufficient to dismiss the hypothesis of AtMRP3 as a transporter of xenobiotic compounds. As demonstrated by our experiments with plants containing a GUS reporter gene under the control of the *AtMRP3* promoter, GUS activity in leaves is not as strong in the mesophyll as in the vascular system, hydathodes and trichomes when the plants are not submitted to xenobiotic stress (see paragraph X.4.1.). This could explain our observations : leaf mesophyll cells (and vacuoles) of unstressed wild-type plants may not contain enough AtMRP3 protein to cause a measurable difference in transport experiments when compared to knockout mutants. It is possible that transport experiment carried with vacuoles isolated from wild-type

plants stressed with a xenobiotic compound, and thus having an enhanced AtMRP3 amount in the leaf mesophyll, would show a difference when compared to vacuoles isolated from leaves of stressed knockout mutants. Furthermore, a transport experiment with vacuoles or protoplasts isolated from a plant overexpressing AtMRP3, or even isolated from trichomes, could provide evidence of the putative transport activity of AtMRP3. Another hypothesis to explain the lack of differences in glutathione import between Col-0 and knockout mutant vacuoles would be that *in planta* AtMRP3 does not transport glutathione conjugates but other forms of Cd complexes one of which could be phytochelatin-Cd complexes. We tested Cd-GSH complexes because (i) the yeast ortholog YCF1 has been demonstrated in yeast and plants to transport Cd-GSH complexes (Li et al., 1997) and (ii) since transporters involved in phytochelatin-Cd complexes such as the *S. pombe* HMT1 transporter do not belong to the MRP subfamily of ABC transporters (Ortiz et al., 1995).

X.4.1. Transgenic *AtMRP3*-promoter lines exhibit xenobiotic inducible changes in reporter gene expression

The overall spatial expression pattern of *AtMRP3* revealed by GUS analysis of the five independent MTER lines, of the *mrp3-2* allele and of the two *promM3-GUS-ternos* lines was almost identical in spite of the different constructs used to analyse GUS activity. Thus, some reliable conclusions can be drawn. The observed *AtMRP3*-dependent GUS activity was strong in the whole vascular system : in roots of the MTER lines and of the *mrp3-2* mutants (GUS activity in the roots of the two *promM3-GUS-ternos* lines was not tested), in stems and leaves of all lines. GUS expression was not limited to the phloem or the xylem but appeared in the entire vascular bundle, including phloem, xylem and bundle sheet cells. Strong GUS activity was also found in hydathodes (all lines) , in trichomes (most lines) and at the root tip (all MTER lines, but not in the *mrp3-2* allele). The overall GUS activity in mesophyll cells was present but clearly weaker when compared to the strong expression in the abovementioned tissues and cell types. In contrast, *AtMRP3*-controlled GUS activity in stomatal guard cells was observed in only one MTER line and GUS activity in the basal epidermal cells supporting the trichomes was observed only in the two *promM3-GUS-ternos* lines, raising the question whether these expression patterns are a result of a positional effect of the T-DNA insertion.

When submitted to cadmium or prosulfuron stress, all MTER lines exhibited an enhanced GUS expression in the vascular system, both in roots and shoots and at the root tip ; the four

lines exhibiting GUS activity in trichomes displayed an increased staining of these organs after cadmium or prosulfuron treatment. Finally, the line showing GUS activity in stomata without stress displayed also enhanced GUS activity under cadmium or prosulfuron stress. However, in all MTER lines, the increase in GUS activity under cadmium or prosulfuron stress was much more dramatic in mesophyll cells. In contrast to the rather weak GUS activity in the absence of stress, treatments with cadmium or prosulfuron lead to a strong increase in the mesophyll.

All these observations are in line with previous data demonstrating strong induction of expression of *AtMRP3* (Bovet et al., 2003, 2005 ; Glombitza et al., 2004), but with one remarkable novelty : in our experiments prosulfuron clearly induced GUS activity in roots whereas Glombitza et al. (2004) did not study the expression of *AtMRP3* in the roots in response to prosulfuron. However, it should be noted that in our experiments the roots of the MTER seedlings were directly in contact with prosulfuron during the spraying, due to the fact that the roots were at the surface of the agarose medium. It would be interesting to study the response of the roots when the contact with the herbicide would be strictly limited to the leaves. With the information about the spatial and inducible activity pattern of the *AtMRP3* promoter, it is possible to refine our previous hypothesis. In the unstressed situation, AtMRP3 could be involved in the detoxification of endogenous toxic compounds, of traces of xenobiotics or transport of essential metabolites, which are mainly carried in the vascular system, in hydathodes, in trichomes and at the root tip, and to a reduced degree in the leaf mesophyll cells. However, under xenobiotic stress the contribution of AtMRP3 to detoxification of xenobiotics is strongly activated. More specifically, strong induction of promoter activity in mesophyll cells strongly argues for the fact that either the promoter and/or the terminator must contain elements that apart from a general stress induction controls the specific activation in the mesophyll, thus a clear change in the spatial pattern of gene activity.

X.5.1. A global hypothesis on the role of *AtMRP3 in planta*

The major question arising from the results presented in this thesis is whether AtMRP3 *in planta* acts as a transporter for toxic substances. The observations made with the short term and long term cadmium accumulation experiments clearly demonstrate that AtMRP3 plays a role in long-distance distribution of the heavy metal cadmium from the root to the shoot. Thus, either AtMRP3 transports Cd^{2+} ions, probably in a conjugated form, or AtMRP3 affects

indirectly such a transport mechanism. In spite of the overall effect of absence of AtMRP3 on cadmium allocation, direct proof of AtMRP3-mediated transport by comparing wild-type and mutant protoplasts and vacuoles is missing. As a consequence and in spite of the demonstration that AtMRP3 expressed in yeasts acts as glutathione conjugate pump (Tommasini et al., 1998), it cannot be excluded that AtMRP3 itself is not a transporter involved in toxic compound transport but rather regulates these processes. In support of this hypothesis, it has been demonstrated that the close homolog AtMRP5 acts as an ion channel regulator controlling the anion channel activity in guard cells although heterologously expressed AtMRP5 is as well active as a glutathione conjugate pump (Gaedeke et al., 2001; Klein et al., 2003; Suh et al., 2006).

Nevertheless, AtMRP3 has the ability to partially complement the cadmium-hypersensitive phenotype of the Δycf1 yeast mutant (Tommasini et al., 1998) and YCF1 has been shown to act as a glutathione-Cd^{2+}-complex transporter (Li et al., 1997) which supports the simpler hypothesis that AtMRP3 itself actively transports toxic compounds or their conjugates. Lack of a measurable difference in the transmembrane transport activities in *atmrp3* mutants may primarily be due to a compensation by other MRP-type transporters which form a gene family in Arabidopsis that could redundantly share overlapping functions and expression patterns. Expression of the Arabidopsis ABC transporters AtMRP4 and AtMRP7 resulted in changes in cadmium resistance in the Δycf1 yeast mutant (Plaza et al., 2005) suggesting that at least three of the 14 Arabidopsis MRPs are involved in cadmium resistance.

The observation of an important role of AtMRP3 in translocation of Cd^{2+} ions from the root to the shoot is in accordance with the expression pattern. GUS activity in our reporter plants suggests that AtMRP3 is expressed in a way that a continuous network from the root tip to the hydathodes is formed, mainly by expression in the vascular system. This pattern proposes that AtMRP3 modulates xylem loading in roots, xylem unloading in the shoot, global repartition, storage and final excretion of Cd^{2+}. If we consider that AtMRP3 acts as a Cd^{2+} importer into the vacuole and keeping in mind that increased Cd^{2+} import into the vacuole will result in a increased overall cellular Cd^{2+} import into the cell through the plasma membrane (see paragraph X.3.1.), the following model can be proposed describing the potential contribution of AtMRP3 to cadmium resistance :

- As actively growing and meristematic tissues, the elongation zone of the root and the root tip has to be specifically protected from all kinds of physiological stresses. However, root growth in contaminated soils will result in overall exposure of all root parts including the root tip to heavy metals. The abundant transcription of *AtMRP3* in

the root tip could protect these cells by sequestering Cd^{2+} in their vacuole, thus avoiding the deleterious cytosolic effects of the heavy metal. The capacity of directly energized transporters to create steep concentration gradients would allow also only partially vacuolated cells to efficiently remove toxic compounds from the cytosol.

- Abundant presence of AtMRP3 in the vascular cylinder of the roots could act as a sink for the transfer of Cd^{2+} ions absorbed at the root epidermis and at the root hair to the inner cells surrounding the xylem. The inner cells would thus concentrate most of the Cd^{2+} absorbed, protecting the outer cells from the accumulation large amounts of Cd^{2+} and creating a flux of these ions from the root surface to the region close to the xylem. We can suppose that in a second step the Cd^{2+} ions stored in the vacuoles of the cells of the vascular cylinder would be remobilised by other transporters and would be diverted upward by the close sap flow. In short, AtMRP3 would prevent stagnation of Cd^{2+} at the root surface and indirectly promote xylem loading with the heavy metal.
- In leaves, AtMRP3 is abundant in the vascular tissue. It thus could act to form a temporary store and allow a control in unloading Cd^{2+} ions from the xylem. As a result, AtMRP3 would prevent the free distribution in the leaf of the toxic ions by concentrating Cd^{2+} in the vacuoles of parenchymatic cells of the vascular bundle and of the bundle sheet. As a consequence, diffusion of Cd^{2+} in the leaf apoplast with the transpiration stream could be diminished, as well as the transfer to mesophyll cell through plasmodesmatal connections. High levels of specific ions in the bundle sheet have already been documented, as well as the possibility of remobilisation of these ions and of their subsequent transfer through non apoplastic pathways, for example for phosphate ions in *Nicotiana tabacum* (Canny, 1993 ; Karley et al. 2000).
- Low *AtMRP3* promoter activity in mesophyll cells could result in moderate or low amounts of Cd^{2+} ions in these vacuoles.
- AtMRP3 could promote the concentration of Cd^{2+} in the secretory organs of the leaves by vacuolar deposition. As mentioned above, *AtMRP3* is strongly expressed in the hydathodes, in trichomes and maybe also in stomata guard cells. If the Cd^{2+} ions stored in the bundle sheet and in the mesophyll would be remobilized and transferred to secretory organs, AtMRP3 could promote this transfer and the subsequent storage. Finally, the fate of Cd^{2+} ions would be to be excreted. The excretion of cadmium through trichomes has already been documented in *Nicotiana tabacum* : the heavy metal is first accumulated into specialized vacuoles in the head cells of trichomes, forming crystals, and then the crystals thus formed are expelled, probably through

exocytosis (Choi et al., 2001). One could imagine that a similar mechanism exists in *Arabidopsis*, AtMRP3 promoting the accumulation of Cd^{2+} in specialized vacuoles of trichome cells, vacuoles which would later undergo exocytosis, resulting in cadmium excretion. Although it is not known if *Arabidopsis* hydathodes are active, hydathodes of other plants, such as rye, wheat and barley, are well-known for their capacity to secrete diverse compounds by guttation, including organic compounds – mainly sugars – and mineral nutrients – mainly potassium (Goatley and Lewis, 1966). Furthermore, it has been proposed that *Arabidopsis* hydathodes play a role in aluminium resistance by excreting Al^{3+} ions (Larsen et al., 2005). As trichome cells, hydathodes could accumulate Cd^{2+} in specialized vacuoles through the action of AtMRP3. The content of these vacuoles would be later expelled through exocytosis, resulting in cadmium excretion. Since hydathodes are directly linked to the vascular bundle, they could be part of a direct pathway for excretion of Cd^{2+} ions, directly from the xylem unloading step to the excretion step.

- In case the plant would be confronted to high amounts of Cd^{2+}, the expression pattern of *AtMRP3* would change : *AtMRP3* transcription would be increased at the root tip, all along the vascular system and in the secretory organs to enhance the previously described mechanisms of protection of the cells of the root tip, of transfer of the heavy metal from the root surface to the vascular cylinder, of storage of Cd^{2+} in the vascular bundle and in the bundle sheet and of final transfer to the secretory organs. But the most important change would take place in the leaf mesophyll, where the transcription of *AtMRP3* increases from low to a level comparable to that of the vascular system. In case of confrontation to high concentrations of Cd^{2+}, the plant would not be able to excrete immediately enough heavy metal to prevent the accumulation of large amounts of Cd^{2+} in the leaves. In that case, the leaf mesophyll would have to play the role of a storage organ for the heavy metal. In consequence, the increase in *AtMRP3* transcription would allow the mesophyll cells to sequestrate more Cd^{2+} in their vacuoles, promoting import of Cd^{2+} from the xylem and avoiding deleterious stagnation of the heavy metal in their cytosol.

According to this model, AtMRP3 enhances xylem loading, xylem unloading and vacuolar storage of Cd^{2+} ions. All these mechanisms are supposed to form the basis of the increased resistance capacities of hyperaccumulator plants (Clemens et al., 2002). As a consequence, this model explains the observation that *atmrp3* mutants are more sensitive to Cd^{2+} and have a

reduced capacity to transfer Cd^{2+} ions from the root to the shoot. Furthermore, the expression pattern of *AtMRP3* resembles that of the *Arabidopsis ALS3* gene which encodes an ABC-transporter-like protein (Larsen et al., 2005) : *ALS3* expression also forms a continuous network from the root tip to hydathodes, including the phloem. Again, also *ALS3* expression is induced in response to metal stress (in that case aluminium) which is also associated with changes in the spatial expression pattern. *ALS3* is known to mediate resistance against aluminium stress and is supposed to operate by promoting long-distance transport and excretion of Al^{3+} ions through guttation.

Within the *AtMRP* gene family of *Arabidopsis*, the expression pattern of the *AtMRP7* is comparable to the expression pattern of *AtMRP3* : the transcription of AtMRP7 in roots is also induced by cadmium stress (Bovet et al., 2003) and Pro_{AtMRP7}*::GUS* activity is high in the primary and secondary phloem and xylem (Plaza et al., 2005). AtMRP7 has been suggested to be implicated in Cd^{2+} root to shoot transport because knockout mutants in the *AtMRP7* gene having a reduced root/shoot ratio of cadmium distribution when compared to wild-type plants (Plaza et al., 2005). AtMRP7 has been localized to the plasma membrane through the use of an AtMRP7-GFP fusion protein (Plaza et al., 2005). One could suppose in our model that AtMRP3 and AtMRP7 work together, AtMRP7 allowing Cd^{2+} import into the cells of the vascular bundle through the plasma membrane and AtMRP3 transporting the ions further in the cell, into the vacuole. Another AtMRP could also be a possible partner for AtMRP3 : AtMRP4 : this protein has also been localized to the plasma membrane as a GFP fusion protein (Klein et al., 2004), Pro_{AtMRP4}*::GUS* activity is present all over the organism but in leaves a stronger activity was found in the vascular tissue (Plaza et al., 2005) and knockout mutants in the AtMRP4 gene also have a reduced root/shoot ratio of cadmium concentration when compared to wild-type plants (Plaza et al., 2005).

The question arises if our model of the role of AtMRP3 can be transferred to the detoxification of organic xenobiotic compounds, since the results of our growth experiments are a strong indication in favour of the hypothesis of AtMRP3 promoting resistance to prosulfuron. In fact, if we accept the idea that AtMRP3 is able to transport conjugated prosulfuron, we can propose a model of the role played by AtMRP3 in prosulfuron detoxification quite similar to the previously described model of its role in Cd^{2+} detoxification:

- In case the plant is exposed to the herbicide, prosulfuron would typically enter through the cuticular layer and through the stomata into the leaves. Transcription of *AtMRP3* into the mesophyll would increase, allowing the mesophyll cells to sequestrate

conjugated prosulfuron into their vacuoles, avoiding the toxic effects of the herbicide in the cytoplasm and allowing its subsequent detoxification by the phase IV reactions.

- Sequestration of conjugated prosulfuron into the vacuoles of the cells of the vascular bundle and of the bundle sheet through the action of AtMRP3 would drain the herbicide from the sap, preventing its diffusion throughout the plant by the vascular system as well as its diffusion into the apoplast.
- Through the same mechanisms previously described for cadmium, conjugated prosulfuron would be concentrated in the vacuoles of the cells of secretory organs and finally excreted.

X.6.1. Possible practical applications resulting from this study

Since plants lacking *AtMRP3* have a reduced resistance to cadmium or prosulfuron and have a lower root to shoot transfer rate of cadmium, it can be supposed that plants overexpressing *AtMRP3* would be more resistant to cadmium and prosulfuron and accumulate more cadmium in their shoot. Following the phytoremediation concept to clean up contaminated soils by the production of plants that have an increased capacity to extract metals from soils and deposit them in their shoot, it will be an interesting aim to investigate whether plants overexpressing *AtMRP3* tolerate more cadmium in soils and how the shoot/root ratio will behave. Actually, a low number of transgenic *Arabidopsis* plants overexpressing *AtMRP3* gene under the control of the CaMV 35S promoter have been produced. These lines seem to have an enhanced capacity to accumulate cadmium, while no obvious difference has been observed with respect to the resistance to herbicides (Lucien Bovet, personal communication).

The *AtMRP3* promoter controls *AtMRP3* expression in the root tip, in the vascular system, in the leaf mesophyll, in hydathodes and trichomes. This pattern of expression allows a contribution of AtMRP3 in the transfer of cadmium from root to shoot. Thus, the promoter could be useful to specifically express other transporters in these cells types which could for example promote the distribution and thereby the availability of limiting nutrients in the shoot. In addition, *AtMRP3* expression is strongly enhanced by exposure to cadmium or prosulfuron. In preliminary studies using stable transformation of a construct into tobacco and Arabidopsis resulted in only very low GUS activity induction by cadmium exposure (Klein and Martinoia, unpublished). As a consequence, we chose here to include the specific terminator as well, which could possess elements necessary for the specific response to the treatments with selected toxic substances. Transgenic *Arabidopsis* carrying this

Pro$_{AtMRP3}$::GUS::Ter$_{AtMRP3}$ reporter exhibited clearly enhanced GUS activity under xenobiotic stress, especially in the leaf mesophyll. Thus, the *AtMRP3* promoter and terminator can be used to specifically express resistance genes only in the case that they also face the toxic stress in their environment. For example, transgenic crop plants that carry an inducible gene conferring resistance to prosulfuron would only produce the corresponding protein after a prosulfuron treatment in the field. Furthermore, the *Pro$_{AtMRP3}$::reporter::Ter$_{AtMRP3}$* could principally be used to generate reporter plants that indicate the pollution in the soil as a visible phenotype produced by the reporter protein.

A problematic aspect is still that *AtMRP3* has a basal transcription pattern. Consequently, future work must isolate the elements either present in the promoter or terminator of the *AtMRP3* gene that are responsible for the induction of the gene expression in order to create promoters that are inactive in the absence of stress.

With respect to phytoremediation or 'safe food' strategies, generation of plants either hyperaccumulating or excluding toxic compounds will need the manipulation of different steps involved in the detoxification of these compounds one part of which will be the specific expression of transporters. This work on AtMRP3 may help to understand a mechanism implicated in heavy metal allocation and possibly excretion as a step towards a complete full understanding of resistance mechanisms involved in heavy metal tolerance.

X.7.1. Conclusion and outlook

The role of AtMRP3 *in planta* is now better understood. It seems to act as a versatile vacuolar importer of xenobiotics that promotes root to shoot transfer of these compounds. The suggested vacuolar membrane localization has been proven. The importance of this protein for the plant in response to prosulfuron or Cd^{2+} stress, but also under normal conditions has been demonstrated. Furthermore, the expression pattern of the protein has highlighted a common feature with another protein implied in metal stress resistance (see paragraph X.5.1.): as ALS3, AtMRP3 is strongly expressed in the vascular system and in hydathodes. We can suppose that this tissue distribution of a metal transporter in the plant specifically promotes the transfer from root to shoot, as well as the subsequent excretion through the hydathodes of the transported metal. Thus, it is possible that other metal transporters share the same expression pattern in order to promote root to shoot transfer and hydathode excretion of the metal they transport, also as a detoxification mechanism.

The elements of the *AtMRP3* promoter or terminator which induce enhanced transcription under xenobiotic stress are still unknown. Furthermore, the importance of the *AtMRP3* terminator for this induction has until now not been tested experimentally. However, we have now produced different four different reporter gene cassettes, with the two different reporters GUS or luciferase, under the control either of the sole *AtMRP3*-promoter or of the *AtMRP3*-promoter and *AtMRP3*-terminator. These cassettes are in now in vectors that allow either transitory expression or stable transformation of plants. Once transgenic plants containing these constructs are generated (a few plants containg the Pro_{AtMRP3}*::GUS::*Ter_{nos} and the Pro_{AtMRP3}*::LUC::*Ter_{AtMRP3} constructs have already been generated), it would be easy to compare the reporter gene activity in plants containing a construct with the sole *AtMRP3*-promoter with the reporter gene activity in plants containing a construct with the *AtMRP3*-promoter and *AtMRP3*-terminator, in the presence or absence of xenobiotics. Similar experiments could be devised with cell cultures transiently transformed with the constructs.
Direct observation of the AtMRP3 transport activity *in planta* is also lacking. Thus, further investigations of AtMRP3 can still lead to interesting discoveries.

XI. Bibliography

Abdel-Ghany SE, Muller-Moule P, Niyogi KK, Pilon M, Shikanai T. The Plant Cell 2005 Apr;17(4):1233-51 : "Two P-type ATPases are required for copper delivery in *Arabidopsis thaliana* chloroplasts."

Bauer BE, Wolfger H, Kuchler K. Biochemica et Biophysica Acta 1999 Dec 6;1461(2):217-36 : "Inventory and function of yeast ABC proteins: about sex, stress, pleiotropic drug and heavy metal resistance."

Bauer J, Hiltbrunner A, Weibel P, Vidi PA, Alvarez-Huerta M, Smith MD, Schnell DJ, Kessler F. The Journal of Cell Biology 2002 Dec 9;159(5):845-54 : "Essential role of the G-domain in targeting of the protein import receptor atToc159 to the chloroplast outer membrane."

Bert V, Meerts P, Saumitou-Laprade P, Salis P, Gruber W, Verbruggen N. Plant and Soil 2003 Feb;249(1):9-18 : "Genetic basis of Cd tolerance and hyperaccumulation in *Arabidopsis halleri*."

Bloss T, Clemens S, Nies DH. Planta 2002;214:783-791 : "Characterization of the ZAT1p zinc transporter from *Arabidopsis thaliana* in microbial model organisms and reconstituted proteoliposomes."

Bolwell GP , Bozak K, Zimmerlin A. Phytochemistry 1994 Dec;37(6):1491-1506 : "Plant cytochrome p450."

Boominathan R, Doran PM. Biotechnology and bioengineering 2003 Jul 20;83(2):158-67 : "Cadmium tolerance and antioxidative defenses in hairy roots of the cadmium hyperaccumulator, *Thlaspi caerulescens*."

Borevitz JO, Xia Y, Blount J, Dixon RA, Lamb C. The Plant Cell 2000 Dec;12(12):2383-2394 : "Activation tagging identifies a conserved MYB regulator of phenylpropanoid biosynthesis."

Bovet L, Eggmann T, Meylan-Bettex M, Polier JE, Kammer P, Marin E, Feller U, Martinoia E. Plant, Cell and Environment 2003 Mar;26(3):371-381 : "Transcript levels of AtMRPs after cadmium treatment: induction of AtMRP3."

Bovet L, Feller U, Martinoia E. Environment International 2005 Feb;31(2):263-7 : "Possible involvement of plant ABC transporters in cadmium detoxification: a cDNA sub-microarray approach."

Bovet L, Kammer PM, Meylan-Bettex M, Guadagnuolo R. Matera V. Environmental and Experimental Botany 2006 Aug;57(1-2): 80-88 : "Cadmium accumulation capacities of *Arabis alpina* under environmental conditions."

Bringezu K, Lichtenberg O, Leopold I, Neumann D. Journal of Plant Physiology 1999;154:536-546 : "Heavy metal tolerance in *Silene vulgaris*."

Brune A, Urbach W, Dietz KJ. Plant, Cell en Environment 1994;17:153-162 : "Compartmentation and transport of zinc in barley primary leaves as basic mechanisms involved in zinc tolerance."

Callahan DL, Baker AJ, Kolev SD, Wedd AG. Journal of Biological Inorganic Chemistry 2006 Jan;11(1):2-12 : "Metal ion ligands in hyperaccumulating plants."

Canny, MJ. Philos. Trans. R. Soc. London Ser. B 1993:341, 87–100 : "The transpiration stream in the leaf apoplast: water and solutes."

Choi YE, Harada E, Wada M, Tsuboi H, Morita Y, Kusano T, Sano H. Planta 2001 May;213(1):45-50 : "Detoxification of cadmium in tobacco plants: formation and active excretion of crystals containing cadmium and calcium through trichomes."

Clemens S, Antosiewicz DM, Ward JM, Schachtman DP, Schroeder JI. Proceedings of the National Academy of Sciences of the United States of America 1998 Sep 29;95(20):12043-8 : "The plant cDNA LCT1 mediates the uptake of calcium and cadmium in yeast."

Clemens S. Planta 2001;212:475-486 : “Molecular mechanisms of plant metal tolerance and homeostasis.”

Clemens S, Palmgren MG, Krämer U. Trends in Plant Science 2002 Jul;7(7):309-315 : “A long way ahead: understanding and engineering plant metal accumulation.”

Clough SJ, Bent AF. The Plant Journal 1998 Dec;16(6):735-43 : “Floral dip: a simplified method for Agrobacterium-mediated transformation of *Arabidopsis thaliana*.”

Cobbett CS. Current Opinion in Plant Biology 2000 Jun;3(3):211-6 : “Phytochelatin biosynthesis and function in heavy-metal detoxification.”

Cobbett CS. Plant Physiology 2000 Jul;123(3):825-32 : “Phytochelatins and their roles in heavy metal detoxification.”

Cobbett CS, Hussain D, Haydon MJ. New Phytologist 2003;159:315-321: “Structural and functional relationships between type 1_B heavy metal-transporting P-type ATPases in *Arabidopsis*.”

Colangelo EP, Guerinot ML. Current Opinion in Plant Biology 2006 Jun;9(3):322-30 : “Put the metal to the petal: metal uptake and transport throughout plants.”

Cole SPC, Bhardwaj G, Gerlach JH, Mackie JE, Grant CE, Almquist KC, Stewart AJ, Kurz EU, Duncan AMV, Deeley RG. . Science 1992;258:1650-1654 : “Overexpression of a transporter gene in a multidrug resistant human lung cancer cell line.”

Cole SP, Deeley RG. Trends in Pharmacological Sciences 2006 Aug;27(8):438-46 : “Transport of glutathione and glutathione conjugates by MRP1.”

Coleman JOD, Blake-Kalff MMA, Davies TGE. Trends in Plant Science 1997;2(4):144-151 : “Detoxification of xenobiotics by plants: chemical modification and vacuolar compartmentation.”

Curie C, Panaviene Z, Loulergoue C, Dellaporta SL, Briat JF, Walker EL. Nature 2001;18 :346-349 : "Maize yellow stripe1 encodes a membrane protein directly involved in Fe(III) uptake."

Czempinski K, Frachisse JM, Maurel C, Barbier-Brygoo H, Mueller-Roeber B. The Plant Journal 2002 Mar;29(6):809-20 : "Vacuolar membrane localization of the *Arabidopsis* 'two-pore' K+ channel KCO1."

Desbrosses-Fonrouge AG, Voigt K, Schroder A, Arrivault S, Thomine S, Krämer U. FEBS letters 2005 Aug 1;579(19):4165-74 : "*Arabidopsis thaliana* MTP1 is a Zn transporter in the vacuolar membrane which mediates Zn detoxification and drives leaf Zn accumulation."

DiDonato RJ Jr, Roberts LA, Sanderson T, Eisley RB, Walker EL. The Plant Journal 2004 Aug;39(3):403-14 : "*Arabidopsis* Yellow Stripe-Like2 (YSL2): a metal-regulated gene encoding a plasma membrane transporter of nicotianamine-metal complexes."

Diener AC, Gaxiola RA, Fink GR. The Plant Cell 2001 Jul;13(7):1625-38 : "*Arabidopsis* ALF5, a multidrug efflux transporter gene family member, confers resistance to toxins."

Eren E, Arguello JM. Plant Physiology 2004 Nov;136(3):3712-23 : "*Arabidopsis* HMA2, a divalent heavy metal-transporting P(IB)-type ATPase, is involved in cytoplasmic Zn^{2+} homeostasis."

Frelet A, Kolukisaoglu UH, Azevedo L, Hörtensteiner S, Marinova K, Weder B, Schulz B, Klein M. "Functional characterization of AtMRP2 and AtMRP5, two plant multidrug resistance-associated proteins of *Arabidopsis thaliana*" 2006;86-121 : "Comparative mutant analysis of *Arabidopsis* Multidrug-Associated Proteins: only AtMRP2 but not AtMRP1, 11 and 12 contribute to detoxification, vacuolar organic anion transport and chlorophyll degradation."

Fulton TM, Chunwongse J, and Tanksley SD. Plant Molecular Biology Reporter 1995;13(3):207-209 : "Miniprep protocol for extraction of DNA from tomato and other herbaceous plants."

Frear DS, Swanson HR. Journal of Agricultural and Food Chemistry 1996;44:3658-3654 : "Cytochrome P450-dependent hydroxilation of prosulfuron (CGA 152005) by wheat seedling microsomes."

Gaedeke N, Klein M, Kolukisaoglu U, Forestier C, Muller A, Ansorge M, Becker D, Mamnun Y, Kuchler K, Schulz B, Mueller-Roeber B, Martinoia E. The EMBO journal 2001 Apr 17;20(8):1875-87 : "The *Arabidopsis thaliana* ABC transporter AtMRP5 controls root development and stomata movement."

Gaillard C, Dufaud A, Tommasini R, Kreuz K, Amrhein N, Martinoia E. FEBS Letters 1994 Sep 26;352(2):219-21 : "A herbicide antidote (safener) induces the activity of both the herbicide detoxifying enzyme and of a vacuolar transporter for the detoxified herbicide."

Geisler M, Girin M, Brandt S, Vincenzetti V, Plaza S, Paris N, Kobae Y, Maeshima M, Billion K, Kolukisaoglu ÜH, Schulz B, Martinoia E. Molecular Biology of the Cell 2004;15:3393-3405 : "*Arabidopsis* Immunophilin – like TWD1 Functionally Interacts with Vacuolar ABC Transporters."

Goatley, JL, Lewis RW. Plant Physiology 1966; 41:373-375 : "Composition of guttation fluid from rye, wheat, and barley seedlings."

Grotz N, Fox T, Connolly E, Park W, Guerinot ML, Eide D. Proceedings of the National Academy of Sciences of the United States of America 1998 Jun 9;95(12):7220-4 : "Identification of a family of zinc transporter genes from *Arabidopsis* that respond to zinc deficiency."

Hall JL. Journal of Experimental Botany 2002 Jan;53(366):1-11 : "Cellular mechanisms for heavy metal detoxification and tolerance."

He ZL, Yang XE, Stoffella PJ. Journal of Trace Elements in Medicine and Biologie 2005;19(2-3):125-40 : "Trace elements in agroecosystems and impacts on the environment."

Hellens RP, Edwards EA, Leyland NR, Bean S, Mullineaux PM. Plant Molecular Biology 2000Apr;42(6):819-32 : "pGreen: a versatile and flexible binary Ti vector for Agrobacterium-mediated plant transformation."

Hellens R, Mullineaux P, Klee H. Trends in Plant Science 2000 Oct;5(10):446-51 : "Technical Focus:a guide to *Agrobacterium* binary Ti vectors."

Higgins CF, Linton KJ. Nature Structural and Molecular Biology 2004 Oct;11(10):918-26 : "The ATP switch model for ABC transporters."

Hipfner DR, Deeley RG, Cole SPC. Biochemica et Biophysica Acta 1999 Dec 6;1461(2):359-76 : "Structural, mechanistic and clinical aspects of MRP1."

Hirayama T, Kieber JJ, Hirayama N, Kogan M, Guzman P, Nourizadeh S, Alonso JM, Dailey WP, Dancis A, Ecker JR. Cell 1999 Apr 30;97(3):383-93 : "RESPONSIVE-TO-ANTAGONIST1, a Menkes/Wilson disease-related copper transporter, is required for ethylene signaling in *Arabidopsis*."

Hirschi KD, Korenkov V, Wilganowski N, Wagner G. Plant Physiology 2000;124:125-134 "Expression of *Arabidopsis* CAX2 in tobacco: altered metal accumulation and increased manganese tolerance."

Howden R, Goldsbrough PB, Andersen CR, Cobbett CS. Plant Physiology 1995 Apr;107(4):1059-66 : "Cadmium-sensitive, cad1 mutants of *Arabidopsis thaliana* are phytochelatin deficient."

Howden R, Andersen CR, Goldsbrough PB, Cobbett CS. Plant Physiology 1995 Apr;107(4):1067-73 "A cadmium-sensitive, glutathione-deficient mutant of *Arabidopsis thaliana*."

Jasinsky M, Ducos E, Martinoia E, Boutry M. Plant Physiology 2003 Mar;131(3):1169-77 : "The ATP-binding cassette transporters: structure, function, and gene family comparison between rice and *Arabidopsis*."

Jentschke G, Godbold DL. Physiologia Plantarum 2000;109:107-116 : “Metal toxicity and ectomycorrhizas.”

Jones PM, George AM. Cellular and Molecular Life Sciences 2004 Mar;61(6):682-99 : “The ABC transporter structure and mechanism: perspectives on recent research.”

Jungwirth H, Kuchler K. FEBS Letters 2006 Feb 13;580(4):1131-8 : “Yeast ABC transporters - a tale of sex, stress, drugs and aging.”

Karley AJ, Leigh RA, Sanders D. Plant Physiology 2000 Mar;122:835-844 : “Differential ion accumulation and ion fluxes in the mesophyll and epidermis of barley.”

Karley AJ, Leigh RA, Sanders D. Trends in Plant Science 2000 Nov;5(11):465-470 : “Where do all the ions go? The cellular basis of differential ion accumulation in leaf cells.”

Klein M, Weissenböck G, Dufaud A, Gaillard C, Kreuz K, Martinoia E. The Journal of Biochemical Chemistry 1996 Nov;271(47):29666-71 : “Different energization mechanisms drive the vacuolar uptake of a flavonoid glucoside and a herbicide glucoside.”

Klein M, Perfus-Barbeoch L, Frelet A, Gaedeke N, Reinhardt D, Mueller-Roeber B, Martinoia E, Forestier C. The Plant Journal 2003 Jan;33(1):119-29 : “The plant multidrug resistance ABC transporter AtMRP5 is involved in guard cell hormonal signalling and water use.”

Klein M, Geisler M, Suh SJ, Kolukisaoglu HU, Azevedo L, Plaza S, Curtis MD, Richter A, Weder B, Schulz B, Martinoia E. The Plant Journal 2004 Jul;39(2):219-36 : “Disruption of AtMRP4, a guard cell plasma membrane ABCC-type ABC transporter, leads to deregulation of stomatal opening and increased drought susceptibility.”

Kobae Y, Uemura T, Sato MH, Ohnishi M, Mimura T, Maeshima M. Plant and Cell Physiology 2004;45:1749-1758 : “Zinc transporter of *Arabidopsis thaliana* AtMTP1 is localized to vacuolar membranes and implicated in zinc homeostasis.”

Kolukisaoglu HU, Bovet L, Klein M, Eggmann T, Geisler M, Wanke D, Martinoia E, Schulz B. Planta 2002 Nov;216(1):107-19 : "Family business: the multidrug-resistance related protein (MRP) ABC transporter genes in *Arabidopsis thaliana*."

Koncz C, Schell J. Molecular and General Genetics 1986;204:383-396 : "The promoter of T_L-DNA gene 5 controls the tissue-specific expression of chimaeric genes carried by a novel type of *Agrobacterium* binary vector"

König J, Nies AT, Cui Y, Leier I, Keppler D. Biochimica et Biophysica Acta 1999 Dec 6;1461(2):377-94 : "Conjugate export pumps of the multidrug resistance protein (MRP) family: localization, substrate specificity, and MRP2-mediated drug resistance."

Koren'kov V, Park S, Cheng NH, Sreevidya C, Lachmansingh J, Morris J, Hirschi K, Wagner GJ. Planta 2006 Jul 15; [Epub ahead of print] : "Enhanced Cd(2+)-selective root-tonoplast-transport in tobaccos expressing *Arabidopsis* cation exchangers."

Korte F, Kvesitadze G, Ugrekhelidze D, Gordeziani M, Khatisashvili G, Buadze O, Zaalishvili G, Coulston F. Ecotoxycology and Environmental Safety 2000;47:1-26 : "Organic toxicants and plants."

Krämer U, Cotter-Howells JD, Charnock JM, Baker AJM, Smith JAC. Nature 1996;379:635-638 : "Free histidine as a metal chelator in plants that accumulate nickel."

Krämer U, Pickering IJ, Prince RC, Raskin I, Salt DE. Plant Physiology 2000 Apr;122(4):1343-53 : "Subcellular localization and speciation of nickel in hyperaccumulator and non-accumulator *Thlaspi* species."

Kreuz K, Tommasini R, Martinoia E. Plant Physiology 1996;111:349-353 : "Old enzymes for a new job – Herbicide detoxification in plants."

Krysan PJ, Young JC, Tax F, Sussman MR. Proceedings of the National Academy of Sciences of the United States of America 1996 Jul 23;93(15):8145-50 : "Identification of transferred DNA insertions within *Arabidopsis* genes involved in signal transduction and ion transport."

Krysan PJ, Young JC, Sussman MR. The Plant Cell 1999 Dec;11(12):2283-90 : "T-DNA as an insertional mutagen in *Arabidopsis*."

Lanquar V, Lelievre F, Bolte S, Hames C, Alcon C, Neumann D, Vansuyt G, Curie C, Schroder A, Krämer U, Barbier-Brygoo H, Thomine S. The EMBO journal 2005 Dec 7;24(23):4041-51 : "Mobilization of vacuolar iron by AtNRAMP3 and AtNRAMP4 is essential for seed germination on low iron."

Larsen PB, Geisler MJ, Jones CA, Williams KM, Cancel JD. The Plant Journal 2005 Feb;41(3):353-63 : "ALS3 encodes a phloem-localized ABC transporter-like protein that is required for aluminum tolerance in *Arabidopsis*."

Lasat MM, Baker A, Kochian LV. Plant Physiology 1996 Dec;112(4):1715-1722 : "Physiological Characterization of Root Zn^{2+} Absorption and Translocation to Shoots in Zn Hyperaccumulator and Nonaccumulator Species of *Thlaspi*."

Lasat MM, Pence NS, Garvin DF, Ebbs SD, Kochian LV. Journal of Experimental Botany 2000;51(342):71-79 : "Molecular physiology of zinc transport in the Zn hyperaccumulator *Thlaspi caerulescens*."

Lee EK, Kwon M, Ko JH, Yi H, Hwang MG, Chang S, Cho MH. Plant Physiology 2004;134:528-538 : "Binding of Sulfonylurea by AtMRP5, an *Arabidopsis* Multidrug Resistance-Related Protein That Functions in Salt Tolerance."

Lee M, Lee K, Lee J, Noh EW, Lee Y. Plant Physiology 2005 Jun;138(2):827-36 : "AtPDR12 contributes to lead resistance in *Arabidopsis*."

Li ZS, Zhao Y, Rea PA. Plant Physiology 1995 Apr;107(4):1257-1268 : "Magnesium Adenosine 5[prime]-Triphosphate-Energized Transport of Glutathione-S-Conjugates by Plant Vacuolar Membrane Vesicles."

Li ZS, Zhen RG, Rea PA. Plant Physiol. 1995 Sep;109(1):177-185 : "1-Chloro-2,4-Dinitrobenzene-Elicited Increase in Vacuolar Glutathione-S-Conjugate Transport Activity."

Li ZS, Szczypka M, Lu YP, Thiele DJ, Rea PA. The Journal of Biological Chemistry 1996 Mar 15;271(11):6509-17 : “The yeast cadmium factor protein (YCF1) is a vacuolar glutathione S-conjugate pump.”

Li ZS, Lu YP, Zhen RG, Szczypka M, Thiele DJ, Rea PA. Proceedings of the National Academy of Sciences of the United States of America 1997 Jan 7;94(1):42-7 : “A new pathway for vacuolar cadmium sequestration in Saccharomyces cerevisiae: YCF1-catalyzed transport of bis(glutathionato)cadmium.”

Lichtenthaler HK and Wellburn AR. Biochemical Society Transactions 1983;11:591-592 : “Determinations of total carotenoids and chlorophylls *a* and *b* of leaf extracts in different solvents.”

Linton KJ, Higgins CF. Molecular Microbiology 1998 Apr;28(1):5-13 : “The Escherichia coli ATP-binding cassette (ABC) proteins.”

Lombi E, Zhao FJ, Dunham SJ, McGrath SP. New Phytologist 2000 Jan;145(1):11-20 : "Cadmium accumulation in populations of *Thlaspi caerulescens* and *Thlaspi goesingense*."

Lombi E, Zhao FJ, McGrath SP, Young SD, Sacchi GA. New Phytologist 2001 Jan;149(1):53-60 : “Physiological evidence for a high-affinity cadmium transporter highly expressed in a *Thlaspi caerulescens* ecotype .”

Linton KJ, Higgins CF. Molecular Microbiology 1998 Apr;28(1):5-13 : “The *Escherichia coli* ATP-binding cassette (ABC) proteins.”

Liu G, Sanchez-Fernandez R, Li ZS, Rea PA. The Journal of Biological Chemistry 2001 Mar 23;276(12):8648-56 : “Enhanced multispecificity of *Arabidopsis* vacuolar multidrug resistance-associated protein-type ATP-binding cassette transporter, AtMRP2.”

Lu YP, Li ZS, Rea PA. Proceedings of the National Academy of Sciences of the United States of America 1997 Jul 22;94(15):8243-8 : “*AtMRP1* gene of *Arabidopsis* encodes a glutathione

S-conjugate pump: isolation and functional definition of a plant ATP-binding cassette transporter gene."

Lu YP, Li ZS, Drozdowicz YM, Hortensteiner S, Martinoia E, Rea PA. Plant Cell 1998 Feb;10(2):267-82 : "AtMRP2, an *Arabidopsis* ATP binding cassette transporter able to transport glutathione S-conjugates and chlorophyll catabolites: functional comparisons with AtMRP1."

Ma JF, Zheng SJ, Matsumoto H. Nature 1997;390:569-570 : "Detoxifying aluminium with buckwheat."

Ma JF, Ryan PR, Delhaize E. Trends in Plant Science 2001;6:273-278 : "Aluminium tolerance in plants and the complexing role of organic acids."

Ma JF, Ueno D, Zhao FJ, McGrath SP. Planta 2005 Mar;220(5):731-6 : "Subcellular localisation of Cd and Zn in the leaves of a Cd-hyperaccumulating ecotype of Thlaspi caerulescens."

Marrs KA. Annual Review of Plant Physiology and Plant Molecular Biology 1996;47:127-158 : "The functions and regulation of glutathione s-transferases in plants."

Martienssen RA. Proceedings of the National Academy of Sciences of the United States of America 1998 Mar 3;95(5):2021-6 : "Functional genomics: probing plant gene function and expression with transposons."

Martinoia E, Grill E, Tommasini R, Kreuz K, Amrhein N. Nature 1993 15 July;364:247-49 : "ATP-dependent glutathione S-conjugate 'export' pump in the vacuolar membrane of plants."

Mäser P, Thomine S, Schroeder JI, Ward JM, Hirschi KD, Sze H, Talke IN, Amtmann A, Maathuis FJ, Sanders D, Harper JF, Tchieu J, Gribskov M, Persans MW, Salt DE, Kim SA, Guerinot ML. Plant Physiology 2001; 126:1646-1667 "Phylogenetic relationships within cation transporter families of *Arabidopsis*."

McElver J, Tzafrir I, Aux G, Rogers R, Ashby C, Smith K, Thomas C, Schetter A, Zhou Q, Cushman MA, Tossberg J, Nickle T, Levin JZ, Law M, Meinke D, Patton D. Genetics 2001 Dec;159(4):1751-63 : "Insertional mutagenesis of genes required for seed development in *Arabidopsis thaliana*."

McGrath SP, Zhao FJ. Current Opinion in Biotechnology 2003 Jun;14(3):277-82 : "Phytoextraction of metals and metalloids from contaminated soils."

Meharg AA, Macnair MR. New Phytologist 1990;116:29-35 : "An altered phosphate uptake system in arsenate-tolerant *Holcus latanus*."

Meharg AA, Macnair MR. Heredity 1992;69:336-341 : "Genetic correlation between arsenate tolerance and the rate of influx of arsenate and phosphate in *Holcus latanus*."

Mentewab A, Stewart CN Jr. Nature Biotechnology 2005 Sep;23(9):1177-80 : "Overexpression of an *Arabidopsis thaliana* ABC transporter confers kanamycin resistance to transgenic plants."

Mills RF, Francini A, Ferreira da Rocha PS, Baccarini PJ, Aylett M, Krijger GC, Williams LE. FEBS Letters 2005 Jan 31;579(3):783-91 : "The plant P1B-type ATPase AtHMA4 transports Zn and Cd and plays a role in detoxification of transition metals supplied at elevated levels."

Moreland DE, Fleischmann TJ, Corbin FT, McFarland JE. Zeitschrift für Naturforschung C 1996;51:698-710 : "Differential metabolism of the sulfonylurea herbicide prosulfuron (CGA-152005) by plant microsomes."

Murashige T and Skoog F. Physiologia Plantarum 1962;15:473-497 : "A revised medium for rapid growth and bioassays with tobacco tissue cultures."

Ortiz DF, Ruscitti T, McCue KF, Ow DW. The Journal of Biological Chemistry 1995 Mar 3;270(9):4721-8 : "Transport of metal-binding peptides by HMT1, a fission yeast ABC-type vacuolar membrane protein."

Perfus-Barbeoch L, Leonhardt N, Vavasseur A, Forestier C. The Plant Journal 2002 Nov;32(4):539-48 : "Heavy metal toxicity: cadmium permeates through calcium channels and disturbs the plant water status."

Pich A, Manteuffel R, Hillmer S, Scholz G, Schmidt W. Planta 2001; 213 :967-976 : "Fe homeostasis in plant cells: does nicotianamine play multiple roles in the regulation of cytoplasmic Fe concentration?"

Plaza S, Bovet L, Kolukisaoglu UH, Tamas M, Azevedo L, Klein M, Martinoia M, Geisler M. "Heavy Metals and Phytoremediation: Combining Molecular and Ecological Approaches" 2005;51-70 : "*Arabidopsis* MRP-like ABC transporters, AtMRP4 and AtMRP7, transport cadmium and maintain the cadmium root-shoot ratio."

Plaza S, Lee OR, Antunes C, Freeman JL, Schoenenberger N, Makam SN, Llemit SM, Bovet L, Geisler M, Murphy AS, Martinoia E, Peer WA. "Heavy Metals and Phytoremediation: Combining Molecular and Ecological Approaches" 2005;165-193 : "Study of *Arabidopsis* species, *A. arenosa* and *A. lyrata*, as heavy metal indicators."

Salt DE, Wagner GJ. The Journal of Biological Chemistry 1993 Jun 15;268(17):12297-302 : "Cadmium transport across tonoplast of vesicles from oat roots. Evidence for a Cd2+/H+ antiport activity."

Salt DE, Rauser WE. Plant Physioly 1995 Apr;107(4):1293-1301 : "MgATP-Dependent Transport of Phytochelatins Across the Tonoplast of Oat Roots."

Salt DE, Prince RC, Baker AJM, Raskin I, Pickering IJ. Environmental Science and Technology 1999;33:712–717 : "Zinc ligands in the metal hyperaccumulator *Thlaspi caerulescens* as determined using X-ray absorption spectroscopy."

Salt DE, Kato N, Krämer U, Smith RD, Raskin I. Phytoremediation of contaminated soil and water. CRC Press LLC. 2000:189-200 : "The role of root exudates in nickel hyperaccumulation and tolerance in accumulator and nonaccumulator species of *Thlaspi*."

Sancenon V, Puig S, Mateu-Andres I, Dorcey E, Thiele DJ, Penarrubia L. The Journal of Biological Chemistry 2004; 279:15348-15355. "The *Arabidopsis* copper transporter COPT1 functions in root elongation and pollen development."

Sánchez-Fernández R, Ardiles-Diaz W, Van Montagu M, Inze D, May MJ. Molecular and General Genetics 1998 Jun;258(6):655-62 : "Cloning and expression analyses of AtMRP4, a novel MRP-like gene from *Arabidopsis thaliana*."

Sánchez-Fernández R, Davies TG, Coleman JO, Rea PA. The Journal of Biological Chemistry 2001 Aug 10;276(32):30231-44 : "The *Arabidopsis thaliana* ABC protein superfamily, a complete inventory."

Santelia D, Vincenzetti V, Azzarello E, Bovet L, Fukao Y, Duchtig P, Mancuso S, Martinoia E, Geisler M. FEBS letters 2005 Oct 10;579(24):5399-5406 : "MDR-like ABC transporter AtPGP4 is involved in auxin-mediated lateral root and root hair development."

Schaaf G, Schikora A, Haberle J, Vert G, Ludewig U, Briat JF, Curie C, von Wiren N. Plant Cell Physioly 2005 May;46(5):762-74 : "A putative function for the *Arabidopsis* Fe-Phytosiderophore transporter homolog AtYSL2 in Fe and Zn homeostasis."

Schmoger ME, Oven M, Grill E. Plant Physiology 2000 Mar;122(3):793-801 : "Detoxification of arsenic by phytochelatins in plants."

Seigneurin-Berny D, Gravot A, Auroy P, Mazard C, Kraut A, Finazzi G, Grunwald D, Rappaport F, Vavasseur A, Joyard J, Richaud P, Rolland N. The Journal of Biological Chemistry 2006 Feb 3;281(5):2882-92 : "HMA1, a new Cu-ATPase of the chloroplast envelope, is essential for growth under adverse light conditions."

Sessions A, Burke E, Presting G, Aux G, McElver J, Patton D, Dietrich B, Ho P, Bacwaden J, Ko C, Clarke JD, Cotton D, Bullis D, Snell J, Miguel T, Hutchison D, Kimmerly B, Mitzel T, Katagiri F, Glazebrook J, Law M, Goff SA. The Plant Cell 2002 Dec;14(12):2985-94 : "A high-throughput *Arabidopsis* reverse genetics system."

Shigaki T, Barkla BJ, Miranda-Vergana MC, Zhao J, Pantoja O, Hirschi KD. Journal of Biological Chemistry 2005; 280:30136-30142 : "Identification of a crucial histidine involved in metal transport activity in the *Arabidopsis* cation/H^+ exchanger CAX1."

Shikanai T, Muller-Moule P, Munekage Y, Niyogi KK, Pilon M. The Plant Cell 2003 Jun;15(6):1333-46 : "PAA1, a P-type ATPase of *Arabidopsis*, functions in copper transport in chloroplasts."

Shitan N, Bazin I, Dan K, Obata K, Kigawa K, Ueda K, Sato F, Forestier C, Yazaki K. Proceedings of the National Academy of Sciences of the United States of America 2003 Jan 21;100(2):751-6 : "Involvement of CjMDR1, a plant multidrug-resistance-type ATP-binding cassette protein, in alkaloid transport in *Coptis japonica*."

Siminszky B, Corbin FT, Ward ER, Fleischmann TJ, Dewey RE. Proceedings of the National Academy of Sciences of the United States of America 1999 Feb;96:1750-1755 : "Expression of a soybean cytochrome P450 monooxygenase cDNA in yeast and tobacco enhances the metabolism of phenylurea herbicides."

Song WY, Sohn EJ, Martinoia E, Lee YJ, Yang YY, Jasinski M, Forestier C, Hwang I, Lee Y. Nature Biotechnology 2003 Aug;21(8):914-9 : "Engineering tolerance and accumulation of lead and cadmium in transgenic plants."

Suh SJ, Frelet A, Grob H, Gaedeke N, Schmidt U, Mueller-Roeber B, Klein M, Martinoia E. "Functional characterization of AtMRP2 and AtMRP5, two plant multidrug resistance-associated proteins of *Arabidopsis thaliana*" 2006;86-121 : "Ectopic expression of *Arabidopsis* AtMRP5 increases drought sensitivity in tobacco and deregulates the guard cell slow anion channel."

Sussman MR, Amasino RM, Young JC, Krysan PJ, Austin-Phillips S. Plant Physiology 2000 Dec;124(4):1465-7 : "The *Arabidopsis* knockout facility at the University of Wisconsin-Madison."

Szczypka MS, Wemmie JA, Moye-Rowley WS, Thiele DJ. The Journal of Biological Chemistry 1994 Sep 9;269(36):22853-7 : "A yeast metal resistance protein similar to human

cystic fibrosis transmembrane conductance regulator (CFTR) and multidrug resistance-associated protein."

Thomine S, Wang R, Ward JM, Crawford NM, Schroeder JI. Proceedings of the National Academy of Sciences of the United States of America 2000 Apr 25;97(9):4991-6 : "Cadmium and iron transport by members of a plant metal transporter family in *Arabidopsis* with homology to Nramp genes."

Thomine S, Lelievre F, Debarbieux E, Schroeder JI, Barbier-Brygoo H. The Plant Journal 2003 Jun;34(5):685-95 : "AtNRAMP3, a multispecific vacuolar metal transporter involved in plant responses to iron deficiency."

Tommasini R, Evers R, Vogt E, Mornet C, Zaman GJ, Schinkel AH, Borst P, Martinoia E. Proceedings of the National Academy of Sciences of the United States of America 1996 Jun 25;93(13):6743-8 : "The human multidrug resistance-associated protein functionally complements the yeast cadmium resistance factor 1."

Tommasini R, Vogt E, Schmid J, Fromentau M, Amrhein N, Martinoia E. FEBS letters 1997 Jul 14;411(2-3):206-10 : "Differential expression of genes coding for ABC transporters after treatment of *Arabidopsis thaliana* with xenobiotics."

Tommasini R, Vogt E, Fromenteau M, Hörtensteiner S, Matile P, Amrhein N, Martinoia E. The Plant Journal 1998 Mar;13(6):773-80 : "An ABC-transporter of *Arabidopsis thaliana* has both glutathione-conjugate and chlorophyll catabolite transport activity."

Tseng TS, Tzeng SS, Yeh CH, Chang FC, Chen YM, Lin CY. Plant and Cell Physiology 1993;34:165-168 : "The heat shock response in rice seedlings - isolation and expression of cDNAs that encode class-I low-molecular-weight heat-shock proteins."

Überlacker B and Werr W. Mol. Breed 1996;2:293–295 : "Vectors with rare-cutter restriction enzyme sites for expression of open reading frames in transgenic plants."

van der Zaal BJ, Neuteboom LW, Pinas JE, Chardonnens AN, Schat H, Verkleij JAC, Hooykaas PJJ. Plant Physiology 1999; 119 :1047-1055 : "Overexpression of a novel

Arabidopsis gene related to putative zinc-transporter genes from animals can lead to enhanced zinc resistance and accumulation."

Verret F, Gravot A, Auroy P, Preveral S, Forestier C, Vavasseur A, Richaud P. FEBS Letters 2005 Feb 28;579(6):1515-22 : "Heavy metal transport by AtHMA4 involves the N-terminal degenerated metal binding domain and the C-terminal His11 stretch."

Vert G, Grotz N, Dedaldechamp F, Gaymard F, Guerinot ML, Briat JF, Curie C. The Plant Cell 2002 Jun;14(6):1223-33 : "IRT1, an *Arabidopsis* transporter essential for iron uptake from the soil and for plant growth."

Vögeli-Lange R, Wagner GJ. Plant Physiology 1990;92:1086-1093 : "Subcellular localization of cadmium and cadmium-binding peptides in tobacco leaves. Implication of a transport function for cadmium binding-peptides."

Voinnet O, Rivas S, Mestre P, Baulcombe D. The Plant Journal 2003 Mar;33(5):949-56 : "An enhanced transient expression system in plants based on suppression of gene silencing by the p19 protein of tomato bushy stunt virus."

Williams LE, Mills RF. Trends in Plant Science 2005;10:491-502: "P(1B)-ATPases — an ancient family of transition metal pumps with diverse functions in plants."

Woeste KE, Kieber JJ. The Plant Cell 2000 Mar;12(3):443-55 : "A strong loss-of-function mutation in RAN1 results in constitutive activation of the ethylene response pathway as well as a rosette-lethal phenotype."

Wolf AE, Dietz KJ, Schroder P. FEBS Letters 1996 Apr 8;384(1):31-34 : " Degradation of glutathione s-conjugates by a carboxypeptidase in the plant vacuole."

Wollgiehn R, Neumann D. Journal of Plant Physiology 1999;154:547-553 : "Metal stress response and tolerance of cultured cells from *Silene vulgaris* and *Lycopersicon peruvianum*: role of heat stress proteins."

Yang YY, Jung JY, Song WY, Suh HS, Lee Y. Plant Physiology 2000 Nov;124(3):1019-26 : "Identification of rice varieties with high tolerance or sensitivity to lead and characterization of the mechanism of tolerance."

Zhou J, Goldsbrough PB. The Plant Cell 1994;6:875-884 : "Functional homologs of fungal metallothionein genes from *Arabidopsis*."

XII. Acknowledgements

A PhD thesis is not a work carried out by a single person. It is a team work and so I would to express my gratitude to many persons for the invaluable help they gave me during these years. So…

For their participation in my work, for their practical and theoretical help and for their advice, many thanks to :

Dr. Birgit Agne, Aurélien Bailly, Dr. Lucien Bovet, Dr. Claire Bréhélin, Bo Burla, Thomas Eggmann, Nadège Fahrni, Michael Federer, Thomas Flura, Dr. Markus Geisler, Hanne Grob, Dr. Michal Jasinski, Sibylle Infanger, Pr. Beat Keller, Pr. Felix Kessler, Dr. Markus Klein, Dr. Ute Krämer, Regis Mack, Dr. Krasimira Marinova, Pr. Enrico Martinoia, Dr. Virginie Matera, Marlyse Meylan, Dr. Valérie Page, Aurélie Pédezert, Dr. Sonia Plaza, Dr. Diana Santelia, Maja Schellenberg, Dr. Ulrike Schmidt, Magali Schnell, Joanne Schwaar, Jana Smutny, Dr. Pia Stieger, Damien Sudre, Dr. Nicola Tomasi, Dr. Pierre-Alexandre Vidi, Vincent Vincenzetti, Barbara Weder, Dr. Petra Weibel, Dr. Laure Weisskopf.

For their constant support and caring, for their friendship and love, for their help at all levels, for their encouragements, for believing in me, because without them I would never have been able to complete the present work, my infinite thanks and love to :

Augusto Azevedo, Elvira Azevedo, Lorenz Bigler, David Borel, Dr. Anne-Frédérique Antonioni-Bourquin, Marie-Jeanne De Jong, Dr. Sandrine Gouinguene, Madeleine Grize, Christian Haenny, Dr. Philippe Jeanbourquin, Robin Lièvre, Marc Nobel, Sister Paulette, Aurélie Pédezert, Master Henry Plée, Nicolas Rákóczi, Julien Renaud, Louis Renaud, Lionel Schilli, Sébastien Villalba, Raphaël Weiss, all the friends of the "Paris group".

For literally saving my life, for taking me from hell to a real rebirth, my eternal gratefulness to :

Philippe Buil, Dr. Jean-Jacques Brugger, Vianney Catteau, Bernard Denel, André Frésard, Denis Labouré, Marc Neu, Denis Vipret, all the staff of the Hôpital de la Providence.